UiT
THE ARCTIC
UNIVERSITY
OF NORWAY

Faculty of health sciences, Institute for Medical Biology

The oncoproteins gelsolin, periostin and thrombospondin are enriched in Merkel cell carcinoma exosomes, and their promoter activity is stimulated by Large T-antigen of Merkel cell polyomavirus

Ida Sofie Furuholmen-Jenssen

Master's thesis in Biomedicine 15.05.2017

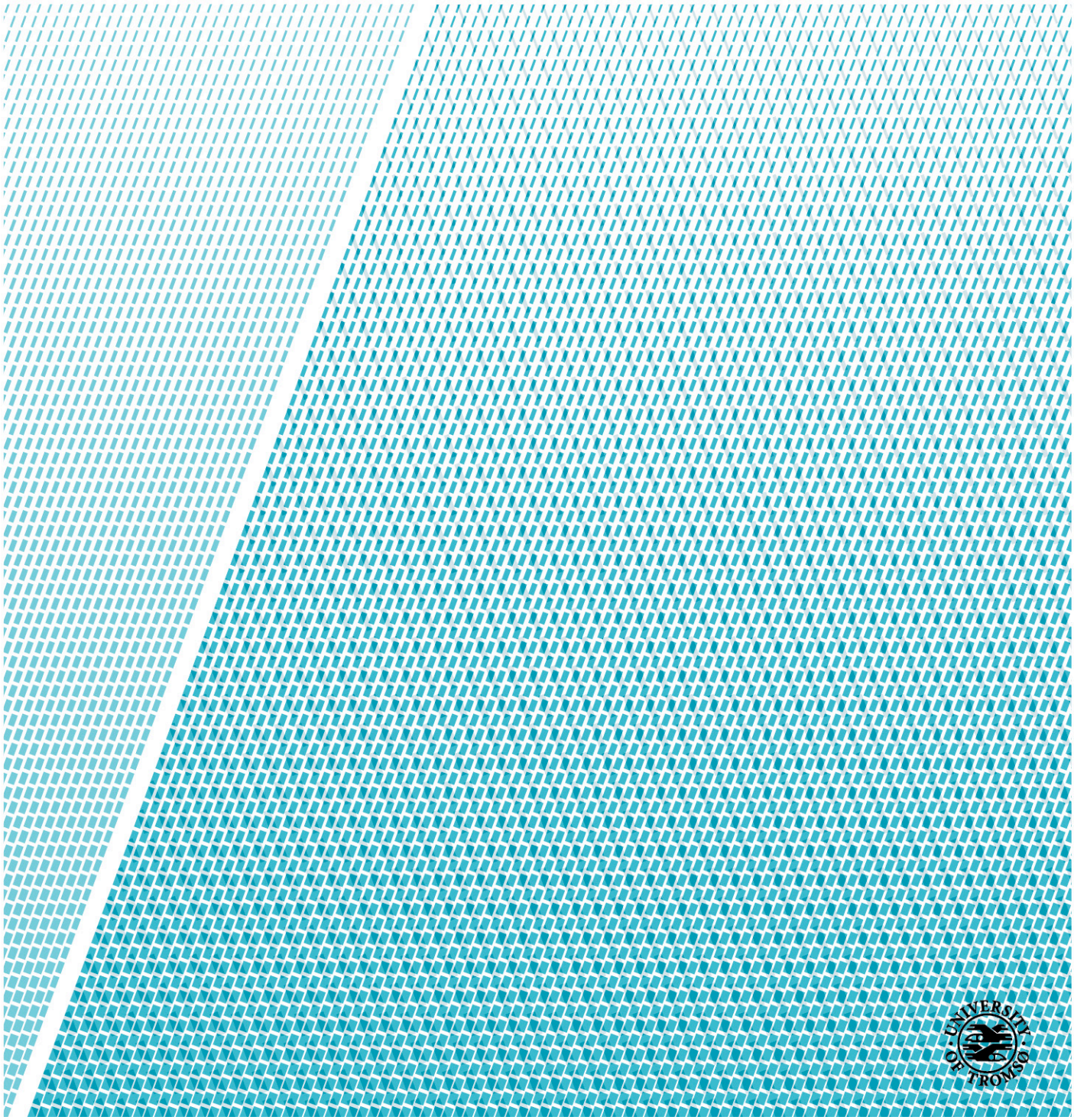

Acknowledgements

This thesis was written under the Molecular Inflammation Research Group (MIRG), at the Department of Medical Biology, University of Tromsø, the Arctic University of Norway.

First and foremost I want to thank my main supervisor Professor Ugo Moens for sharing his expertise regarding laboratory technical methods and for his help with result interpretation. I am truly grateful for his thorough and efficient proof reading, and constructive criticism during the writing of this thesis. I also want to thank him for his support and encouraging words when I needed them the most.

A special thanks goes to PhD candidate Aelita Konstantinell for giving me the opportunity to be a part of her project and for helping me out in the lab. I want to thank Professor Baldur Sveinbjørnsson, my co-supervisor, for his bright ideas regarding experimental design and progression. I also want to thank Gianina Dumitriu and Maria A. Ludvigsen, the engineers of the group research group, PhD candidate Conny Tümler and PhD candidate Kashif Rasheed for giving me advices and sharing their experiences with me.

Finally, Aud-Malin Hovds help and support especially regarding Prism7 related problems and statistical analysis of the data is highly appreciated.

Abstract

Merkel cell carcinoma (MCC) is a rare, aggressive neuroendocrine form of skin cancer with high mortality rate and increasing incidence. Around 80 % of MCC tumours are positive for Merkel cell polyomavirus (MCPyV), the only polyomavirus known to induce cancer in humans. Continuous expression of the viral oncogenes LT-ag and st-ag is necessary for MCPyV positive MCC tumour cell survival, suggesting that it could be a causative agent in MCC. Exosomes are 30-150 nm vesicles of endocytic origin that play a crucial role in cell-cell communication both under normal and pathophysiological conditions like cancer, through transfer of various nucleic acid species, proteins, lipids or viral particles.

The role of exosomes in MCC remains elusive. Previous proteomic studies from our group have demonstrated that MCC-derived exosomes contain the proteins gelsolin, periostin and thrombospondin, all of which have tumorigenic properties. It is not known whether the MCPyV proteins LT-ag or/and st-ag affect the expression of these proteins and their exosomal concentrations. By using western blot and RT-PCR we confirmed that gelsolin, periostin and thrombospondin were present and possibly enriched in exosomes derived from four MCC cell lines. The effect of LT-ag and st-ag on gelsolin, periostin and thrombospondin promoter activity was also studied using transient transfection studies with luciferase reporter constructs, and it was found that LT-ag but not st-ag induces promoter activity of the genes encoding these proteins. Furthermore, the effect of the three proteins on cell proliferation was assessed using MTT assay. However, the addition of increasing concentrations of recombinant proteins to MCC cell cultures did not give conclusive results.

In conclusion, the results suggest that MCPyV LT-ag may contribute to MCC by enhancing the expression of the oncoproteins gelsolin, periostin and thrombospondin. Furthermore, the proteins seem to be enriched in MCC exosomes and therefore may play a role in exosome-mediated processes in carcinogenesis.

Table of Contents

1. Introduction 1
1.1. Merkel cells 1
1.2. Merkel cell carcinoma 2
1.3. Human polyomaviruses and MCPyV 3
1.4. MCPyV oncogenes 5
1.5. Exosomes 8
1.6. Exosomes - mediators of cell-cell communication under normal and pathophysiological conditions 10
1.7. Exosomes unambiguous role in the immune system 14
1.8. Periostin 16
1.9. Thrombospondin 17
1.10. Gelsolin 19
1.11. Aim of the study 20
2. Materials 21
3. Methods 31
3.1. Mammalian cell cultures 31
3.1.1. Thawing of cells 31
3.1.2. Cultivating cells 32
3.1.3. Sub-culturing of cells 32
3.1.4. Removal of bovine exosomes 33
3.1.5. Counting and seeding out cells 33
3.1.6. Mycoplasma test 34
3.1.7. Freezing down cells in liquid nitrogen 35
3.2. Isolation of exosomes 36
3.3. Verification of Exosomes using Photon Correlation Spectroscopy (PCS) 36
3.4. Verification of periostin, thrombospondin and gelsolin using Western blot 38
3.5. Detection of periostin and thrombospondin transcripts using Reverse Transcription Polymerase Chain Reaction (RT-PCR) 41
3.5.1. RNA isolation 42
3.5.2. cDNA synthesis 43
3.5.3. PCR 44
3.5.4. Agarose gel electrophoresis 46

3.6. Assessing the effect of LT-ag and st-ag on periostin, thrombospondin and gelsolin promoter activity using transient Transfection 47
3.6.1.Transformation of plasmid DNA into *E.coli* DH5 47
3.6.2. Plasmid purification 48
3.6.3. Transient transfection and luciferase assay 51
3.6.4. Luciferase assay 53
3.6.5. Protein quantification assay 54
3.7. Cell viability of MCC13 cells treated with recombinant protein was measured using MTT assay 55
3.8. Statistical analysis 56
4. Results 57
4.1. Two distinct populations of vesicles were detected in the four MCC cell lines used in the study using Nicomp particle sizing system (PSS) 57
4.2. Western blot detected gelsolin, periostin and thrombospondin in exosomes of MCC cell lines 61
4.3. LT-ag protein was detected in MKL-1, but not in MKL-2 cells using Western blot 64
4.4. Periostin and thrombospondin were detected in MCC cell lines by RT-PCR 66
4.5. LT-ag mRNA was detected in virus positive MCC cell lines using RT-PCR 69
4.6. LT-ag, but not st-ag activates the gelsolin, periostin and thrombospondin promoters . 70
4.7. Cell viability was not enhanced following exposure to recombinant gelsolin, periostin and thrombospondin proteins 76
5. Discussion 82
5.1. Exosomes were successfully isolated from MCC cell lines 82
5.2. Gelsolin, periostin and thrombospondin transcripts were detected in MCC exosomes and cells using western blot and RT-PCR 83
5.3. Western blot and RT-PCR shows that LT-ag expression is higher in MKL-1 than in MKL-2 cells and confirms the lack of LT-ag in MCC13 and MCC26 cells 85
5.4. MCPyV LT-ag, but not st-ag, significantly stimulates gelsolin, periostin and thrombospondin promoter activity in MCC13 cells 85
5.5. Increased cell proliferation was not measured after incubation with recombinant gelsolin, periostin thrombospondin proteins followed by MTT assay 86
5.6. Future perspectives 88
Bibliography 90
Appendices 102

Appendix 1. Alignment of MKL-1 and MKL-2 genomes 102

Appendix 2. ANOVA tables generated from luciferase assays with gelsolin, periostin and thrombospondin promoters 111

Appendix 3. Two-way ANOVA tables generated from MTT experiments with recombinant gelsolin, thrombospondin and periostin from two different suppliers. 123

Appendix 4. Putative LT-ag binding sites 129

Putative LT-ag binding sites in the gelsolin promoter 129

Putative LT-ag binding sites in the thrombospondin promoter 130

Putative LT-ag binding sites in the periostin promoter 130

List of abbreviations

APRT = Adenine phosphoribosyltransferase

Akt = Oncogene identified in the mouse AKR retrovirus which can cause thymomas

ALTO = Alternative open reading frame

APC = Antigen presenting cells

ATP = Adenosine triphosphate

BKPyV = BK polyomavirus

β-ME = β mercaptoethanol

Bp = Base pair

CD = Cluster of differentiation

CK 20 = Cytokeratin 20

DC = Dendritic cell

DMSO = Dimethyl sulfoxide

DNA = Deoxyribonucleic acid

dsDNA = Double stranded DNA

EBV= Epstein-Barr virus

ECM = Extracellular matrix

EGF = Epidermal growth factor

EGFR = Epidermal growth factor receptor

ERB-b2 = Epidermal growth factor 2

ERK = Extracellular signal Regulated Kinase

EMT = Epithelial to Mesenchymal Transition

ESCERT = Endosomal sorting complexes required for transport

FGF = Fibroblast growth factor

gDNA= Genomic DNA

GTP = Guanosine triphosphate

HCV = Hepatitis C virus

Hsp = Heat shock protein

ILV = Intraluminal vesicle

ITG = Integrin

JCPyV = JC polyomavirus

KSHV = Kaposi sarcoma associated virus

LMP1= Latent membrane protein 1

lncRNA = Long non-coding RNA

LRP = Low-density receptor-related protein

LSD = LT- stabilizing domain

LT-ag = Large T-antigen

MAC = Membrane attack complex

MAE = Methyl amino ethanol

MAPK= Mitogen activated protein kinase

MCC = Merkel cell carcinoma

MCPyV = Merkel cell polyomavirus

MDCK = Madin Darby Canine Kidney (cell line)

MHC = Major histocompatibility complex

MMP = Matrix metalloproteinase

mRNA= Messenger RNA

miRNA = Micro RNA

MPyV = Mouse polyomavirus

mT-ag = Middle T-antigen

MVB = Multivesicular body

NCCR = Non coding control region

NK-cell = Natural killer cell

NSCLC = Non-small cell lung cancer

Ori = Origin of replication

OSF-2 = Osteoblast specific factor 2

PAGE = Polyacrylamide gel electrophoresis

PI3K = Phospoinositide-3-kinase

PLCγ = Phospholipase Cγ

PP2A = Holoenzyme protein phosphatase 2A

pRb = Retinoblastoma protein

RRP = Receptor related protein

RT = Room temperature

SDS = sodium dodecyl sulphate

siRNA = Small interfering RNA

st-ag = Small t-antigen

ssDNA = Single stranded DNA

SV40 = Simian virus 40

TBP = TATA binding protein

TCA= Trichloric acid

TCR = Transcription control region

TGF-β =Transforming growth factor-β

THBS1= Thrombospondin type 1

TNF-α = Tumour necrosis factor-α

TRAIL= tumour necrosis factor-related apoptosis-inducing ligand

TSG = Tumour susceptibility gene

VEGF = Vascular endothelial growth factor

1. Introduction

1.1. Merkel cells

Merkel cells are specialized cells in the skin that may function as mechanoreceptors with importance in two-point discrimination, and were first described by Friedrich Sigmund Merkel in 1975. Merkel cells are large, pale cells with lobulated nuclei that are located in the basal layer of the epidermis in close proximity to terminal endings of myelinated nerve fibres. They are abundant in sensitive areas of the skin and mucosal areas derived from the ectoderm (Halata, Grim, & Bauman, 2003). Even though the exact function of Merkel cells is unknown, it is clear that they are required for the characteristic neurophysiological response of Merkel cell-neurite complexes after exposure to mechanical stimuli. Merkel cell-neurite complexes are touch receptors composed of sensory afferent nerves and Merkel cells, and it has been demonstrated that mice lacking Merkel cells in their foot pads completely lack the neurophysiologic responses normally observed (Maricich, Wellnitz, Nelson et al., 2009). It is currently debated whether Merkel cells are derived from the neural crest or if they are of epidermal origin. Grim and Halata demonstrated that avian Merkel cells are of neural crest origin using chick/quail transplantation experiments (Grim & Halata, 2000; Halata, Grim, & Christ, 1990). Szeder et al. (2003) similarly concluded that Merkel cells descend from the neural crest, as they express β-galactosidase. This conclusion was drawn based on the knowledge that Wnt1 expression during embryogenesis is transient and limited to neural crest cells and some central nervous system cells. They used double transgenic Wnt1-cre/R26R mice, in which neural crest cells and their derivatives are marked. The Wnt1 promoter controls the expression of cre recombinase in Wnt1-cre mice. In R26R mice, cre induces the expression of β-galactosidase. Thus, the transient expression of cre recombinase under the control of the Wnt1 promoter in double transgenic mice activates expression of R26R-derived β-galactosidase in neural crest cells (Szeder, Grim, Halata et al., 2003). Morrison and colleagues, however, found conclusive evidence for an epidermal origin in their 2009 study. They selectively knocked out the gene *Atoh1* (necessary for the development of Merkel cells) from both neural crest cells and skin cells, and found that selective deletion of *Atoh1* from the neural crest and its derivatives had no effect on the Merkel cell population, while deletion in the epidermal lineage resulted in an absence of Merkel cells in the skin (Morrison, Miesegaes, Lumpkin et al., 2009). Likewise, Van Keymeulen et al. found that conditional deletion of

Atoh1/Math1 in the embryonic epidermis resulted in the absence of Merkel cells at all body locations (Van Keymeulen, Mascre, Youseff et al., 2009). Immunohistochemical detection of Cytokeratin 20 (CK20) is often used as a specific marker for Merkel cells. Moll et al. demonstrated that it could be used to identify Merkel cells in normal squamous epithelia of humans, pigs, and mice (Moll, Kuhn, & Moll, 1995). Since the most prevalent Merkel cell marker is an epithelial marker, Merkel cells are often thought of as modified keratinocytes. However, low molecular mass cytokeratins have also been detected in other non-epithelial cells, such as glial cells. Hence, the expression of cytokeratins does not necessarily mean that Merkel cells are of epidermal origin (Grim & Halata, 2000). General markers of neuroendocrine cells, such as neuron-specific enolase, protein gene product 9.5, synaptophysin, and chromogranin A, have also been used to identify Merkel cells immunohistochemically (Halata et al., 2003).

1.2. Merkel cell carcinoma

Merkel cell carcinoma (MCC) is a rare, aggressive neuroendocrine form of skin cancer with rising incidence and a high mortality rate (Albores-Saavedra, Batich, Chable-Montero et al., 2010; Lemos & Nghiem, 2007). While MCC treatment is effective at early stages of the disease and survival rate quite high in patients with local disease (64 % at five years), the five year relative survival rate of patients with lymph node metastasis is 39 %, and only 18 % for those individuals with distant metastases (Lemos & Nghiem, 2007). Toker et al. initially described the cancer in 1972, as a trabecular cancer of the dermis with high risk of lymphoid metastasis (Toker, 1972). Elderly people with fair skin, people exposed to excessive UV-radiation or immuno-compromised patients are most susceptible to the cancer. The most common primary site is in the head and neck region with 45 % of the cases, and the onset of the disease often occurs at more than 50 years of age. The disease appears more often in men than in women, with men comprising 61 % of the cases (Lemos & Nghiem, 2007). Merkel cell polyomavirus (MCPyV) is the only known polyomavirus that is directly linked to a human cancer (Liu, Yang, Payne et al., 2016; Moens, Rasheed, Abdulsalam et al., 2015). MCPyV DNA is clonally integrated in 80 % of the MCC tumours and continuous expression of MCPyV oncogenes is required for MCC tumour cell survival, suggesting that that the virus could be a causative agent in MCC tumour initiation and progression (Feng, Shuda, Chang et al., 2008; Houben, Shuda, Weinkam et al., 2010; Nghiem, Bhatia, Lipson et al., 2016; Van

Ghelue & Moens, 2011). MCC tumour cells share several markers with normal Merkel cells, and the disease is diagnosed based on histological analysis combined with positive immunohistochemical staining for CK20, Cam 5.2 and CD56 as well as neuroendocrine markers such as chromogranin A, synaptophysin and neuron specific enolase (Heymann, 2008).

1.3. Human polyomaviruses and MCPyV

Polyomaviruses are a family of non-enveloped viruses with a circular double stranded DNA (dsDNA) genome of approximately 5,000 bp. They infect fish, birds and mammals (Calvignac-Spencer, Feltkamp, Daugherty et al., 2016), while polyomavirus sequences but not virus particles have been detected in amphibians, reptiles and some invertebrates (Buck, Van Doorslaer, Peretti et al., 2016). The viral genome contains the origin of replication and transcription regulatory elements, as well as the early and late coding regions. Polyomavirus replication origins contain a central region, referred to as site 1/2 in murine polyomavirus (MPyV) and site II in JC polyomavirus (JCPyV) and BK polyomavirus (BKPyV). Repeated pentameric 5'-G(A/G)GGC-3' sequences are recognised by the early gene large T-antigen (LT-ag) in order to start viral replication. However, the amount of repeats and the spacing between them varies between the polyomavirus family members (Figure 1) (Harrison, Meinke, Kwun et al., 2011).

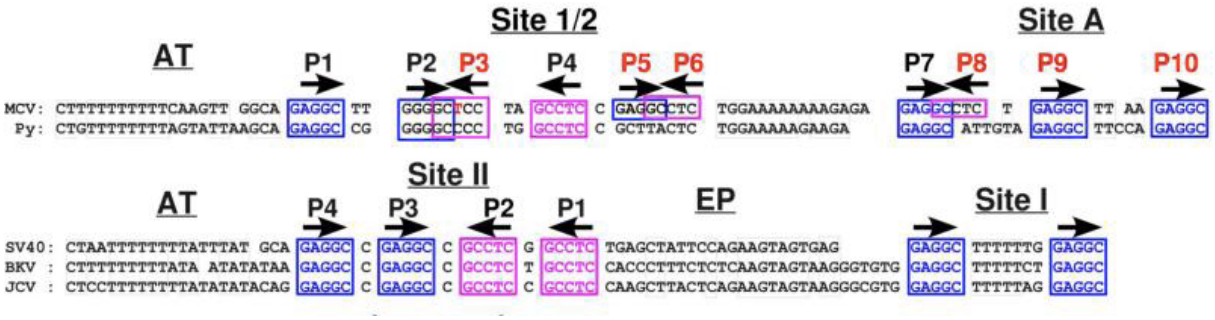

Figure 1. The pentameric LT-ag binding sites are illustrated for MCPyV (MCV in the figure) and MPyV (Py) and for SV40, BKPyV (BKV) and JCPyV (JCV) respectively. G(A/G)GGC repeats are boxed in blue and the inverse complement, GCCTC, in pink. EP = early palindromic region and AT = AT rich region. For MCPyV and MPyV three pentameric sequences P1, P2 and P4 of site ½ and P7 from site A is necessary for viral replication. All pentameric sequences in site II are involved in viral replication, but the site I sequences is not required for *in vitro* replication. The figure is modified from Figure 1 in Harrison et al 2011 (Harrison et al., 2011).

The genes of the early region (T-antigens) are expressed in the early phase of infection before viral DNA replication and encode regulatory proteins crucial for viral DNA replication. Different T-antigen proteins are created as a result of differential splicing of the common exon 1 sequences on the T-antigen locus. LT-ag and small t-antigen (st-ag) of polyomaviruses have received most attention in cancer studies because of their potential to transform cells and induce tumours in animal models (Moens, Van Ghelue, & Johannessen, 2007). These viral proteins are also thought to be the main drives of oncogenesis in MCC (Wendzicki, Moore, & Chang, 2015). Other early proteins include Middle T-antigen (mT-Ag) that is present in some polyomaviruses but not in MCPyV, and 17-kT-antigen that is present in Simian virus (SV40) (Chang & Moore, 2012). The late region of the polyomavirus genome is transcribed after the onset of viral replication and encodes the capsid proteins VP1 and VP2 and sometimes VP3. The VP1 and VP2 proteins are derived from alternatively spliced transcripts, while VP3 is translated from an internal ATG start codon in the VP2 mRNA (DeCaprio & Garcea, 2013). SV40 and several other polyomaviruses also encode a small agnoprotein that is important for viral replication and release (Saribas, Coric, Hamazaspyan et al., 2016). The non-coding control region (NCCR) consisting of origin of replication and transcription control region controls viral DNA replication and transcription of the early and late genes. It is located between the early and late region (Figure 2) (Moens & Johannessen, 2008).

In accordance with other polyomaviruses, the MCPyV genome consists of 5,387 bp, and is divided into early and late coding regions separated by a NCCR. The MCPyV early region encodes LT-ag, st-ag and 57-kT, while the late region encodes VP1 and VP2 all of which are expressed after the onset of viral DNA replication (Chang & Moore, 2012). However, no agnoprotein open reading frame seems to be present in the MCPyV genome (Chang & Moore, 2012). More recently, an alternative open reading frame (ALTO) has also been detected in the MCPyV genome. ALTO shares some sequence features with mT-Ag of other polyomaviruses, but its function largely remains unknown. However, its absence does not seem to affect viral replication (Carter, Daugherty, Qi et al., 2013). One single precursor miRNA that produces two mature miRNAs, termed mcv-miR-M1-5p and -3p, has also been detected in the MCPyV genome (Seo, Chen, & Sullivan, 2009; Theiss, Günther, Alawi et al., 2015). Theiss et al. showed that this miRNA binds to the early transcripts and negatively affects LT-ag expression to the extent that it limits MCPyV genome replication. Furthermore, they showed that MCPyV-miR-M1 causes prolonged episomal persistence of MCPyV genomes. This in turn may increase the overall chances of integration events that are very low

in natural infection yet regarded as a prerequisite for MCPyV positive MCC (Theiss et al., 2015).

The cells in which MCPyV replicate are not known, but skin keratinocytes, skin progenitor cells, or Merkel cells are likely candidates (Woo, Stumpfova, Jensen et al., 2010). A recent study by Liu et al. identified dermal fibroblasts as the preferred host for viral infection (Liu et al., 2016).

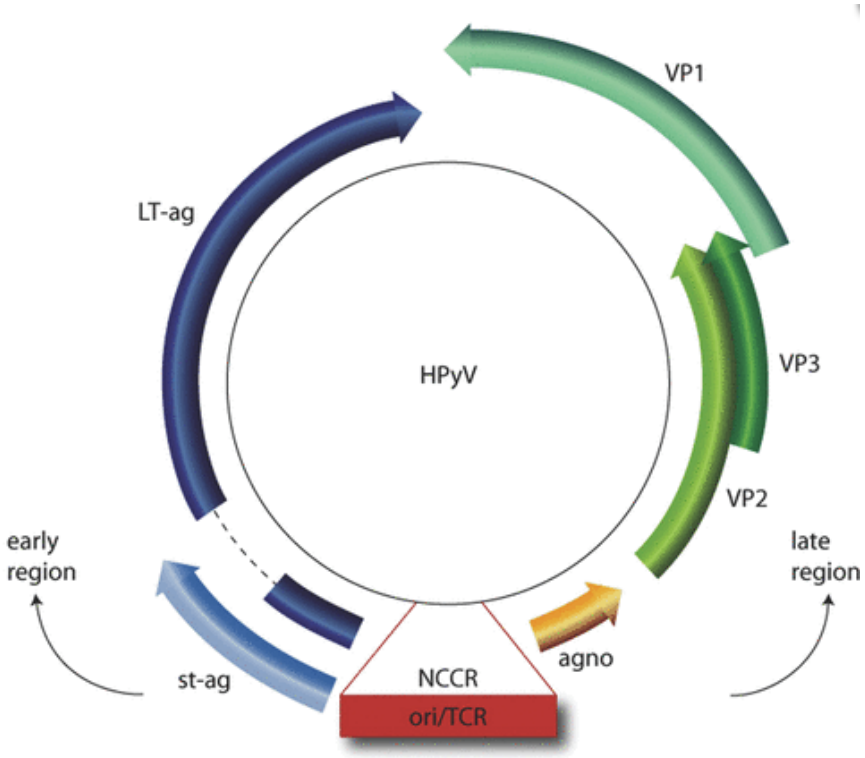

Figure 2.The polyomavirus genome consists of approximately 5,000 bp and can be divided into three functional regions. The proteins encoded by the early region are involved in viral DNA replication. The major early proteins are st-ag and LT-ag. The genes of the late region genes encode the capsid proteins VP1, VP2 and VP3. The noncoding control region (NCCR) consists of the origin of replication (ori) and the transcription control region (TCR) and is in charge of viral replication and expression of early and late genes. Used with permission from John Whiley and sons: *J Dtsch Dermatol Ges* (Moens & Johannessen, 2008).

1.4. MCPyV oncogenes

LT-ag is thought to be the main oncoprotein in MCPyV induced MCC, while st-ag is thought to have an auxiliary role (Houben et al., 2010; Van Ghelue & Moens, 2011; Wendzicki et al., 2015). Studies conducted on SV40 shows that LT-ag is essential for viral replication, as it

forms a complex with DNA polymerase/primase-α, replication protein A and topoisomerase. It also possesses helicase activity, allowing it to unwind the DNA-strands during replication. Furthermore, it can bind to the tumour suppressor proteins p53 and retinoblastoma (pRb), hence forcing the cells to replicate their DNA during S-phase of the cell cycle (Cheng, DeCaprio, Fluck et al., 2009; Van Ghelue & Moens, 2011). p53 is known as the guardian of the genome and is normally involved in DNA repair, repressing cell cycle proliferation, inhibiting angiogenesis and inducing apoptosis (Vousden & Lane, 2007). The main role of pRb is to prevent excessive cell division by inhibiting cell cycle progression until a cell is ready to divide (Alberts, Johnson, Lewis et al., 2008). LT-ag functions as a mitogen partly because it has a LXCXE motif that functions as a pRb pocket. Binding of LT-ag to pRb leads to activation of E2F and hence expression of E2F-responsive genes required for S-phase initiation and progression (Richards, Guastafierro, Shuda et al., 2015). In absence of LT-ag or other mitogenic factors (such as G1-cdk complexes) E2F-dependent gene expression and S-phase initiation is inhibited by retinoblastoma - E2F-interaction (Alberts et al., 2008). DnaJ is another LT-ag domain involved in regulating the pRb through inducing the intrinsic ATP-ase activity of heat shock protein 70 (Hsc70). The energy produced by DnaJ mediated hydrolysis of ATP is used to split pRb/E2F complexes, and hence induces viral replication, transactivation of viral promoters and viral assembly. The C-terminal domain of LT-ag can also bind the tumour suppressor p53 (Van Ghelue & Moens, 2011).

Alternative splicing of the T-antigen locus generates the st-ag protein. This protein shares approximately 80 N-terminal residues with LT-ag, and hence contains the DnaJ segment. Nevertheless, it lacks a pRb pocket making it irrelevant for E2F dependent gene activation. St-ag mainly exerts its effect through abrogating the catalytic activity in the holoenzyme protein phosphatase 2A (PP2A), that in turn can lead to altered signalling cascades, altered gene expression, inhibition of apoptosis/increased survival of the cells, changes in protein stability, stimulation of telomerase activity, disruption of the cytoskeleton and chromosome instability (Moens et al., 2007; Van Ghelue & Moens, 2011).

All MCC tumour tissues examined so far express a C-terminal truncated form of LT-ag due to a non-sense mutation (Freze Baez, Cirauqui Diaz, Baeta Cavalcanti et al., 2014; Schmitt, Wieland, Kreuter et al., 2012). However, the LXCXE pRb protein-family binding domain is retained (Richards et al., 2015). Shuda et al. investigated nine sequences derived from MCC tumours and found that all the sequences contained mutations that caused a truncated MCPyV

LT-ag helicase. This truncated form of LT-ag was not identified in control tissue. Further, they showed that the mutated LT-ag did not affect retinoblastoma tumour suppressor protein binding, but eliminated viral replication capacity. Hence, suggesting a selection for a truncated version of LT-ag in MCC, as autoactivation of integrated virus replication would ultimately cause cell lysis. Because this truncation in the LT-ag gene renders the virus replication-incompetent, it is implicated that the virus causes MCC and does not secondarily infect MCC tumours (Shuda, Feng, Kwun et al., 2008). So far, only integrated MCPyV DNA encoding truncated LT-ag has been found in MCC (Van Ghelue & Moens, 2011).

Houben et al. provided experimental evidence for LT-ag and st-ag's effect on virus positive MCC. In their study, they knocked down MCPyV T-antigen expression in virus-positive MCC cell lines by targeting the exon 1 of the T-antigen locus using short hairpin RNAs. The authors found that the three virus-positive MCC cell lines used in their study experienced growth arrest and/or cell death upon T-antigen knockdown, while the virus negative control cell line was unaffected by the inactivation. This implies that T-antigen expression is necessary for the maintenance of MCPyV-positive MCC, and that MCPyV is the infectious cause of MCPyV-positive MCC (Houben et al., 2010). Shuda et al. looked at st-ag's effect on MCC tumour progression. They found that knockdown of st-ag alone was sufficient to inhibit MCPyV positive cell growth. They also found that MCPyV st-ag differed from other polyomavirus st-ag's, as the transforming capacity was not linked to PP2A or heat shock protein–binding activities. They showed that MCPyV st-ag reduced turnover of a translation initiation inhibitor, hyperphosphorylated 4E-BP1, resulting in increased eIF4E activity important for translation initiation (Shuda, Kwun, Feng et al., 2011). Likewise, Kwun et al. also demonstrated an st-ag transforming mechanism not linked to the PP2A domain. The researchers identified the LT-Stabilization Domain (LSD) responsible for inhibiting the SCF^{Fbw7} E3 ubiquitin ligase. This ubiquitin ligase normally targets LT-ag and causes its degradation. Hence, st-ag has a supportive role leading to increased LT-ag levels in the cell and enhanced viral replication (Kwun, Shuda, Feng et al., 2013). *In vivo* studies have also confirmed the oncogenic potential of LT-ag and st-ag. For example, Spurgeon and colleagues investigated LT-ag and st-ag's oncogenic activity in a transgenic mouse study and found that MCPyV T antigen expression in the stratified epithelium induces both histological and molecular changes consistent with neoplastic progression (Spurgeon, Cheng, Bronson et al., 2015). Verhagen et al. also used transgenic mice and found that st-ag functions as an oncogenic driver in MCC. They demonstrated that expression of MCPyV st-ag alone is

sufficient for rapid neoplastic transformation *in vivo*. Furthermore, they found that this transforming activity was linked to the Fbxw7 binding domain of st-ag and not the PP2A tumour suppressor complex (Verhaegen, Mangelberger, Harms et al., 2015). Shuda et al. used transgenic mice manipulated to express MCPyV st-ag in response to tamoxifen administration, and demonstrated that high expression of st-ag was in fact lethal for the mice. Lower doses of tamoxifen caused dermal and epidermal hyperplasia in ear tissue of the mice. The researchers also showed that a p53 null setting caused MCPyV st-ag transgenic mice to develop tumours (Shuda, Guastafierro, Geng et al., 2015).

1.5. Exosomes

Exosomes are small membranous vesicles (30–150 nm in diameter) of endocytic origin (Beach, Zhang, Ratajczak et al., 2014; Yu, Cao, Shen et al., 2015). They were initially considered to be involved in garbage disposal (Johnstone, Bianchini, & Teng, 1989). However, more recent experiments have revealed that exosomes are important mediators for intracellular communication and subject to specific sorting mechanisms under both normal and pathophysiological conditions, like cancer (Beach et al., 2014). Increasing evidence suggests that exosomes are important in tumour growth and progression, cancer metastasis, avoiding apoptosis and providing drug resistance (Al-Nedawi, Meehan, Micallef et al., 2008; Azmi, Bao, & Sarkar, 2013). Moreover, it has been shown that exosomes derived from virus-infected cells, including the human tumour viruses Hepatitis C-virus (HCV), Epstein- Barr virus (EBV) and Kaposi's sarcoma associated herpes virus (KSHV), can contain both functional viral proteins and nucleic acids that can aid oncogenesis. It has also been suggested that non-enveloped viruses deploy exosomes for infecting cells and immune system avoidance (Meckes, 2015).

Exosomes are created when intraluminal vesicles (ILVs) are formed by inward budding of the endosomal membrane. These ILVs then cluster together to generate multivesicular bodies that fuse with the plasma membrane, and release their content as exosomes in the extracellular compartment (Figure 3) (Mathivanan, Ji, & Simpson, 2010; Soung, Nguyen, Cao et al., 2016; Yu et al., 2015).

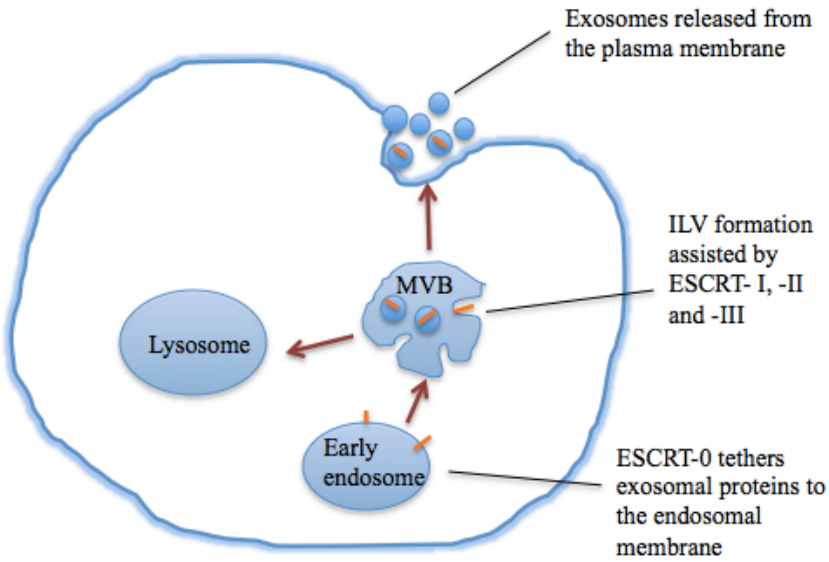

Figure 3. The endosomal sorting complexes required for transport (ESCRT) plays a crucial role in the formation of ILVs .The ESCRT complex is composed of ESCRT-0, -I, -II and -III. ESCRT-0 helps cluster and attach ubiquitinated proteins to the endosomal membrane. The proteins are then absorbed into the endosome via direct budding into the lumen to form an ILV by the aid of ESCRT-I and -II. Finally, ESCRT-III pinches of the vesicle by forming a ring-like structure around the vesicles (Hewson & Morris, 2016; Soung et al., 2016). The MVBs are either transported to the lysosome for proteolytic degradation or to the plasma membrane where the ILVs are released as exosomes when the MVBs fuse with the plasma membrane, depending on the subsets of ILVs (Mathivanan et al., 2010; Soung et al., 2016).

Exosomal vesicles can contain proteins, lipids, mRNAs, long non-coding RNAs (lncRNAs), microRNAs (miRNAs) as well as viral genes, transcripts and protein and even prion genes (Figure 4), that can be transferred to target cells (De Toro, Herschlik, Waldner et al., 2015; Yu et al., 2015; Zhang, Yuan, Shi et al., 2015). The exosomal lipid content reflects both the lipid content of the plasma membrane, and the endosomal compartments of the cell of origin. The lipids provide the exosomes with both structural integrity and take part in cell-cell communication (Azmi et al., 2013). The protein content of exosomes mainly consists of membrane proteins derived from endosomes, cytoplasm or the plasma membrane. Canonical exosomal proteins are often involved in intracellular membrane fusions and transport, as well as multivesicular body biogenesis (Soung et al., 2016). Exosomal proteins involved in membrane fusion and transport include Rab GTPases, annexin and flotilin, while the tumour susceptibility gene proteins TSG101 and Alix are involved in multivesicular body biogenesis and endosomal sorting. Membrane associated proteins like tetraspanins (CD9, CD63, CD81 and CD82) and cytoplasmic proteins such as the heat shock proteins Hsp60, Hsp70 and

Hsp90 are frequently used as exosomal markers, as they are highly conserved (Azmi et al., 2013; De Toro et al., 2015; Soung et al., 2016; Yu et al., 2015). The assortment of exosome-derived proteins is also cell type specific, depending on the cell of origin (Soung et al., 2016; Zhang et al., 2015). Moreover, cancer exosomes contain cancer antigens that can elicit immune responses, as well as various nucleic acids including mRNA, miRNA and lncRNA that can alter the gene expression in recipient cells and aid an oncogenic transformation (De Toro et al., 2015; Yu et al., 2015).

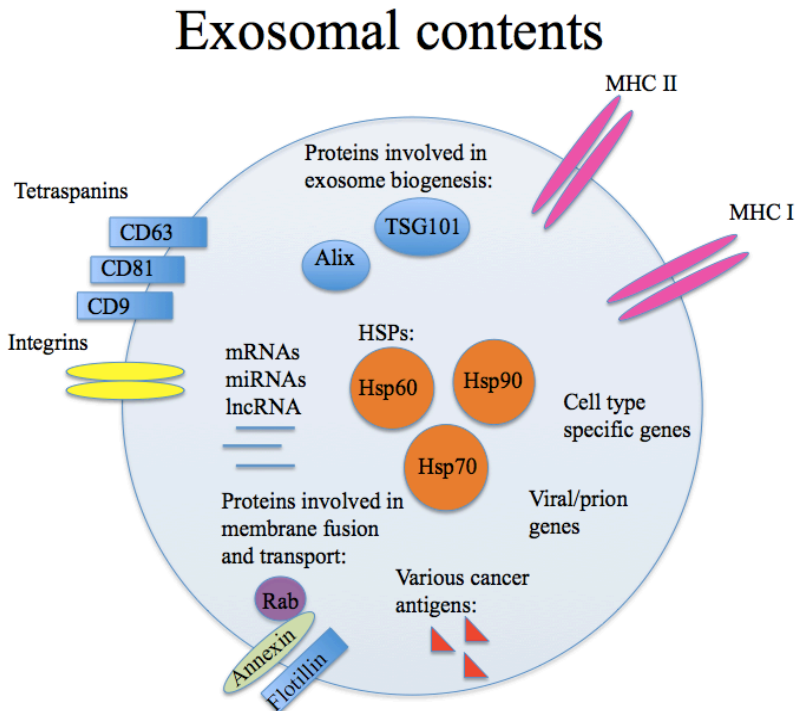

Figure 4. Exosomal contents. Exosomes are small membranous particles involved in cell-cell communication. Typically they contain various proteins involved in membrane fusion and transport as well as exosome biogenesis. Several membrane proteins such as tetraspanins and integrins as well as major histocompatibility complexes (MHC) type I and II molecules can be located on the exosomal membrane (Thery, Ostrowski, & Segura, 2009; Yu et al., 2015). Heat shock proteins (HSPs), cell type specific proteins, mRNAS, miRNAs, lncRNAs, various cancer antigens and viral genes, transcripts and proteins are also frequently found in exosomes (Yu et al., 2015).

1.6. Exosomes - mediators of cell-cell communication under normal and pathophysiological conditions

The exact biological function of exosomes is not known. However, it is believed that exosomes are important mediators of cell-cell communication and that they elicit an important

role in the immune system (De Toro et al., 2015).

The belief that extracellular vesicles act as paracrine or endocrine effectors both under normal and diseased conditions is based on evidence showing that they can transport bioactive molecules to both neighbouring cells and to cells at a different location via the endocrine system (Zhang & Grizzle, 2014). For example argosomes, microvesicles derived from endosomes that closely resemble exosomes, are important mediators of morphogens during early development of the embryo. Greco et al. demonstrated in their study that argosomes enabled the spread of Wingless in drosophila imaginal disc epithelium, and thus caused tissue development and differentiation (Greco, Hannus, & Eaton, 2001). The authors proposed two potential mechanisms of argosome transfer from one cell to another. It is uncertain whether these argosomes are transferred from one cell to another in the same way as exosomes (where multivesicular bodies are formed and released outside the cell) or whether they are directly internalized by the adjacent cells in a manner reminiscent of that used by *Listeria* to spread through sheets of Madin-Darby Canine Kidney (MDCK) epithelial cells or the endocytosis of transmembrane ligands observed for Boss/Sevenless or Delta/Notch signalling (Greco et al., 2001). Nevertheless, the study demonstrated that microvesicles are used to transfer specific information from one cell to another. Likewise, a study by Gross et al. showed that Wnts, a family of ligands that function as important morphogens during development, are secreted in exosomes both during *Drosophila* development and in human cells. Their study revealed that exosomes carry Wnts on their surface and induce Wnt signalling activity in target cells (Gross, Chaudhary, Bartscherer et al., 2012).

It has also been demonstrated that exosomes derived from cancer cells transfer various nucleic acids and oncogenic proteins to adjacent cells or to anatomically distant sites. The exosomal content can aid and even direct oncogenesis, by inducing signalling pathways or directly alter the phenotype of specified recipient cells aiding an oncogenic transformation (Hoshino, Costa-Silva, Shen et al., 2015; Wendler, Favicchio, Simon et al., 2017). Al Nevadi et al. found that a truncated oncogenic form of the EGF-receptor was transported in exosomes from glioma cells to distally located cells lacking the mutated receptor. The transfer of the truncated receptor leads to constitutive activation of the mitogen-activated protein kinase (MAPK) and Akt signalling pathways, thereby stimulating cancer progression and invasiveness (Al-Nedawi et al., 2008). Moreover, Luga et al. found that exosomes secreted from fibroblasts promote motility and protrusive activity in breast cancer cells via Wnt-planar cell polarity signalling (Luga, Zhang, Viloria-Petit et al., 2012). Hood and colleagues

demonstrated, in their *in vivo* study, that melanoma exosomes showed a prominent homing to sentinel lymph nodes when compared with artificial liposomes of similar size (Hood, San, & Wickline, 2011). It has also been demonstrated that the exosomal integrin expression patterns determines the sites of metastasis in an organ specific manner. It was established by Hoshino et al. that tumour-derived exosomes prepare a favourable microenvironment at future metastatic sites and mediate metastasis in a non-random fashion. They found that exosomal integrins ITG$\alpha_6\beta_4$ and ITG$\alpha_6\beta_1$ mediate lung tropism, whereas exosomal integrin ITG$\alpha_v\beta_5$ is associated with liver metastasis (Hoshino et al., 2015). This study implies that specific integrin combinations on exosomes contribute to organ specific metastasis, and hence could be used as a prognostic marker to predict future metastasis. Furthermore, tumorigenic viruses such as EBV and KSHV can manipulate the content of exosomes and lead to activation of cell signalling pathways and activation of the surrounding stroma. For example, Meckes et al. found that exosomes derived from EBV-infected cells may manipulate the tumour microenvironment to influence the growth of neighbouring cells through the intercellular transfer of viral Latent Membrane Protein 1 (LMP1), signalling molecules, and viral miRNAs (Meckes, Shair, Marquitz et al., 2010). The cancer exosomes caused activation of the ERK and AKT signalling pathways in recipient cells through transfer of EGFR, which is induced by LMP1. The increased amount of miRNA detected in cancer exosomes implies that some of the viral miRNAs may be selectively packed into exosomes (Meckes et al., 2010). In a follow up study Meckes et al. investigated the proteome of exosomes derived from B-cells infected with EBV and KSHV or both, and compared the content to uninfected cells (Meckes, Gunawardena, Dekroon et al., 2013). They found that the proteome of exosomes derived from virus-infected cells was markedly different from the exosomes produced by the uninfected B-cell control exosomes. The differing content indicated that exosomes derived from both EBV and KSHV likely have an impact on cell death and survival, ribosome function, protein synthesis, and mammalian target of rapamycin signalling. Exosomes produced by KSHV positive cells were found to particularly affect cellular metabolism, while exosomes from EBV infected cells were found to activate cell-signalling pathways through integrins, actin, interferon (IFN), and NFκB. The specific proteome identified in exosomes from virus-positive cells suggests that the oncogenic viruses use exosomes to modulate the tumour microenvironment. Hence, the specific proteins could be used as diagnostic markers for EBV and KSHV associated malignancies (Meckes et al., 2013). Cancer exosomes have also been found to affect the development of stromal cells like myofibroblasts or cancer associated fibroblasts (Wendler et al., 2017). For instance, Webber et al. found that cancer-derived

exosomes expressing TGF-β in association with the transmembrane proteoglycan betaglycan on their surface could trigger (among other changes) elevated α-smooth muscle actin expression consistent with the process of fibroblast differentiation into myofibroblasts. They demonstrated that the TGF-β - betaglycan complex induced downstream SMAD signalling (Webber, Steadman, Mason et al., 2010). Moreover, exosomes released from cells undertaking an Epithelial to Mesenchymal Transition (EMT) can aid oncogenesis. Gopal et al. provide evidence for the first time that exosomes derived from cancer cells undergoing different stages of EMT induced angiogenesis in recipient endothelial cells *in vitro* and *in vivo* through transfer of the known angiogenic proteins Rac1/PAK2. The ability to induce angiogenesis increased with the EMT spectrum of the cells (Gopal, Greening, Hanssen et al., 2016).

These studies imply that exosomes and other extracellular vesicles are able to reprogram the cellular metabolism and change cellular interactions. Several types of RNAs including mRNAs, miRNAs and lncRNAs are also transported between cells in exosomes, leading to a genetic reprogramming in the recipient cells (Kosaka, Yoshioka, Fujita et al., 2016; Zhang et al., 2015). Furthermore, exosomes have proved to prolong the half-life of various RNA species in circulation, and the transported mRNAs, miRNAs or lncRNAs are functional in the recipient cells (Yu et al., 2015). Especially miRNAs have been connected to cancer initiation, invasion, metastasis and recurrence, as well as drug resistance (Kosaka et al., 2016; Melo, Sugimoto, O'Connell et al., 2014). For example, Zhuang et al. found that the exosomal miR-9 from cancer cells promotes endothelial proliferation and angiogenesis (Zhuang, Wu, Jiang et al., 2012). Another angiogenic miRNA, mir210, that is secreted by exosomes was also found to promote angiogenesis and metastasis and to influence the microenvironment in favour of cancer progression (Kosaka, Iguchi, Hagiwara et al., 2013). Moreover, miRNA from cancer exosomes have been connected to drug resistance and expulsion. For example, ΔNp73 miRNA was enriched in tumour-derived exosomes, suggesting that it is actively sorted into tumour exosomes. What the authors did was overexpress this miRNA in a colon cell line (HCT116) and then they observed that ΔNp73 ended up in the exosomes. They also found that this miRNA was higher in plasma exosomes from cancer patients than normal controls The team of researchers reported that the transfer of exosome cargo to various cell types led to increased proliferative abilities and drug resistance in the acceptor cells. They also concluded that ΔNp73 had a prognostic value for colon cancer patients (Soldevilla, Rodriguez, San Millan et al., 2014).

1.7. Exosomes unambiguous role in the immune system

Several studies have confirmed that exosomes derived from professional antigen presenting cells (APCs), such as dendritic cells (DCs) and B-lymphocytes, express peptide MHC-I and MHC-II complexes as well as co-stimulatory molecule, allowing them to directly activate both $CD4^+$ and $CD8^+$ T-cell responses (Thery et al., 2009). Because of this, several studies have attempted to determine cancer exosomes potential in cell free anti-cancer vaccines. The concept behind a cell based cancer vaccine is to generate and culture *ex vivo* DCs derived from a mouse or a patient and pulse them with cancer antigens before the DCs are injected into the subject again to stimulate antigen-specific T-cells *in vivo*. In a cell free anti-cancer vaccine exosomes are isolated from for example DCs pulsed with cancer antigens and injected into the mouse or patient again (Kunigelis & Graner, 2015). Raposo et al. showed that exosomes derived from both human and murine B-lymphocytes induced antigen-specific MHC class II-restricted T-cell responses *in vitro* (Raposo, Nijman, Stoorvogel et al., 1996). Zitvogel et al. demonstrated that exosomes produced by DCs express MHC-I and MHC-II molecules in addition to costimulatory molecule B-7. They showed that injection of DC-derived exosomes containing peptide MHC-I and MHC-II complexes as well as co-stimulatory molecule led to tumour regression in a murine model, caused by activation of $CD8^+$ and $CD4^+$ T-cells respectively (Zitvogel, Regnault, Lozier et al., 1998). A study by Thery et al. revealed that the main mechanism used by cancer-derived exosomes is indirect activation of T-cells, where DCs use exosomes as an exogenous source of antigen (Thery, Duban, Segura et al., 2002). Similarly, Vincent-Schneider et al. found that exosomes bearing MHC-II molecules need DCs to effectively initiate a specific T-cell response (Vincent-Schneider, Stumptner-Cuvelette, Lankar et al., 2002). Such a mechanism may increase the number of DCs displaying a specific peptide, and hence cause stronger immunogenicity. Zeelenberg et al. showed that exosome bound cancer antigens caused more efficient tumour regression than soluble antibodies in a murine fibrosarcoma model. They also tested the membrane bound and the soluble form of the antigen in DNA vaccination protocols, and found that the vesicle bound antigen induced stronger delay in tumour growth than the soluble antigen form (Zeelenberg, Ostrowski, Krumeich et al., 2008). A phase I clinical trial conducted by Dai et al. found that exosomes derived from ascites could induce anti-tumour immunity in colorectal cancer patients (Dai, Wei, Wu et al., 2008).

However, these promising results *in vitro* and in murine models have not proved to be transmittable to all clinical trials. A clinical I trial undertaken by Escudier et al. showed that

no significant increase in T-cell responses could be detected when metastatic melanoma patients were vaccinated with autologous DC-derived exosomes. However, they observed enhanced NK-cell effector functions following exosome exposure. Thus, it was assumed that exosomes could induce anti-tumour responses by acting on other MHC unrestricted immune effector cells (Escudier, Dorval, Chaput et al., 2005). A later clinical trial showed that DC-derived exosomes directly enhanced natural killer-cell (NK-cell) number in 7 out of 14 patients (Chaput, Flament, Viaud et al., 2006). Immune activating functions in tumour exosomes have been reported mainly in relation to cancer cells exposed to stress. Stressed cancer cells often secrete exosomes with Hsps on their surface, and the Hsps induce NK-cell activation and induce macrophages to secrete TNF-α that induces inflammation and inhibits tumourigenesis (Lv, Wan, Lin et al., 2012; Thery et al., 2009).

Despite the antigenic properties of tumour exosomes, substantial evidence suggests that exosomes play an important role in immune evasion, mostly by antigen-independent mechanisms (Yang, Kim, Bianco et al., 2011). In fact, considerable evidence shows that exosomes aid immune evasion (Huber, Fais, Iero et al., 2005; Liu, Yu, Zinn et al., 2006; Naito, Yoshioka, Yamamoto et al., 2017; Yu et al., 2015). Tumour-derived exosomes have been connected to the function of effector T-cells and NK-cells, as well as the inhibition of DC maturation. Human colorectal cancer cells induce T-cell apoptosis through the release of exosomes containing Fas ligand and tumour necrosis factor-related apoptosis-inducing ligand (TRAIL), and thus evade the immune system (Huber et al., 2005). A study undertaken by Liu et al. demonstrated that treatment with tumour exosomes caused increased tumour growth in both BALB/C and nude mice. Furthermore, they found that the cytotoxic activity performed by NK-cells was inhibited due to exposure to tumour-derived exosomes (Liu et al., 2006). Lundholm et al. also found that NK and $CD8^+$ T-cells showed impaired cytotoxic abilities after exposure to prostate tumour derived exosomes (Lundholm, Schröder, Nagaeva et al., 2014). In a murine model, Yu et al. found that exosomes block the differentiation of myeloid precursor cells into DCs *in vitro* (Yu, Liu, Su et al., 2007). Pilzer and Fishelson demonstrated that cancer cells avoid lysis mediated by the complement system by removing the membrane attack complex (MAC) by exosome vesiculation induced by mortalin (Pilzer & Fishelson, 2005). These immune evasive properties raise concerns about the use of exosomes as anti-tumour vaccines. Furthermore, anti-cancer therapies can also be subject to exosomal efflux, leading to lower drug concentrations in the cell interior (Azmi et al., 2013). The various functions of exosomes are summarised in Figure 5.

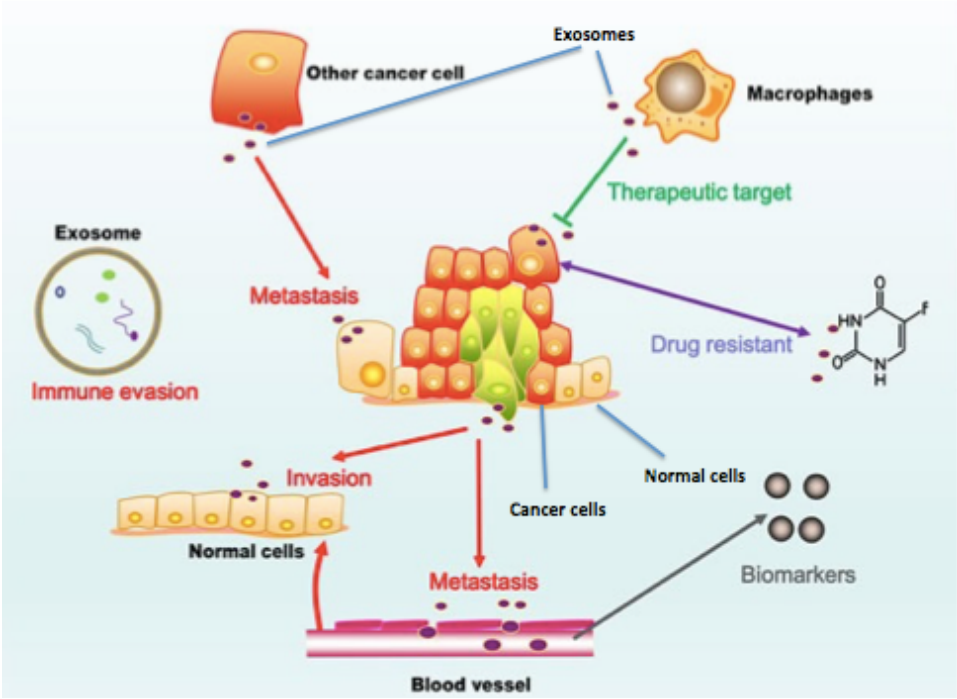

Figure 5. The role of exosomes in tumourigenesis and cancer therapy. Tumour promoting activities like metastasis, invasion, immune evasion and drug resistance, as well as exosomes potential role as cancer biomarkers, their use in anticancer vaccines and drug transport vehicles are illustrated. Modified from figure 2 in Wu et al. 2016 (Wu, Zeng, Cao et al., 2016).

1.8. Periostin

Periostin or osteoblast-specific factor 2 (OSF-2) is a 90 kDa secreted matricellular protein. The matricellular proteins are located in the extracellular matrix without playing a primarily structural role in this location (Liu, Zheng, & Ouyang, 2014), and often function as adaptors or modulators of interactions between cells and their extracellular microenvironment (Wang, Xiong, Mao et al., 2016). Periostin was first identified in a mouse osteoblast cell line as a cell adhesion protein with importance for bone formation, and it has high homology with the insect protein fascilin 1 (Takeshita, Kikuno, Tezuka et al., 1993). Six different isoforms of the protein, caused by different splicing in the C-terminal domain, have been identified (Morra, Rechsteiner, Casagrande et al., 2012). The protein is involved in extracellular matrix formation, cell migration and wound healing, and therefore it is also involved in various pathophysiological conditions, including fibrosis, arthritis, atherosclerosis and other inflammatory diseases, as well as tumourigenesis and metastasis (Liu et al., 2014; Mosher, Johansson, Gillis et al., 2015; Wu, Chen, Xie et al., 2016). Periostin is up-regulated in several human cancers such as non-small-cell lung carcinoma (NSCLC), breast cancer, colon cancer,

head and neck cancer, ovarian cancer, pancreatic cancer and neuroblastoma (Bao, Ouyang, Bai et al., 2004; Baril, Gangeswaran, Mahon et al., 2007; Erkan, Kleeff, Gorbachevski et al., 2007; Gillan, Matei, Fishman et al., 2002; Kudo, Ogawa, Kitajima et al., 2006; Morra et al., 2012; Ruan, Bao, & Ouyang, 2009; Sasaki, Sato, Kondo et al., 2002; Shao, Bao, Bai et al., 2004). Periostin up-regulation in cancer promotes tumour invasion and metastasis via EMT (Hu, Tong, Zhao et al., 2015). Hu et al. showed that periostin overexpression promoted increased cell proliferation, invasion, and migration in prostate cancer cells. It was also demonstrated that EMT markers were up-regulated in response to periostin exposure (Hu et al., 2015). Gillan and colleagues found that periostin increased ovarian epithelial cells invasive properties by promoting $\alpha_V\beta_3$ or $\alpha_V\beta_5$ integrin-dependent adhesion and migration (Gillan et al., 2002). Furthermore, several studies have showed that periostin primes the surrounding stroma for future metastasis, by creating a tumour supporting microenvironment (Erkan et al., 2007; Fukuda, Sugihara, Ohta et al., 2015; Wang et al., 2016; Wu, Luo, & Ouyang, 2015). Aberrant periostin expression has also been found to affect various signalling pathways leading to induction of angiogenesis (Shao et al., 2004) and promotion of cell survival (Bao et al., 2004). Due to periostin's prominent role in cancer progression and metastasis and its up-regulation in several cancers, the protein is a potential prognostic biomarker.

1.9. Thrombospondin

Thrombospondin (THBS1), a 450 kDa homotrimeric protein that consists of three disulfide-linked 142 kDa chains, is another matricellular protein that plays multiple roles in cell-matrix and cell-cell interactions (Huang, Wang, Liu et al., 2017; Lawler, Slayter, & Coligan, 1978). The protein is secreted from blood platelets in response to thrombin and was first isolated from blood platelets in 1978 (Lawler et al., 1978). Its main role is assumed to be in negative control of angiogenesis, and it was the first angiogenic inhibitor to be identified (Good, Polverini, Rastinejad et al., 1990; Mirochnik, Kwiatek, & Volpert, 2008). Thrombospondin inhibits angiogenesis by antagonizing the effect of Vascular Endothelial Growth Factor (VEGF), and has effects on endothelial cell migration, proliferation, survival and apoptosis (Lawler & Lawler, 2012). Results by Gupta et al. suggest that THBS1 inhibits angiogenesis by at least two mechanisms: Firstly, it binds directly to VEGF and mediates the uptake and clearance of VEGF from the extracellular space. Secondly, it binds heparin with stronger

affinity than VEGF. The researchers also found that the heparin binding domain of VEGF was responsible for about 35 % of its mitogenic activity (Gupta, Gupta, Wild et al., 1999). Wang et al. demonstrated that the N-terminal domain of THBS1 mediates binding to heparin sulphates as well as the endocytic receptor low-density receptor-related protein (LRP). The binding of heparin sulphates is necessary for LRP mediated endocytosis and clearance of thrombospondin and associated proteins like for example matrix metalloproteinases (MMPs) and VEGF (Wang, Herndon, Ranganathan et al., 2004). Thrombospondin binds with high affinity to fibroblast growth factor-2 (FGF-2) that possesses angiogenic properties, and therefore limits its bioavailability and activity (Margosio, Rusnati, Bonezzi et al., 2008). In a transgenic mouse study where THBS1 was either overexpressed or knocked out, Rodriguez-Manzaneque et al. found that the tumour burden and vasculature were significantly increased in THBS1-deficient animals and that mice overexpressing THBS1 showed delayed tumour growth. They also showed that absence of THBS1 resulted in upregulation of MMP-9 (Rodriguez-Manzaneque, Lane, Ortega et al., 2001). Another transgenic mouse study indicated that expression of THBS1 prevented the development of adenomas in the large intestine (Soto-Pantoja, Sipes, Morris et al., 2015). Thrombospondin's positive effects have also been reported in human carcinoma. Down-regulation of the secretion of THBS1 was found to be a key event in the change from an anti-angiogenic to an angiogenic phenotype during bladder tumourigenesis (Campbell, Volpert, Ivanovich et al., 1998). Grossfield et al. found that patients with low thrombospondin expression exhibited increased recurrence rates and decreased overall survival, and that it could be used as an independent predictor of relapse and disease outcome (Grossfeld, Ginsberg, Stein et al., 1997). Likewise Goddard et al. showed that low THBS1 expression indicated high risk of muscle invasive or metastatic disease in bladder carcinoma (Goddard, Sutton, Jones et al., 2002). Thrombospondin has also been found to inhibit downward VEGF signalling pathways. In this study the three anti-angiogenic domains (3TSR) of THBS were found to induce both intrinsic and extrinsic apoptosis in primary endothelial cells by up-regulating the expression of TRAIL receptors in a CD36 and Jun NH_2-terminal kinase-dependent manner (Ren, Song, Parangi et al., 2009). Another study also showed that endothelial cells treated with thrombospondin up-regulated the Fas/FasL receptor/ligand pair, hence inducing apoptosis (Volpert, Zaichuk, Zhou et al., 2002). Despite the huge evidence supporting thrombospondin's anti-tumorigenic effects some studies have linked increased expression of THBS1 to tumour differentiation. A recent study reported that increased expression of THBS1 was linked to invasive properties of human gastric cancer cells. The authors also found that THBS1 expression was regulated by

fibroblast growth factor 7 (FGF7) and FGF2 signalling (Huang et al., 2017). Similarly, Borsotti et al. concluded that THBS1 expression was higher in cancerous tissue than normal. They also found that THBS1 is regulated by VEGF and FGF2 that are both known to be involved in melanoma progression (Borsotti, Ghilardi, Ostano et al., 2015). Silencing of THBS1 by hyper-methylation has also been shown to have a protective effect in oligodendrogliomas. The study concluded that THBS1 could be used as a prognostic marker, as THBS1 hyper-methylation is clearly associated with bad prognosis (Perez-Janices, Blanco-Luquin, Tuñón et al., 2015).

1.10. Gelsolin

Several gelsolin isoforms exist, but the plasma isoform of 86 kDa, the cytoplasmic isoform of 81 kDa and a 82 kDa isoform most involved in myelin and CNS development are the most documented ones (Li, Arora, Chen et al., 2012). Gelsolin superfamily members have an important role in regulation of the actin filaments of the cytoskeleton. They are Ca^{2+}-dependent, multidomain regulators that sever actin filaments, cap the barbed ends of actin filaments and under certain conditions nucleate actin monomers (Li et al., 2012; Mannherz, Mazur, & Jockusch, 2010; Nag, Larsson, Robinson et al., 2013). Actin filament assembly and disassembly are important for essential cellular processes like cell division and motility (Alberts et al., 2008). Gelsolin can also both induce and prevent apoptosis depending on the circumstances. Various caspases cleave gelsolin and the N-terminal half of gelsolin contributes to apoptosis. Full length gelsolin on the other hand is generally anti-apoptotic (Li et al., 2012). Numerous studies have revealed that gelsolin is down regulated in various cancers and that increased gelsolin expression leads to a less invasive phenotype (Li et al., 2012). For example, a study conducted by Asch et al. showed that gelsolin expression was decreased in human, mouse and rat mammary carcinomas (Asch, Head, Dong et al., 1996), Ni et al. detected lower gelsolin protein levels in pancreatic cancer compared to normal pancreatic tissue (Ni, Zhou, Wang et al., 2008) and in a recent study Li and colleagues found that up-regulation of gelsolin expression significantly reduced the invasive properties of colorectal cancer cells (Li, Yang, Hong et al., 2016). Other studies point to a correlation between increased gelsolin expression and invasion as well as poor clinical outcome. Gelsolin was up-regulated in oral cancer and the increased expression correlated with increased tumour size, invasive growth and bad prognosis (Shieh, Chen, Wei et al., 2006). Shieh et al.

investigated gelsolins effect on NSCLC and found that gelsolin expression correlated negatively with patient survival (Shieh, Godleski, Herndon et al., 1999). Gelsolin expression has also been shown to be prominent at the invasive end of colorectal tumours (Zhuo, Tan, Yan et al., 2012). Several important signalling pathways that are often aberrantly expressed in cancer are regulated by gelsolin. A study by Thor et al. investigated EGFR/ Epidermal growth factor 2 (erb-B2) mediated motility and the importance of gelsolin in breast cancer. EGFR and erbB-2 receptors are located in the membrane and signal through phosphatidylinositol 3'-kinase (*PI 3-kinase*), the Rac GTPase, and phospholipase Cγ (PLCγ) when stimulated. These signalling pathways all induce cell movement through dynamic changes in the actin cytoskeleton with gelsolin as an important mediator. The researchers found that tumour gelsolin was associated with overexpression of erbB-2 and EGFR, as well as with an aggressive tumour phenotype. However, tumour gelsolin alone could not be used as a prognostic factor. Overexpression of all three factors, on the other hand, significantly predicted poor clinical outcome (Thor, Edgerton, Liu et al., 2001). Even though gelsolin's role in tumourigenesis and invasiveness is still not fully understood and most probably context specific, gelsolin can be considered as a potential drug target or a prognostic marker due to its role in actin remodelling and induction of apoptosis. Recombinant mouse studies have shown that lack of gelsolin is not lethal for the animals, making the protein a relatively safe therapeutic option (Li et al., 2012).

1.11. Aim of the study

The overall aims of the study are to investigate whether exosomes derived from MCC may play a role in this cancer, and whether exosomal proteins or microRNAs can be used as prognostic or diagnostic markers of this malignant disease. Comparative proteomic analysis performed by PhD candidate Aelita Konstantinell of exosomes derived from two MCPyV-positive and two MCPyV-negative MCC cell lines have shown exosomal proteins that are common for all cell lines, proteins that are common for the virus-negative and virus-positive cell lines respectively, and proteins unique for each cell line. The proteins gelsolin, periostin and thrombospondin are known to have oncogenic potential, and were detected in high numbers by proteomics in all four MCC cell lines. The specific aims of this master thesis is to:

- Verify the presence of the proteins gelsolin, perisotin and thrombospondin, detected by proteomics, in MCC derived exosomes.
- Study the effect of the MCPyV oncoproteins LT-ag and st-ag on the expression of these three exosomal proteins.
- Investigate the effect of gelsolin, periostin and thrombospondin on cell proliferation.

2. Materials

Table 1. Growth mediums used in this study.

Growth medium	**Manufacturer/Contents**	**Purpose**
RPMI-1640 Medium supplemented with 10 % exosome depleted FBS Media Heat Inactivated	450 ml RPMI-1640 Medium, Sigma Life sciences, R8758-500ML (With L-glutamine and sodium bicarbonate, liquid, sterile filtered suitable for cell culturing) + 50 ml Exo-FBSHI Exosome depleted FBS Heat Inactivated, System Biosciences, Exo-FBSHI-250A-1	Mammalian cell culture
RPMI-1640 Medium supplemented with 10 % FBS (fetal bovine serum)	450 ml RPMI-1640 Medium, Sigma Life sciences, R8758-500ML (With L-glutamine and sodium bicarbonate, liquid, sterile filtered suitable for cell culture) + 50 ml FBS	Mammalian cell culture
DMEM (Dulbecco's modified Eagles Medium) +10 % FBS	450 ml Dulbecco's modified Eagles Medium, Sigma Aldrich, D5546-500ML (With 1000 mg glucose/L, L-glutamine, and sodium bicarbonate, without L-glutamine, with pyridoxine, liquid sterile filtered, suitable for cell culture) + 50 ml FBS	Mammalian cell culture

LB (Luria Bertani) broth	950 ml dH_2O, 20g bactotryptone, 5 g yeast extract, 10 g NaCl, NaOH up to pH 7 (0.2 ml), appropriate antibiotics, dH_2O up to 1000 ml	Transformation of bacterial cells
LB agar plates	LB broth, 15 g bacto-agar/L	Transformation of bacterial cells
SOC broth	950 ml dH_2O, 20 g bactotryptone, 5g bacto-yeast extract, 0.5 g NaCl, 20 mM glucose, 10 ml 250 mM KCl, NaOH up to pH 7 (0.2 ml), dH_2O up to 1000 ml	Transformation of bacterial cells
Opti-MEM®, Reduced Serum Medium	Thermo Fisher Scientific, 11058021	MTT-assay

Table 2. Enzymes used in this study.

Enzyme	**Manufacturer**	**Purpose**
AccuStart™ II Geltrack™ PCR Supermix (2x)	Quanta biosciences, 89235-014	PCR
JumpStart™ REDTaq® ReadyMix™ Reaction Mix	Sigma Aldrich, p0982	PCR
Phusion High Fidelity DNA polymerase	New England Biolabs, M0530S	PCR

Table 3. Buffer solutions and chemicals used in this study.

Buffer solutions and chemicals	**Content/Manufacturer**	**Purpose**
DMSO	Sigma Aldrich, D8418	Cryo protectant
Exo-Quick reagent	System biosciences, EXOQ5A-1	Exosome precipitation
Ripa buffer	Thermo Fisher Scientific, 89900	Cell lysis, western blot

NuPAGE® LDS Sample Buffer (4X)	Thermo Fisher Scientific, NP0007	Western blot
Methanol, anhydrous	Sigma Aldrich, 322415	Western blot
Blotting buffer	5.8 g Tris base, 29 g glycin, 200 ml methanol, 800 ml ddH_2O	Western blot
CDP Star substrate (12.5 mM concentrate)	Thermo Fisher Scientific, T2306	Western blot
10 x washing buffer	10mM Tris HCl pH 9.5, 100 mM NaCl, 10 mM $MgCl_2$ and dH_2O up to 1000 ml. Working dilution 1:10	Western blot
Blocking buffer	150 ml PBS, 7.5 g dry milk, 150 µl Tween 20	Western blot
Blocking buffer phospho antibodies	150 ml TBST, 7.5 g dry milk	Western blot
TBST	1xTBS + 0.1% Tween 20	Western blot
PBST	1xPBS + 0.1% Tween 20	Western blot
CDP Star buffer	5 ml DEA in 420 ml dH_2O, bring to pH9.5, add $MgCl_2$ up to 500 ml	Western blot
Super signal West Femto Luminol Enhancer Solution	Thermo Fisher Scientific, 34095	Western Blot
Super signal West Femto Stable Peroxide Buffer	Thermo Fisher Scientific, 34095	Western blot
Restore™ PLUS Western blot stripping buffer	Thermo Fisher Scientific, 46428	Western blot
Magic Marker™ XP Western standard	Invirtogen, LC5602	Western blot
Precision Plus Protein™ Dual Color Standards	Biorad, #1610374	Western blot

Buffer RES + RNase	Macherey-Nagel, 740410.100	Plasmid purification (resuspension)
Buffer LYS	Macherey-Nagel, 740410.100	Plasmid purification (lysis)
Buffer NEU	Macherey-Nagel, 740410.100	Plasmid purification (neutralization)
Buffer EQU	Macherey-Nagel, 740410.100	Plasmid purification (equilibration)
Buffer WASH	Macherey-Nagel, 740410.100	Plasmid purification (wash)
Buffer ELU	Macherey-Nagel, 740410.100	Plasmid purification (elution)
Isopropanol	Fluka analytical, 34965-1L	Plasmid purification (precipitation)
Ethanol 96 %	Sigma Aldrich, 16368	Plasmid purification (drying)
TE buffer	10 mM Tris, bring to pH 8.0 with HCl, 1 mM EDTA	Plasmid purification
jetPRIME buffer	Polyplus transfection®, 114-01	Transfection
jetPRIME® Transfection reagent	Polyplus transfection®, 114,01	Transfection
Tropix® lysis buffer supplemented with 0,5 µM DTT	Applied biosystems	Luciferase assay
Luciferase buffer	Promega	Luciferase assay
Protein solving buffer (PSB)	Macherey-Nagel, 740967.50	Protein quantification assay
Quantification reagent	Macherey-Nagel, 740967.50	Protein quantification assay

PBS (g/1000 ml)	900 ml H_2O, 8.0 g NaCl, 0.20 g KCl, 1.42 g NaH_2PO_4, 0.24 g KH_2PO_4, brig to pH 7.4, add H_2O up to 1000 ml	Mammalian cell culture
Trypsin 0.25 %	Sigma Aldrich, T4049	Mammalian cell cultures
TAE 50x (1000 ml)	242 g Tris base, 57 ml Acetic acid, 200 ml 0.5 M EDTA, bring to pH 8, add H_2O till the total volume reaches 1000 ml	Gel electrophoresis
Loading buffer 6x	100 mg Bromophenol Blue, 100 mg Xylene Cyanol FF, 6 g Ficoll, add dH_2O to 40 ml	Gel electrophoresis
SeaKem® LE Agarose	Lonza, CAM50004	Gel electrophoresis
Gel Red	Biotium, 41003-1	Gel electrophoresis
1 Kb+ ladder	Invitrogen, 10787-026	Gel electrophoresis
5x iScript reaction mix	Biorad, 170-8890	cDNA synthesis
iScript reverse transcriptase	Biorad, 170-8890	cDNA synthesis
RPE buffer	Qiagen, 74104	RNA isolation
RLT buffer +β-ME	Qiagen, 74104	RNA isolation
RW1 buffer	Qiagen, 74104	RNA isolation
RNase free H_2O	Qiagen, 74104	RNA isolation
DTT	ApliChem, A3668, 0100	Cell lysis
MycoAlert™ PLUS reagent	Lonza, LT07-701	Mycoplasma testing
MycoAlert™ PLUS Substrate	Lonza, LT07-701	Mycoplasma testing
MycoAlert™ PLUS Assay Buffer	Lonza, LT07-701	Mycoplasma testing
MycoAlert™ Assay Control	Lonza, LT27-235	Mycoplasma testing

MTT (3-(4,5-dimethylthiazol-2-yl)-2,5-diphenyltetrazolium bromide)	Sigma Aldrich, M5655	MTT-assay
Stop solution MTT	Acidic isopropanol, isopropanol supplemented with 0.04 M HCl	MTT-assay

Table 4. Primary antibodies used in this study.

Primary antibodies	**Manufacturer and catalogue nr.**	**Dilution**
Anti-Periostin antibody (rabbit polyclonal)	Abcam, ab152099	1:1000
Anti-Gelsolin antibody (rabbit polyclonal)	Abcam, ab74420	1:1000
Anti-Thrombospondin antibody (rabbit polyclonal)	Abcam, ab85762	1:900
Anti-CD63 Antibody (rabbit anti-human, mouse, rat)	System Biosciences, EXOAB-CD63A-1	1:2500
MCPyV large T-antigen (mouse monoclonal)	Santa Cruz biotechnology, sc-136172	1:1000
ERK-2 (rabbit polyclonal IgG)	Santa Cruz biotechnology, sc-154	1:1000

Table 5. Secondary antibodies used in this study.

Antibody	**Manufacturer**	**Dilution**	
Polyclonal Rabbit anti mouse IgG/AP	Dako, DO314	1:2000	Detection of LT-ag

Polyclonal goat anti rabbit IgG/HRP	Abcam, AB6721	1:20,000	Detection of periostin/thrombospondin/gelsolin
Goat anti-rabbit secondary antibody	System biosciences, EXOAB-HRP	1:20,000	Detection of CD63
Rabbit Anti-Mouse IgG H&L (HRP)	Abcam, Ab97046	1: 20,000	Detection of LT-ag

Table 6. Primers used in this study.

Protein	**Primer sequence**	**Product size**
Periostin	Forward 5′-GATGGAGTGCCTGTGGAAAT-3′ Reverse 5′-AACTTCCTCACGGGTGTGTC-3′	239 bp
Thrombospondin	Forward 5′-CCTATGCTGGTGGTAGACTA-3′ Reverse 5′-ACGTTCTAGGAGTCCACACT-3′	235 bp
Large T antigen	Forward 5′-TACAAGCACTCCACCAAAGC-3′ Reverse 5′-TCCAATTACAGCTGGCCTCT-3′	423 bp
APRT	Forward 5′-CCCGAGGCTTCCTCTTTGGC-3′ Reverse 5′-CCTCGCTTAAGGGCAGGGAG-3′	302 bp (RNA) 805 bp (DNA)

Table 7. Promoters used in this study.

Promoter	**Provided by**	**Manufacturer/reference**
Gelsolin promoter -384/+35 pGL3-Basic	GenScript	SC1692

Periostin promoter pGL3-basic	A kind gift from Dr. Melino, University of Leicester, United Kingdom	(Landré, Antonov, Knight et al., 2016)
Thrombospondin promoter pGL3-basic	A kind gift from Dr. Cohn, University of Chicago, United States	(Yang, Liu, Tian et al., 2003)

Table 8. Recombinant proteins used in this study.

Recombinant proteins	**Manufacturer and catalogue nr.**
Human Gelsolin protein	Abcam, ab114280
Recombinant Human Periostin/OSF-2	Biotechne, 3548-F2
Recombinant Human Thrombospondin-1	Biotechne, 3074-TH
Periostin/OSF-2 Recombinant Protein Antigen	Novus, NBP1-82472PEP

Table 9. Cell lines used in this study.

Cell line	**Provided by**	**MCPyV**	**Reference**
MKL-1	Dr. Akgül; university of Cologne, Germany	Positive	(Shuda et al., 2008)
MKL-2	Dr. Akgül; university of Cologne, Germany	Positive	(Guastafierro, Feng, Thant et al., 2013)
MCC13	Dr. Akgül; university of Cologne, Germany	Negative	(Leonard, Ramsay, Kearsley et al., 1995)
MCC26	Dr. Akgül; university of Cologne, Germany	Negative	(Leonard, Williams, Walters et al., 1996)

Merkel cell carcinoma cell lines MCC13, MCC26, MKL-1 and MKL-2 were used. Merkel cell carcinoma cell lines have historically been categorized into subtypes I–IV based on morphology. This classification has been adapted from Small Cell Lung Cancer (SCLC), as the cells are similar in morphology and growth characteristics. Subtypes I and II grow in dense, floating, spherical aggregates. Type I is more densely packed than type II and often show central necrosis. Type III cells form looser aggregates with a 2-dimensional appearance, and type IV are adherence dependent cells growing in a monolayer (Leonard, Dash, Holland et al., 1995). MCC13 and MCC26 are both MCPyV-negative, adherence dependent cells (type IV) with a large low contrast appearance. MKL-1 and MKL-2 are both MCPyV-positive suspension cells. They grow in loose aggregates and can hence be classified as type III cells (Figure 6) (Guastafierro et al., 2013).

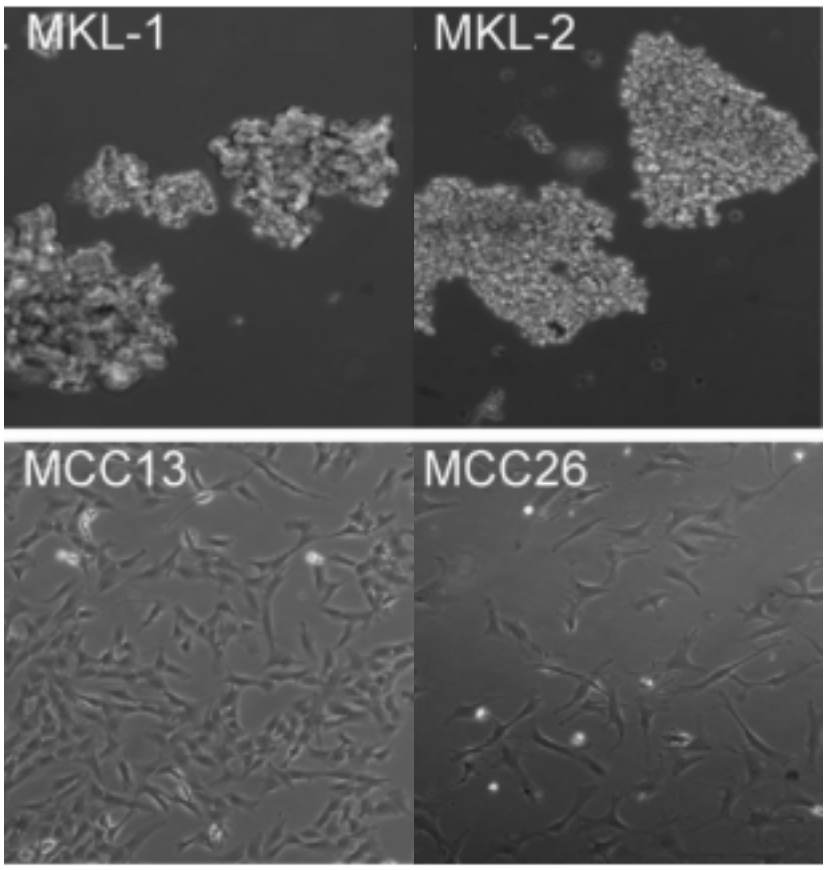

Figure 6. Morphology of MCC cell lines used in the study. MKL-1 and MKL-2 are both MCPyV-positive suspension cells that grow in loose aggregates. MCC13 and MCC26 are both MCPyV-negative, adherence dependent cells with a large low contrast appearance. The figure is modified from Figure 1 in Guastafiero et.al. (Guastafierro et al., 2013).

Table 10. Bacterial strain used in this study.

Bacterial strain	Description	Purpose
Escherichia coli DH5	Competent strain	Amplification of plasmid vectors

Table 11. Equipment used in this study.

Equipment	Manufacturer	Purpose
Microfuge 22R refridgerated centrifuge	Beckman Coulter™, California, USA	Centrifugation eppendorf tubes
Kubota 5100 centrifuge	Kubota, Tokyo, Japan	Centrifugation of 15 ml tubes
Avanti J-26 XP ultracentrifuge	Beckman Coulter™, California, USA	Centrifugation of 50 ml tubes
Sonication machine	Heat systems ultrasonics, New York, USA	Sonication of cell lysate Western Blot
T-100 Thermal cycler	Biorad, California, USA	PCR
AccuBlock™ digital dry bath	Labnet, North Carolina, USA	Heating block Western blot
Vortex	VWR, Pennsylvania, USA	Mixing of samples
CLARIOstar® microplate reader	BMG Labtech, Ortenberg, Germany	Luciferase assay, protein quantification
Lumi Analyst machine (LAS-4000)	Fujifilm, Tokyo, Japan	Luminescent image analyser
X-cell SureLock™ mini cell electrophoresis system	Thermo Fischer Scientific, Massachusetts, USA	SDS PAGE/Western blot
Submicron Particle sizer 370	Nicomp PSS, Florida, USA	Particle size determination

Millipore Scepter handheld cell counter	Merck Millipore, California, USA	Cell counting
Direct Detect	Merck Millipore, California, USA	Protein measurement
Electrophoresis power supply	Amersham Biosciences, Little Chalfont, UK	Gel electrophoresis

3. Methods

Based on proteomic analysis of exosomes originating from MCPyV-negative and MVPyV-positive MCC cell lines performed by PhD candidate Aelita Konstantinell, three proteins with known oncogenic properties, gelsolin, periostin and thrombospondin, were chosen for further investigation. Exosomes were first isolated from MCC cell lines using a commercially available precipitation kit, before the size of the exosomes was confirmed using particle size determination. The presence of the oncogenic proteins and their transcripts in MCC cells and exosomes was verified using western blot and RT-PCR, respectively. Subsequently, the effect of MCPyV LT-ag and st-ag on the gelsolin, periostin and thrombospondin promoter activity was assessed using a luciferase reporter transient transfection assay. The respective proteins' effect on cellular metabolism was also attempted examined using MTT-assay.

3.1. Mammalian cell cultures

3.1.1. Thawing of cells

In order to start a new cell culture cells had to be retrieved from the nitrogen tank and thawed.

Protocol:

The desired cells were retrieved from the liquid nitrogen tank and washed with 96 % ethanol before the tube was brought into the laminar air flow (LAF) bench. Here, 1/4 of the cap was opened to allow any potentially trapped liquid nitrogen to evaporate to avoid the risk of explosion caused by temperature differences. The cap was retightened before the tube was

transferred to a water bath. Immediately after thawing, the tube was sterilised with ethanol again before it was brought back to the LAF bench where the cells were transferred to a 15 ml tube in order to remove the cryo protectant. Five ml of the appropriate medium containing 10 % Foetal Bovine Serum (FBS) was then added drop wise to the cells before 10 more ml was added more quickly. The tube was centrifuged at 900 rpm (Kubota centrifuge 5100) for 5 minutes before the supernatant was removed by water suction and 5 ml new medium was added to the cells. The cells were subsequently transferred to a medium (75 cm^2) flask containing 14 ml complete growth medium and the flask was incubated in the 37 ºC 5 % CO_2-incubator.

3.1.2. Cultivating cells

Cells were cultivated in appropriate cultivation medium supplemented with 10 % FBS or exosome depleted FBS and incubated in the 37°C, 5 % CO2 incubator until they reached approximately 70 % confluence.

3.1.3. Sub-culturing of cells

In order to avoid overcrowding and metamorphosis of the cultured cells in the flask, the cells have to be split and transferred to a new flask when they are approximately 70 % confluent. Before splitting the cells, fresh RPMI-1640 medium containing 10 % FBS was preheated in the 5 % CO_2 37°C warming cabinet for approximately 1 hour. Sub-culturing of cells can either be performed mechanically by scraping or enzymatically by adding trypsin, a proteolytic enzyme.

Protocol:

When sub-culturing the adherent cell lines MCC13 and MCC26 for use in exosome isolation and size determination, the cells were detached from the flask mechanically. The old medium was removed by water suction before 3 ml of fresh medium was added. The cells were then detached from the flask surface using a cell scraper before the cell suspension was transferred to a centrifuge tube. The cell suspension was centrifuged at 900 rpm (Kubota centrifuge 5100) for 5 minutes at room temperature before the supernatant was removed by water suction. The pelleted cells were resuspended in 1 ml fresh RPMI-1640 and transferred to the new flask containing the preheated medium.

The suspension cells MKL-1 and MKL-2 were split by transferring the cell suspension to two centrifuge tubes, followed by centrifugation for 5 minutes at 900 rpm (Kubota centrifuge 5100) at room temperature. The supernatant was then removed by water suction, and the pelleted cells were resuspended in 1 ml fresh RPMI-1640 and transferred to the new flasks containing preheated medium. All cell types were incubated in a 5 % CO_2 humidified incubator at 37℃.

The cells used in either transfection studies or MTT-assay, were split by trypsinization. RPMI-1640 medium supplemented with 10 % FBS and 100 μg/ml streptomycin plus 100 units/ml penicillin was removed from the cells by water suction before 1 or 2 ml of Trypsin (depending on the size of the flask) was added to the cells. The flask was subsequently incubated in the CO_2 cabinet for approximately 2 minutes or until the cells had dislodged from the bottom of the flask and rounded up. Four ml of fresh medium was then added to the cells in order to stop the trypsinization reaction. An appropriate amount of cell suspension was transferred to a new flask containing fresh cultivation medium.

3.1.4. Removal of bovine exosomes

The cells used for exosome isolation, western blot and RT-PCR were cultivated in RPMI-1640 medium supplemented with exosome depleted FBS in order to avoid contamination with bovine exosomes. The cells were passed four times in the medium containing exosome depleted FBS in order to assure that bovine exosomes from normal FBS had been washed away. After the fourth passage the supernatant was collected (for exosome isolation) and cells were harvested (as a positive control for western blot and for use in RT-PCR) and stored at -70℃.

3.1.5. Counting and seeding out cells

When performing various experiments it is vital to seed out an equal amount of cells in each well. How many cells to seed out in each well depends on the degree of confluence preferred by the cells, how long they have to be incubated and how fast they are growing. In this thesis

the amount of cells seeded out varied from 35,000 cells/well to 250,000 cell/well depending on the experiment.

Protocol:

The cells were first washed with PBS and detached from the surface of the flask using trypsin. The trypsinization reaction was stopped by adding fresh medium to a total of 5 ml. Subsequently, a 1/10 dilution of PBS and cell suspension (90 µl PBS and 10 µl cell suspension) was made in order to count the cells using a Millipore Scepter handheld cell counter.

Calculations:

Adjusting for dilution:

$$Cell\ count * 10$$

Seeding out e.g. 250,000 cells in 12 wells using the formula $C1 * V1 = C2 * V2$:

$$Cells/ml * V1 = 250{,}000 cells * 15\ wells$$

$$V1 = \frac{250{,}000 cells * 15 wells}{Cells/ml}$$

3.1.6. Mycoplasma test

All cell lines used in the study were tested for mycoplasma using the MycoAlert™ PLUS Mycoplasma Detection Kit from Lonza. Worldwide, Mycoplasma has been detected in 15 % - 35 % of all continuous cell cultures. This is a huge problem in contemporary research, as infections can extensively affect the physiology and metabolism of the cells and thus impact the reliability and reproducibility of the results obtained with these cultures (Nikfarjam & Farzaneh, 2012).

The MycoAlert™ PLUS kit exploits mycoplasma specific enzymes that convert ADP to ATP. When the viable mycoplasma are lysed the enzymes react with the MycoAlert™ PLUS Substrate, catalyzing the conversion of ADP to ATP by the following reaction:

$$Luciferin + O_2 + ATP \rightarrow oxyluciferin + CO_2 + AMP + diphosphate + light$$

The amount of ATP in the sample is measured both before and after the addition of MycoAlert™ PLUS Substrate, and hence a ratio indicating the presence of mycoplasma can be obtained by dividing the measurement prior to the addition of the substrate by the measurement taken after the addition of the substrate (Lonza, 2012).

Protocol:

The MycoAlert™ PLUS Reagent and substrate were first reconstituted in 1.2 ml MycoAlert™ PLUS Assay Buffer. Supernatant from a cultivation flask containing cells of more than 70 % confluence was collected and centrifuged for 5 minutes at 1500 rpm (Microfuge 22R) before 100 µl of the supernatant was transferred to a 96 well plate. Three wells (undiluted, 1:10 and 1:100 dilution in Assay buffer) containing 100 µl of the positive control MycoAlert™ Assay Control were prepared. As negative control 100 µl MycoAlert™ Assay Buffer was loaded in a well in the 96 well plate, and 100 µl of the MycoAlert™ PLUS Reagent was added to each well and incubated for 5 minutes before the luminescence was measured (measurement A) using CLARIOstar® microplate reader. Next 100 µl of MycoAlert™ PLUS Substrate was added to the wells and incubated for 10 minutes before the second measurement (measurement B) was undertaken. Measurement B/measurement A gives a ratio indicative of mycoplasma contamination. An B/A ratio of <1 is negative for mycoplasma, 1-1.2 is borderline and >1.2 is mycoplasma positive (Lonza, 2012).

3.1.7. Freezing down cells in liquid nitrogen

Cells cultivated in exosome depleted FBS were frozen down in liquid nitrogen in order to avoid the timely process of removing bovine exosomes for later studies. Cells were frozen down in 90 % serum and 10 % at a concentration of ~10^6 cells/ml.

The cultivation medium was removed from the cells by water suction before they were washed with 10 ml preheated PBS. The cells were detached from the bottom of the flask by adding 1-2 ml Trypsin (depending on the size of the flask). When the cells were fully detached from the growth surface, 5-10 ml of preheated medium was added to the cells in order to stop the trypsinization reaction. Subsequently the cells were transferred to a 15 ml centrifuge tube and centrifuged for 5 min at 900 rpm (Kubota centrifuge 5100). The supernatant was removed by water suction and n x 900 µl exo-depleted serum (n= number of tubes you want to freeze) was added to the cells. Thereafter n x100 µl DMSO was added drop

wise to the cells. The content of the tube was carefully mixed by pipetting up and down, since the cells are fragile after adding DMSO. The cryo tubes were marked with name of cell line, amount of cells and date before 1000 µl cell suspension with DMSO was transferred to each tube. The tubes were snap-frozen in liquid nitrogen.

3.2. Isolation of exosomes

Exosomes were isolated from medium derived from MKL-1, MKL-2, MCC13 and MCC26 cell cultures cultivated in exosome depleted FBS, and their size was subsequently determined using the Submicron Particle Sizer. Exosomes were also isolated for further use in western blot analysis where the relative amount of protein in cells and exosomes respectively was compared. Exosome isolation was performed using a commercial precipitation reagent, ExoQuick-TCTM Exosome Precipitation Solution followed by centrifugation.

Protocol:

The supernatant was first centrifuged at 3,000 x g for 15 minutes at 4℃ in order to get rid of cell debris. The supernatant was then carefully removed and transferred to a tray. A syringe was used to absorb 10 ml of the supernatant before it was filtered through a 0.2 µM filter placed on the tip of the syringe, and transferred to a 15 ml centrifuge tube. Subsequently 2 ml ExoQuick reagent was added to each centrifuge tube containing 10 ml filtrated supernatant in order to precipitate the exosomes. The content of the tubes was mixed by pipetting up and down and by inverting the tubes several times. The tubes were incubated over night at 4℃. The following day, the tubes were centrifuged for 30 minutes at 1,500 x g before the supernatant was removed by water suction. In order to remove excess supernatant, the tubes were centrifuged again for 5 minutes at 1,500 x g and the residual medium was removed by water suction.

3.3. Verification of Exosomes using Photon Correlation Spectroscopy (PCS)

In order to verify that MCC exosomes had been successfully isolated, the size of the isolated exosomes were determined using the Nicomp Particle Sizing System (PSS) Submicron Particle sizer 370 with software version C-370 V-1.51a.

This machine determines particle size based on the intensity of light scattered and detects particles between 3 nm and 5 μm. A 632.8 nm, 5 mW He-Ne laser passes through the diluted sample and the PCS detects the intensity of scattered light at a 90° angle (ANALYSTA, 2017). As individual particles pass through the laser beam, the light scattered by the particle is collected by a detector and interpreted. This corresponds to the cross sectional area of the particle and hence particle size. The molecular weight, size, and shape of a particle as well as the refractive indices of the particle and solvent affect the amount of scattered light collected. Due to interference between the light beams scattered from different particles that move randomly in a liquid, random fluctuations in time can be expected (Particle Sizing Systems, 2016).

The PSS programme offers two data analysis tools; either a Gaussian calculation suitable for monodisperse samples or a Nicomp distribution analysis that is more suitable for more complex samples. Most samples are not monodisperse, i.e. they consist of several different populations of particles. Since a conventional Gaussian analysis would not be able to separate the different mean diameters and would present a result with a mean diameter somewhere in the middle of the different populations, the Nicomp analysis was used on all the samples as they consisted of more than one population of vesicle particles (Particle Sizing Systems, 2016).

Protocol:

First the pelleted exosomes were dissolved in 150 μl sterile filtered PBS. The specialized PSS tubes were sonicated in water before use, and sample preparation was carried out in a LAF bench to avoid contamination with dust particles. The tubes were then rinsed three times in sterile filtered PBS using a 5 ml syringe. The sample was then added to the tube using a 5 ml syringe, and sterile PBS was added until 2/3 of the tube's total volume was occupied. The content of the tube was mixed gently with the sample syringe in order to avoid bubbles in the test tube. The tube was subsequently wiped with a lens paper before it was placed in the PSS machine. Ideally, the display on the instrument should show a frequency between 250-350kHz. If the frequency is lower, the cycle time has to be adjusted, as at least 1000 particles should be measured in order to trust the measurement. On the computer, the PSS programme was opened and the option particle sizing and the sub-category control sizing was chosen. The settings were adjusted according to the room temperature, and the angle was set to 90°. Auto print save menu was then selected and three cycles and appropriate measurement time were

selected before the measurement was started by selecting “GO”. The settings were then changed from solid to vesicle particle. The machine accurately detects particles in the size range 10-990 nm, and a variance of lower than 0.7 is acceptable.

3.4. Verification of periostin, thrombospondin and gelsolin using Western blot

Western blot was used to verify the presence of gelsolin, periostin and thrombospondin in both isolated exosomes and harvested cells. Furthermore, the supernatant from the harvested exosomes was also tested by western blot in order to check whether the proteins of interest are exclusively excreted via exosomes or actively secreted by the cell or the result of cell leakage.

Western blot is an immunoassay based on the specific binding of antibodies directed to the protein of interest. The proteins are first denatured using sodium dodecyl sulphate (SDS) before they are separated by size on a polyacrylamide gel (PAGE). SDS is a powerful negatively charged detergent that binds to the hydrophobic regions of the proteins and causes them to unfold due to repulsion. Moreover, SDS helps transport the proteins through the polyacrylamide gel as it covers the proteins in negative charged detergent molecules, and masks the proteins intrinsic charge (Alberts et al., 2008). The separated proteins are further transferred to a membrane, also called blotting. This membrane is in turn treated with a primary antibody specific for the protein of interest. In order to detect and amplify the signal from the primary antibody-antigen complex, a secondary antibody targeted for the Fc-region of the primary antibody is added (Alberts et al., 2008; Mahmood & Yang, 2012). If the primary antibody is made in goat, the secondary antibody must be an anti-goat antibody. The secondary antibody is conjugated with either alkaline phosphatase (AP) that converts its substrate, CDP-Star, into a detectable product, Horseradish peroxidase (HRP) that produces light when oxidizing luminol substrates (Veitch, 2004) or it can be tagged with a fluorescent compound (Eaton, Hurtado, Oldknow et al., 2014).

Protocol:

Before the proteins can be detected using western blot, cells and exosomes have to be lysed. Here, Ripa buffer containing phosphatase inhibitor and sonication was used. The pelleted exosomes were kept at 4℃ while phosphatase inhibitor 1:100 dilution was added to the Ripa buffer. The samples were protected in aluminium foil, as the phosphatase inhibitor is light

sensitive. Fifty µl Ripa buffer was then added to MCC13, MCC26, MKL-1 and MKL-2 cells retrieved from the -70℃ freezer, and the samples were incubated at room temperature for 15 minutes. The cell lines were used as positive controls during the western blot analysis. Fifty µl Ripa buffer was added to the tubes containing pelleted exosomes after this 15 minute incubation. The cells were subsequently lysed by sonication and incubated 15 minutes on ice. The lysate was then centrifuged for 5 minutes at 13, 000 x g before the supernatant was transferred to new Eppendorf tubes (System Biosciences, 2013). The protein concentration of the samples was measured using Direct Detect.

In order to separate and detect the desired proteins in cells and exosomes, 30 µg protein was loaded on to each well on a polyacrylamide gel. A mixture of LDS sample buffer, DTT (1M), ddH_2O and the protein sample was made accordance to Table 12, to a total volume of 20 µl because the wells of a 12-well acrylamide gels used for western blot can accommodate maximum 20 µl.

Table 12. Protein sample preparation for loading on PAGE-gel.

Protein sample	x µl
NuPAGE LDS sample buffer (4x)	5 µl
DTT	2 µl
ddH_2O	Up to 20 µl
Total volume	20 µl

The samples were heated for 10 min at 70 ℃ (Accublock) to denature the proteins, and then placed on ice until they were loaded on the acrylamide gel. The gel was removed from the plastic wrapping and rinsed in water. Next, the comb was removed and the wells were rinsed in running buffer. The white tape covering a gap at the bottom of the PAGE gel was removed in order to allow the current to pass. Finally, the gel was placed in the X-Cell Sure Lock mini cell with the highest side of the gel-cassette facing out. Both chambers of the X-Cell Sure Lock mini were filled with 1x running buffer. The first well was loaded with 2 µl Protein

Precision Plus and the second with Magic Marker. Subsequently, 20 µl of the samples were loaded onto and the gel was run for approximately 45 minutes at 200 V.

Blotting:

After gel electrophoresis, the proteins were transferred to the membrane by a process called blotting. In order to assemble the gels and membranes in the blotting module, some initial preparations were undertaken. Four filter papers and one membrane were cut to the size of the gel. The membrane was washed 3 sec in methanol, 10 sec in ddH_2O and > 5 min in blotting buffer. Moreover, six blotting pads were soaked in blotting buffer and air bubbles were removed using a roller. Inserting and twisting the gel knife on the three sealed sides of the cassette carefully opened the gel cassettes. The top plate was carefully discarded and the wells and the bottom part of the gel were trimmed of before a wet filter paper was placed on top of the gel. The gel was then flipped over to the filter paper, and assembled in the blotting module in the following way: two blotting pads, two filter paper, first gel, membrane, two filter papers, one blotting pad, two filter papers, second gel, membrane, two filter papers and two blotting pads. Air bubbles were removed for each new layer. The module was placed in the X-Cell Sure Lock and blotting buffer was poured into the upper chamber while cold water was poured into the outer chamber. NuPAGE blotting was chosen in the menu and blotting was run for 1 hour at 30 V. After blotting, the cooling water was removed by water suction and the blotting buffer discarded in the methanol waste container.

Blocking:

The membrane was transferred to a tray containing TBST and incubated on the shaker for 10 minutes to remove traces of acrylamide on the membrane. Next, the TBST was replaced by blocking buffer and the membrane was incubated on the shaker for 1 hour.

Incubation with primary and secondary antibodies:

The membrane was transferred to a 50 ml tube with the side of the membrane containing the proteins facing inward. Three ml blocking buffer and the appropriate primary antibody in the correct dilution were added to the tube. The tube was incubated at the rotating wheel at 4 °C over night. The next day the antibody-blocking buffer solution was discarded before the membrane was washed three times for 5 minutes each with 3-5 ml PBST. After the last washing step, 3 ml blocking buffer and the secondary antibody was added to the tube and

incubated on the rotating wheel at RT for 1 hour. If the secondary antibody was AP-conjugated the developing was performed with CDP star. Here the membrane was washed 2 x 5 min with PBST and 2 x 5 min with washing buffer before 5 ml CDP star buffer and 10 µl CDP star was added to the tube. For HRP-conjugated antibodies, the membrane was first washed 2 x 5 min with TBST and 2 x 5 min in washing buffer, before 1.5 ml Super Signal West Pico Chemiluminecent substrate luminol solution and 1.5 ml Stable peroxide buffer was added to the tube. Regardless of the developing agent the tube was incubated for 5 min at the rotating wheel at RT before the membrane was placed in a plastic seal for analysis on the LumiAnalyst machine LAS 3000/4000. The membrane was protected from light before analysis.

Calculations:

Amount of lysate needed to load 30 µg protein in each well:

$$\frac{30\ \mu g\ protein}{Protein\ concentation\ measured\ by\ Direct\ Detect\ (\frac{\mu g}{\mu l})} = x\ \mu l\ lysate$$

$50 \mu l\ Ripa\ buffer * 12\ samples =$ 600 µl, added phosphatase inhibitor in 1:100 dilution → 7 µl was added to 693 µl Ripa buffer.

Example dilution of Anti-periostin antibody (1:1000) in 3 ml blocking buffer:

$\frac{1}{1000} * 3000\ \mu l =$ 3 µl Anti-Periostin antibody and 3 ml blocking buffer.

3.5. Detection of periostin and thrombospondin transcripts using Reverse Transcription Polymerase Chain Reaction (RT-PCR)

In this thesis, RT-PCR was used to verify the presence of periostin, gelsolin and thrombospondin transcripts in MCC cells. Furthermore, RT-PCR was performed to confirm that the virus positive cell lines MKL-1 and MKL-2 used in the study expressed large-T

antigen while the virus negative cell lines MCC13 and MCC26 did not.

Reverse transcription where RNA is converted to cDNA followed by polymerase chain reaction (PCR) enables the detection and quantification of mRNA and hence the expression of specific genes. The method is very sensitive and easy to reproduce, making it an advantageous method (Pfaffl, 2004).

3.5.1. RNA isolation

The first step in RT-PCR is RNA isolation. DNA-free and non-degraded RNA is needed in order to accurately determine the amount of RNA. In this thesis, the RNeasy mini kit from Qiagen was used for RNA isolation. In this kit, the cells are first lysed before the genomic DNA is trapped in a spin column. The RLT lysis buffer provided by the kit contains guanidine-isothiocyanate that lyses the cell by disrupting hydrophilic bonds in the cell membrane. β-mercaptoethanol (β-ME) is added to the RLT buffer, as it inactivates RNases, thus ensuring isolation of intact RNA. RNases are very stable enzymes due to numerous disulfide bonds. β-ME is used to reduce these disulfide bonds and irreversibly denature the proteins (Nelson & Cox, 2013). The lysate is then loaded onto a gDNA Eliminator spin column and centrifuged in order to remove the genomic DNA. Thereafter, ethanol is added to the flow-through to provide appropriate binding conditions for RNA. The sample is then applied to an RNeasy spin column, where RNA binds to the membrane with high specificity while contaminants are efficiently washed away. The RNA is then eluted in 30 µl, or more, RNase free water (Qiagen, 2014).

Protocol:

The adherent cells first had to be trypsinized before they were resuspended and pelleted by centrifugation together with the suspension cells. The pelleted cells were then resuspended in 350 µl RLT buffer containing β-ME as we had less than 5 x 10^6 cells. The cells were then homogenized by passing the lysate 4-5 times through a syringe. The homogenized cell lysate was then transferred to the gDNA eliminator column placed in a 2 ml collection tube and centrifuged for 30 seconds at 8,000 x g. The flow through was saved and the column discarded. 350 µl (same amount as RLT buffer) 70 % ethanol was added to the flow through and mixed by pipetting. 700 µl of the sample was then transferred to an RNeasy spin column placed in a 2 ml collection tube before it was centrifuged for 30 seconds at 8,000 x g. The

flow through was discarded. The column was washed twice with 700 µl buffer RW1 and 30 seconds centrifugation at 8,000 x g. The spin column was also washed twice with 500 µl RPE-buffer. In the first washing step with RPE the column was centrifuged for 30 seconds at 8,000 x g. In the second washing step, the column was centrifuged for 2 minutes in order to dry the column membrane. The RNeasy spin column was then carefully transferred to a new 1.5 ml collection tube and 40 µl RNase free water was added to the spin column before it was centrifuged for 1 minute at 8,000 x g in order to elute the RNA.

3.5.2. cDNA synthesis

The next step in RT-PCR is cDNA synthesis. Here the RNA is converted to cDNA using the enzyme reverse transcriptase (Nolan, Hands, & Bustin, 2006).

Protocol:

In this thesis, iScript cDNA synthesis kit was used. 5x iScript reaction mix, RNA samples, and nuclease free H_2O were mixed according to Table 13:

Table 13. Sample preparation for cDNA synthesis.

Reagent	**Amount**
5x iScript reaction mix	10 µl
RNA sample	100 ng
iScript reverse transcriptase	2.5 µl
Nuclease free H_2O	Up to 50 µl
Total amount	50 µl

The samples were then placed in the Thermo cycler with the following programme (Table 14):

Table 14. Thermocycler programme for cDNA synthesis.

Thermocycler programme
5 min, 25℃
20 min, 46℃
1 min, 95℃

3.5.3. PCR

The last step in RT-PCR is to amplify the desired genes by PCR. The method is used to amplify DNA *in vitro,* and uses the enzyme DNA polymerase to repeatedly copy the desired stretches of DNA. This enzyme needs artificial DNA oligonucleotide primers to initiate the reaction. The PCR reaction consists of three steps; denaturing of the template DNA by heating, cooling of the sample so that the oligonucleotide primers can anneal to the DNA and extension of the primer by DNA polymerase using the original DNA as template. After an appropriate incubation period the cycle is repeated until the amplification is sufficient (Madigan, Martinko, Stahl et al., 2012).

In order to check the quality of the cDNA transcripts of the housekeeping gene *adenine phosphoribosyltransferase (APRT)* were first amplified by PCR. The APRT primers bind to both cDNA and genomic DNA and the size(s) of the fragment(s) can be used to determine the quality of the cDNA. If the primers amplify cDNA, a fragment of 302 bp is expected. If the sample is contaminated with genomic DNA a fragment of 805 bp is expected because of the presence of an intron in the *APRT* gene.

Protocol:

A premix for five samples containing Accustart PCR mix, forward and reverse primers and ddH_2O was prepared according to Table 15:

Table 15. Premix for PCR with APRT specific primers.

Accustart	75 µl
APRT forward primer (10 µM)	5 µl
APRT reverse primer (10 µM)	5 µl
ddH_2O	55 µl

Subsequently 28 µl premix and 2 µl (~5 ng) cDNA was transferred to each tube. The tubes were placed in the thermo cycler with the following programme:

Table 16. Thermocycler programme for PCR with APRT specific primers.

PCR programme	
2 min, 94°C	
40x	20 sec, 94°C
	30 sec, 62°C
	90 sec, 72°C
10 min, 72°C	
∞, 15°C	

Thereafter, PCR reactions amplifying periostin and thrombospondin cDNA were run. Premixes were prepared as described above, only with periostin and thrombospondin primers instead of APRT.

Table 17. Premixes for PCR with periostin and thrombospondin specific primers.

Accustart	75 µl
Periostin/thrombospondin forward primer (10 µM)	5 µl
Periostin/thrombospondin reverse primer (10 µM)	5 µl
ddH_2O	55 µl

The following PCR programme with an annealing temperature of 52°C for thrombospondin and 59°C for periostin, due to the different melting temperatures of their respective primers, was used:

Table 18. Thermocycler programme for PCR with periostin and thrombospondin specific primers.

PCR programme	
2 min, 94°C	
40x/45x	20 sec, 94°C
	30 sec, 52/59°C
	90 sec, 72°C

10 min, 72℃
∞, 15℃

The samples were then run on a 1 % agarose gel using 1kb+ ladder as a size marker.

3.5.4. Agarose gel electrophoresis

Gel electrophoresis is used to separate, purify and identify DNA fragments. The method uses electricity an electric field to separate DNA fragments by their size and shape as they migrate through an agarose gel. Gel electrophoresis relies simply upon the negative charge of the phosphate backbone of the DNA and the ability to distribute a voltage gradient in a matrix. The negatively charged DNA migrates towards the anode, and the smaller DNA fragments travel faster than the larger fragments when they are exposed to an electric field. A higher concentration of agarose in the gel leads to a closer meshwork and thus more hindrance of the DNA fragments (Madigan et al., 2012). Here gel electrophoresis was used to check the quality of cDNA (no genomic DNA contamination) and to detect the presence of transcripts of the genes encoding the proteins of interest.

Protocol:

Because relatively small PCR products were expected, 1% agarose gels were prepared. Seakem agarose was dissolved in TAE buffer (0.4 g in 40 ml) and heated in the microwave till the agarose solution was boiling. The content was stirred by gently shaking it, and 5 µl Gelred was added in the PCR hood when the solution had cooled a little. The solution was then poured into the tray and left to solidify for approximately 30 minutes. When the gel was firm enough, the comb was removed and the casting tray was placed in the electrophoresis chamber. TAE buffer was poured into the chamber so that the entire gel and the electrodes were covered. Five µl 1kb+ ladder and 10 µl of the samples were loaded onto the gel in separate wells. The lid of the chamber was then correctly placed on top of the electrophoresis chamber and connected to the power supply. The gel was run for approximately 45 min at 90 V.

3.6. Assessing the effect of LT-ag and st-ag on periostin, thrombospondin and gelsolin promoter activity using transient Transfection

The effects of MCPyV LT-ag and st-ag on the gelsolin, periostin and thrombospondin promoters in MCPyV negative MCC cells were studied using transient transfection studies with luciferase reporter plasmids. DNA of the luciferase reporter plasmid with the respective promoters was transformed into *E.coli* DH5 cells for amplification, and plasmid DNA was isolated and transfected into the MCC13 cells. The periostin and thrombospondin luciferase reporter plasmids were obtained from other publications (Landré et al., 2016; Yang et al., 2003) and kindly shipped to us. The gelsolin promoter-luciferase reporter plasmid was not available from other research groups, and it was therefore attempted generated. However, this was unsuccessful (see results). Therefore, the plasmid was purchased from GenScript. This company synthesized part of the gelsolin promoter and cloned it into the luciferase reporter plasmid.

3.6.1.Transformation of plasmid DNA into *E.coli* DH5

The luciferase reporter plasmid pGL3-basic with the promoter of periostin, gelsolin or thrombospondin, as well as DNA of the expression vectors for MCPyV LT-ag and st-ag as well as the empty vector control pcDNA3.1 were transformed into competent *E.coli* DH5 cells and amplified for further use in co-transfection studies.

Bacterial transformation involves the internalization of exogenous DNA. It is a natural process that enables bacteria to adapt to challenging environmental conditions like the presence of an antibiotic substance. In order for genetic transformation to occur, the transformable bacterium needs to express the required genes involved in the process. A bacterium is said to be competent when it is ready to take up exogenous DNA. The genes making the bacterial cells competent are not constitutively expressed, and competence can therefore be seen as a temporary opportunity for DNA internalization and hence subsequent transformation. In many bacterial species competence is triggered by stressful conditions (Johnston, Martin, Fichant et al., 2014).

Protocol:

Competent *E.coli* DH5 cells were available in the lab. The cells were thawed on ice before 200 µl competent cells and 10 ng plasmid DNA was transferred to a cultivation tube. The

cultivation tubes were incubated 30 minutes on ice before they were transferred to a 42℃ water bath and incubated for 90 seconds. Then, 800 µl SOC medium was added and the tubes were incubated in the shaker at 37℃ for 45 minutes. Two hundred µl bacterial suspension was plated on selective agarose plates supplemented with 100 µg/ml ampicillin and incubated over night at 37℃.

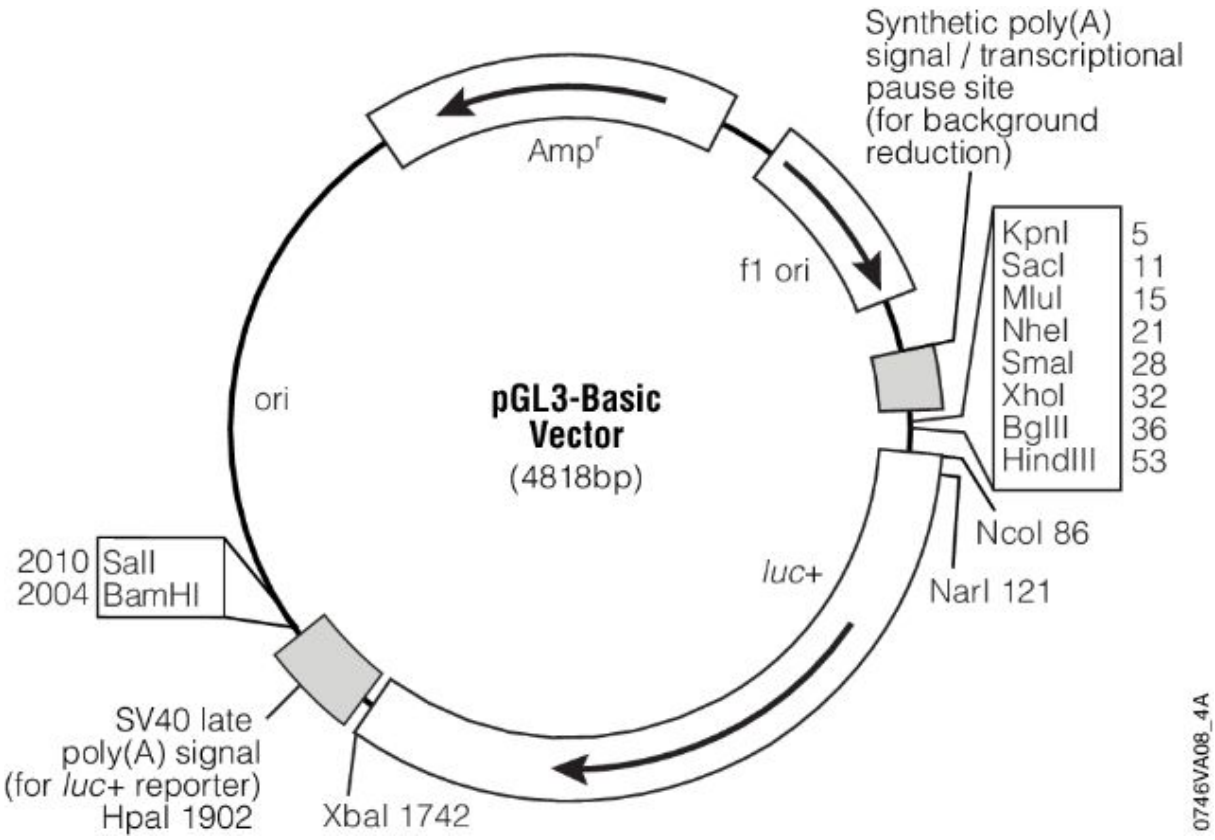

Figure 7. pGl3 basic vector. The vector is a luciferase reporter plasmid optimised for monitoring transcriptional activity in transfected eukaryotic cells (Promega, 2017).

3.6.2. Plasmid purification

DNA of the luciferase reporter plasmids with the promoters of gelsolin, periostin, or thrombospondin and the LT-ag or st-ag expression plasmids were purified from *E.coli* DH5 using the NucleoBond® Xtra Midi kit from Macherey Nagel for further use in co-transfection studies. The NucleoBond® Xtra Midi kit is based on alkaline lysis followed by binding of plasmid DNA to an anion exchange column (Macherey Nagel, 2014).

The principle of alkaline lysis is based on the distinctive properties of different DNA species after lysis. In order to isolate the plasmids, the cells are first treated with lysozyme to weaken the cell wall. Subsequently the cells are lysed completely with SDS and NaOH (Birnboim & Doly, 1979). SDS is a strongly anionic detergent that solubilizes the cell membrane. It also has a denaturing effect on many cell proteins. NaOH degrades the cell wall and disrupts the hydrogen bonding between the DNA bases, converting the dsDNA in the cell, including the genomic DNA and plasmid DNA, to single stranded DNA (ssDNA). When a solution containing both chromosomal DNA and plasmid DNA is neutralised, using e.g. potassium acetate, high molecular weight chromosomal DNA will re-anneal in an unorganized meshwork, while covalently closed circular DNA manages to renature properly because they are topologically intertwined (Birnboim & Doly, 1979; Sambrooke & Russel, 2001). The high concentration of potassium acetate from the neutralization step also causes precipitation of protein-SDS complexes, genomic DNA and other cellular debris (Macherey Nagel, 2014). The cellular debris can hence easily be discarded by loading the lysate on to the NucleoBond® Xtra column filters (Macherey Nagel, 2014). The Xtra Midi kit operates by gravity flow; when the lysate is loaded onto the column it is cleared by the NucleoBond® Xtra Silica Resin that contains hydrophilic, large, porous silica beads coated with methyl-amino-ethanol (MAE). Under acidic conditions, the NH-group provides a high overall positive charge. The positively charged NH-group binds the negatively charged phosphate backbone of plasmid DNA with high specificity. Furthermore, the OH-group can create hydrogen bonds with the DNA (Figure 8). Changing the pH of the column to a slightly more alkaline environment facilitates elution of the plasmid DNA. Larger DNA fragments that are able to re-anneal can form several interactions with the positively charged resin and are therefore eluted later with increasing salt concentration. Smaller DNA fragments and single stranded RNA/DNA carry less charge and bind with less affinity. These fragments are thus eluted at an earlier stage (Macherey Nagel, 2014).

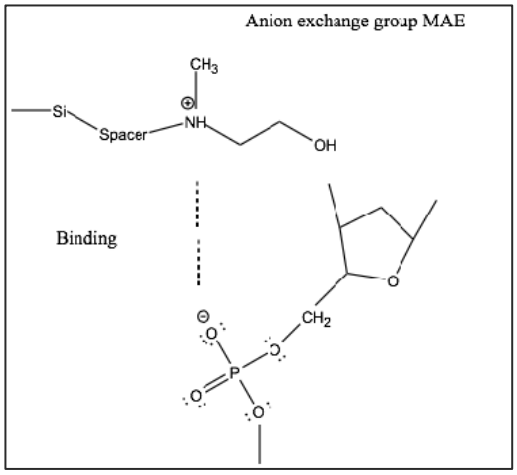

Figure 8. The positively charged NH-group binds the negatively charged phosphate groups of the DNA backbone. The OH-group also enables the formation of hydrogen bonds between MAE and DNA. Modified from a figure in Macherey Nagel 2014 (Macherey Nagel, 2014).

Protocol:

Isolation of plasmids starts with growth and harvesting of the cell culture that contains the plasmid of interest. One colony was picked from the agarose plates containing *E.coli* DH5 transformed with the respective luciferase reporter plasmids as well as the empty vector pcDNA3.1. The colony was subsequently transferred to a cultivation tube containing 1 ml LB broth supplemented with ampicillin. The pre-culture was then transferred to a 100 ml overnight culture after approximately 3.5 hours. The selective growth medium on the plates and in the broth ensures that only the bacteria containing the plasmid of interest grows. The following day, the overnight culture was transferred to sterile 45 ml falcon tubes before they were centrifuged at 5,000 x g for 10 minutes in order to pellet the bacteria containing the plasmids. The supernatant was discarded and the tubes were placed upside down until the pellet was dry. At this stage in the protocol the pellet can easily be frozen down at -20℃, so that the purification process can be completed at a later stage. The pellet was then re-suspended in 8 ml RES buffer from the kit. This buffer contains RNase in order to degrade RNA from the lysate. 8 ml LYS buffer was then added and gently mixed in order to lyse the cells. The samples were incubated at room temperature for 5 minutes before 8 ml of neutralization buffer NEU was added. During the incubation time the specialized nucleospin column was prepared and equilibrated by adding 12 ml of EQU buffer to the rim of the column filter. Inverting the tube and pipetting up and down mixed the content of the tube, before the lysate was transferred to the bottom of the nucleospin column. The column was allowed to empty by gravity flow. The filter was then washed with 5 ml of EQU buffer that

was added at the rim of the filter in order to ensure proper washing of the filter. Next, the filter was discarded before 8 ml of washing buffer WASH was added directly to the samples in order to avoid low purity. The column was placed over an empty 45 ml falcon tube before 5 ml elution buffer ELU was added. Then 3.5 ml of isopropanol was added to precipitate the eluted plasmid DNA. The sample was then centrifuged at 15,000 x g for 30 minutes. The mass was carefully adjusted with isopropanol before centrifugation. The supernatant was discarded before the pellet was washed with 2 ml of 99.6 % ethanol. The tubes were weighed and the mass adjusted with MQ-water before the samples were centrifuged for 10 minutes at 15,000 x g and the supernatant was discarded. The pellet was dried at room temperature and then dissolved in an appropriate volume of AE/TE buffer. The content was transferred to an eppendorf tube and the plasmid concentration was determined using Nano Drop.

3.6.3. Transient transfection and luciferase assay

In order to investigate whether the viral genes LT-ag and st-ag affects the expression of periostin, thrombospondin and gelsolin. MCC13 cells were transiently co-transfected with a luciferase reporter plasmid containing the promoter of periostin, thrombospondin or gelsolin (Table 7) and either empty vector pcDNA3.1 or an expression vector for MCPyV LT-ag or st-ag. These expression vectors contain the cDNA of LT-ag or st-ag in a pcDNA3.1-like backbone vector.

Transfection is the process of delivering exogenous nucleic acids into mammalian cells. The host cells can be transfected either stably or transiently. In stable transfection, the transfected gene is integrated in the genome and passed on when the cells replicate. Transiently transfected genes are not integrated in the host genome and hence they are only expressed for a limited period of time (Kim & Eberwine, 2010). Chemical transfection is the most common transfection method in contemporary research, and the one used here. Chemical transfection reagents are positively charged polymers that mask the intrinsic negative charge of the DNA backbone, and hence allow interaction with the negatively charged cell membrane. It is believed that uptake of nucleic acid/chemical complex is facilitated by endocytosis and phagocytosis (Kim & Eberwine, 2010).

Protocol:

Transient transfection studies were performed in 12-well plates. In these experiments 150,000, 200,000 and 250,000 MCC13 cells (depending on the growth rate of the cells) were

seeded out in each well of a 12-well plate. The following day the cells were ready for transfection. In this thesis, Jet Prime transfection reagent from polypluss transfection was used according to the manufacturers instruction. Due to differences in promoter strengths, we wanted to transfect the cells with 200 ng LT-ag and st-ag expression plasmids and 400 ng of the luciferase reporter plasmids and the empty vector pcDNA 3.1. pcDNA 3.1 was used to adjust the amount of DNA in each tube up to 800 ng, as the amount of DNA added affects the transfection efficiency (Table 19).

300 µl JetPrime buffer and the appropriate amount of DNA were added to each tube according to table 19 before the content was vortexed and spun down. Then JetPrime reagent was added in a DNA:JetPrime reagent ratio of 1:2. The transfection mix was then incubated for 10 min at room temperature before 95 µl was added to each well. The plates were incubated over night in the 37℃, 5 % CO2 incubator.

Table 19. Sample preparation for co-transfection with pGL3- periostin/gelsolin/thrombospondin luciferase constructs and LT-ag and/or st-ag expression vectors.

DNA	**Protein (periostin/gelsolin/thrombospondin) + pcDNA**	**Protein (periostin/gelsolin/thrombospondin) + LT-ag**	**Protein (periostin/gelsolin/thrombospondin) + st-ag**	**Protein (periostin/gelsolin/thrombospondin) + LT-ag and st-ag**
pGL3-periostin/gelsolin/thrombospondin (400 ng)	1.2 µl	1.2 µl	1.2 µl	1.2 µl
LT-ag (200ng)		1.9 µl		0.6 µl
st-ag (200 ng)			0.6 µl	0.6 µl

pcDNA (400ng)	1.2 µl	0.6 µl	0.6 µl	
Final amount of DNA added to each tube	800 ng	800 ng	800 ng	800 ng

3.6.4. Luciferase assay

The luciferase assay was used to measure the effect of LT-ag and st-ag on the periostin, gelsolin and thrombospondin promoter activity. These promoters drive the transcription of the *luciferase* gene and the amount of luciferase protein is monitored indirectly by measuring the activity of this enzyme. Luciferase catalyses the conversion of luciferin into oxoluciferin, and this reaction releases light:

$$Luciferin + O_2 + ATP \rightarrow oxyluciferin + CO_2 + AMP + diphosphate + light$$

The luciferase gene of the firefly *Pythonitus pyralis* was used. The amount of light emitted can be measured precisely using a luminometer and the amount of light emitted reflects the amount of luciferin oxidised, and therefore the amount of luciferin produced by the cells (Sambrooke & Russel, 2001). The method is sensitive, fast and relatively cheap. The disadvantage is that the promoter is studied out of its natural context and that multiple copies of the promoter are introduced into the cells, which is different for the two endogenous copies found in a normal diploid cell. Transcription activators or repressors that are expressed at low levels in the cell may become limited for the high number of promoter copies. Therefore, the promoter activity measured may differ from the endogenous promoter activity (Sambrooke & Russel, 2001).

The luciferase value of each sample was normalized to the protein concentration of the corresponding sample. The protein concentration was determined using the Protein Quantification Assay from Macherey-Nagel.

Protocol:

In order to measure the luciferase values 12 eppendorf tubes corresponding to the wells in the 12 well plate were marked. The medium was carefully removed from the wells and the cells washed with 1 ml PBS. All traces of PBS were removed by suction, and 100 µl TROPIX lysis buffer containing 0.5 µM DTT was added to each well. The cells in each well were harvested by scraping, and subsequently transferred to the corresponding eppendorf tubes. The tubes were then centrifuged for 3 minutes at 13,000 rpm (Microfuge 22R centrifuge) at room temperature. Twenty µl of TROPIX lysis buffer (blank) or of the samples were then loaded onto a white luminometer microtitre plate. Air bubbles were removed with a needle before the luciferase activity was measured using the CLARIOstar® luminometer.

3.6.5. Protein quantification assay

The protein quantification assay is a reliable kit used to determine protein concentration. The basic principle of the kit is to measure light extinction photometrically after the addition of the quantification reagent QR. The kit is based on a method described by Karlsson et al. in 1994, where trichloric acid (TCA) was added to a dilution series with SDS solubilized albumin and increasing turbidity was measured at 570 nm (Karlsson, Ostwald, Kabjorn et al., 1994).

Protocol:

Twenty µl supernatant from each sample was transferred to empty wells in a blank 96 well micro titre plate before 40 µl buffer PSB and then 40 µl quantification reagent QR was added to each well. The content in each well was pipetted up and down until the colour changed completely from blue to yellow. The micro titre plate was then incubated at room temperature for 30 minutes. All air bubbles were removed using a needle. Light extinction was measured photometrically at 570 nm using the CLARIOstar® machine.

3.7. Cell viability of MCC13 cells treated with recombinant protein was measured using MTT assay

The MTT (3-(4,5-dimethylthiazol-2-yl)-2,5-diphenyltetrazolium bromide) tetrazolium reduction assay is an assay for assessing cell metabolic activity. The method is generally used to determine cell viability and proliferation (Riss, Moravec, Niles et al., 2004). Here the assay was used to assess the effect of the proteins periostin, thrombospondin and gelsolin on MCC13 cell proliferation. The assay is based on the fact that viable cells with active metabolism convert MTT into a purple coloured, crystallized formazan product with an absorbance maximum around 570 nm. Since dead cells are not able to convert the MTT reagent to the formazan product, the quantity of purple crystals formed are presumably directly proportional to the number of viable cells. The amount of formazan is determined by recording changes in absorbance at 570 nm using a plate reading spectrophotometer (Riss et al., 2004). Before the MTT reagent is added to the cells the cells are usually starved in order to ensure that their metabolism is low and that the perceived changes are due to the stimulants added. Moreover, it is important that an equal number of cells are seeded out in each well.

Protocol:

Day 1: MCC13 cells were seeded out in triplicates with 35,000 cells/well in starvation medium RPMI-1640 supplemented with 0.1 % FBS (cells were seeded directly in Opti-MEM for the last three experiments conducted with recombinant periostin from Novus). Cells were seeded out in three 24 well plates in a total of 15 wells per plate; 3 wells for the vehicle control containing Opti-MEM supplemented with 1x PBS since the proteins were reconstituted in PBS, for each protein 9 wells with three different protein concentrations, and 3 wells containing Opti-MEM supplemented with 10 % serum as a positive control (RPMI-1640 supplemented with 10 % FBS was used in the three last experiments conducted with recombinant periostin from a second supplier).

Day 2: The medium was first removed from the wells using water suction before they were washed with 500 µl Opti-MEM (this washing step was omitted when the experiment was repeated with periostin from a different supplier). Thereafter, 0.1 ng/µl, 0.5 ng/µl and 1.0 ng/µl recombinant thrombospondin or periostin protein was added to the cells. Premixes containing Opti-MEM and the recombinant proteins as well as positive and negative controls were prepared; Three tubes with 5 ml Opti-MEM containing the protein to the right dilution,

one tube containing 5 ml Opti-MEM supplemented with PBS and one tube containing 5 ml Opti-MEM supplemented with 10 % FBS were prepared. Thereafter 500 µl of the appropriate solution was added in triplicates to the cells on the 24 well plates. The plates were left in the CO_2 incubator for 24, 48 and 72 hours respectively.

At the appropriate time of the assay (after 24 h, 42, h and 72 h) 1:10 dilution of MTT in prewarmed Opti-MEM (22.5 µl Opti-MEM + 2.5 µl MTT) was prepared. First the supernatant in each well was removed by water suction. Subsequently 500 µl MTT solution was added to each well and incubated for 3 hours before 500 µl stop solution (isopropanol/3.3 % HCl) was added to each well. The cells were incubated with the stop solution for up to an hour until all the crystals had been dissolved. At halftime of the incubation, the content of the wells was pipetted up and down and 100 µl from each well was transferred to a 96 well plate (Nunc cell culture plate) and the absorbance at 590 nm was measured using the CLARIOstar® machine.

3.8. Statistical analysis

All statistical tests of significance are based around a null hypothesis. The next step in any statistical analysis is to calculate the probability of the null hypothesis being true. This is expressed with a p-value. If the p-value is small enough one can assume that the differences observed are not due to random chance. It is normal to operate with 95 % ($p<0.05$) and 99 % ($p<0.01$) significance levels (Helbæk, 2001). An Analysis of variance (ANOVA) test is used when three or more groups are compared. The test is used to determine whether the groups compared are significantly statistically different from each other by comparing the means within each group to the means between each group. However, the ANOVA cannot tell you which specific groups were statistically significantly different from each other, only that at least two groups were (Helbæk, 2001). Post hoc tests such as Dunnet's test must be deployed in addition to the ANOVA in order to determine the specific groups that stood out. Dunnett's test is basically a more sophisticated T-test that takes into account the multiple testing problem (if we test two independent true null hypothesises with significance level 0.05 the probability that neither test is significant is 0.95*0.95=0.90, i.e. the probability of getting a significant result increases) (Bland & Altman, 1995; Lowry, 2008). It is used when you want to compare each of a number of treatments with a single control (McHugh, 2011). One- or

two-way ANOVA tests can be used depending on the data. In a one-way ANOVA, one varying factor that affects the outcome is considered. The two-way ANOVA measures the interaction between two varying factors and the possible interaction within these (Helbæk, 2001). In this study, one-way ANOVA was used in the individual luciferase experiments, where the varying factor was different transfection treatments. The two-way ANOVA was used to create a combined graph for all luciferase experiments. Here different transfection treatments and differences between the three individual experiments were considered. Two-way ANOVA was used for all MTT experiments since the experiments vary in both treatment and incubation time. When the ANOVA test detected significant differences in the dataset Dunnet's post hoc test was applied to the dataset in order to determine which groups differed significantly from each other. Only p values obtained from the post hoc tests are showed since the ANOVA does not indicate where in the data the difference is located (ANOVA tables are presented in appendix 2 and 3). Graph pads programme Prism 7 was used to determine the statistical significance. Statistical significance was calculated relative to the empty vector PC DNA 3.1. *= $p \leq 0.05$, statistically significant; ** = $p \leq 0.01$, very statistically significant; *** and **** = $p \leq 0.001$ and $p \leq 0.0001$, extremely statistically significant.

4. Results

4.1. Two distinct populations of vesicles were detected in the four MCC cell lines used in the study using Nicomp particle sizing system (PSS)

In order to verify that the exosome isolation was successful, the size of the isolated exosomes was measured using the Submicron Particle sizer 370. For all the cell lines used (MKL-1, MKL-2, MCC13 and MCC26) two distinct populations of vesicles could be detected after three parallel runs. Vesicles detected in the respective cell lines are shown in Figures 9-12.

For MKL-1 one population with a mean diameter of 48.7 nm $\pm$ 6.8 nm (13.89 %) and one population with a mean diameter of 440.8 nm $\pm$ 39.8 nm (9.04 %) were detected. Run 1 and 2 (MKL-1 001 and MKL-1 002, Figure 9.) are mostly overlapping while there is a clear shift to the right (i.e. increased diameter of the particles) in the third reading. This tendency is likely

due to agglomeration of exosomal vesicles in the sample tube since the content of the tube had not been homogenized for a while. As a consequence, it can be argued that the mean diameter is skewed and that the second population of exosomes is probably closer to 250 nm.

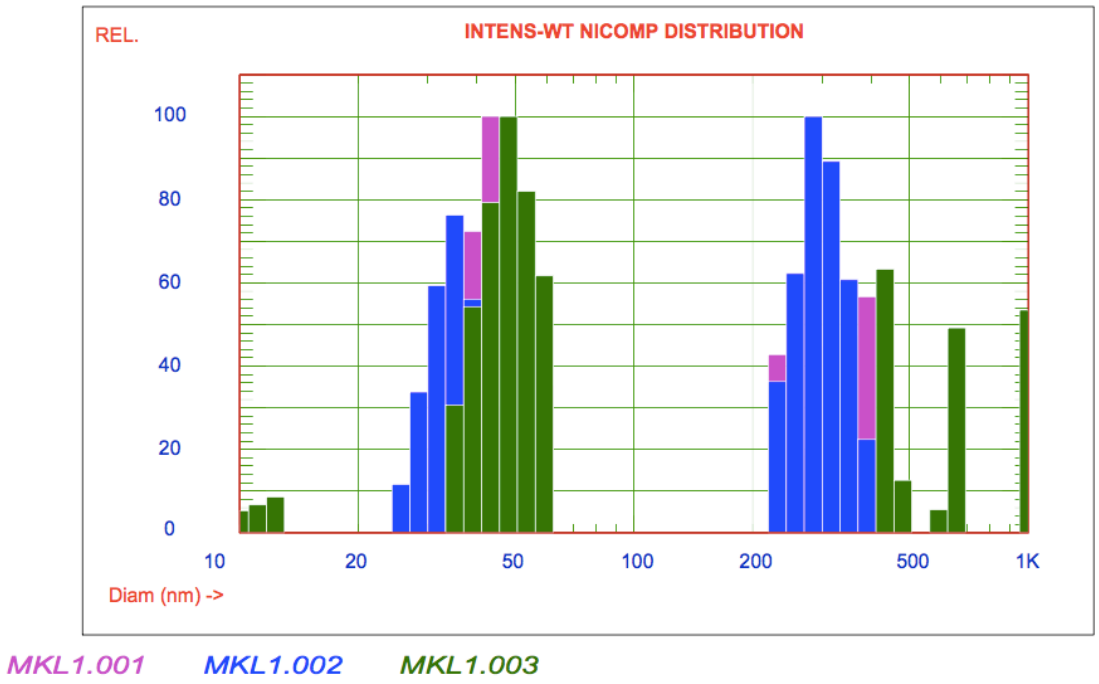

Figure 9. MKL-1 extracellular vesicle size determination. Exosomes isolated from MKL-1 cells were analysed using Nicomp Submicron Particle Sizer. The time of each run was adjusted so that ~1000 particles were measured. The Nicomp distribution after three parallel runs showed two distinct populations of MKL-1 exosomes. The diameter of the vesicles (nm) is shown in X-axis and intensity weighted scattering is shown in the Y-axis. The first population had a mean diameter of 48.7 nm ± 6.8 nm (13.89 %), while the second population had a mean diameter of 440.8 nm ± 39.8 nm (9.04 %).

For MKL-2 cells, the Nicomp PSS analysis showed that the first population of exosomes had a mean diameter of 39.9 nm ± 3.4 nm (8.57 %). The mean diameter of the second population was not calculated by the programme, but from the graph it can be estimated that the mean diameter is ~150 nm (Figure 10).

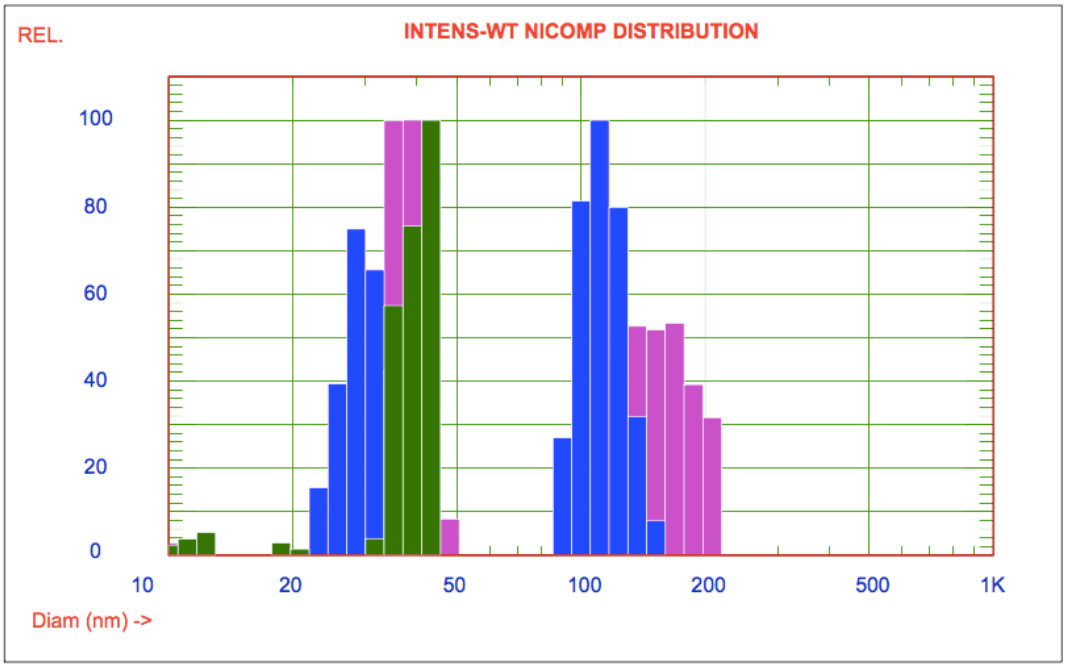

Figure 10. MKL-2 extracellular vesicle size determination. Exosomes isolated from MKL-2 cells were analysed using Nicomp Submicron Particle Sizer. The time of each run was adjusted so that ~1000 particles were measured. For MKL-2 cells two separate populations of exosomes were detected after three parallel runs on the PSS machine. The Nicomp PSS analysis showed that the first population of exosomes showed a mean diameter of 39.9 nm ± 3.4 nm (8.57 %). The mean diameter of the second population, on the other hand, was not detected by the programme, but can be estimated to be ~150 nm.

Two respective populations of MCC13 exosomes were detected by the Nicomp analysis (Figure 11). The first exosome population is narrowly distributed with a mean diameter of 39.4 nm ± 5nm (12.69 %). The second peak shows a population of vesicles with a mean diameter of 325.9 nm ± 41.6 nm (12.75 %). Interestingly, the second parallel run shows larger vesicles than the third parallel run. The reason for this is not known. Nevertheless, the second vesicle population is most likely composed of agglomerated smaller vesicles as MCC exosomes have been found to be in the size range 30-150 nm (Konstantinell, Bruun, Olsen et al., 2016).

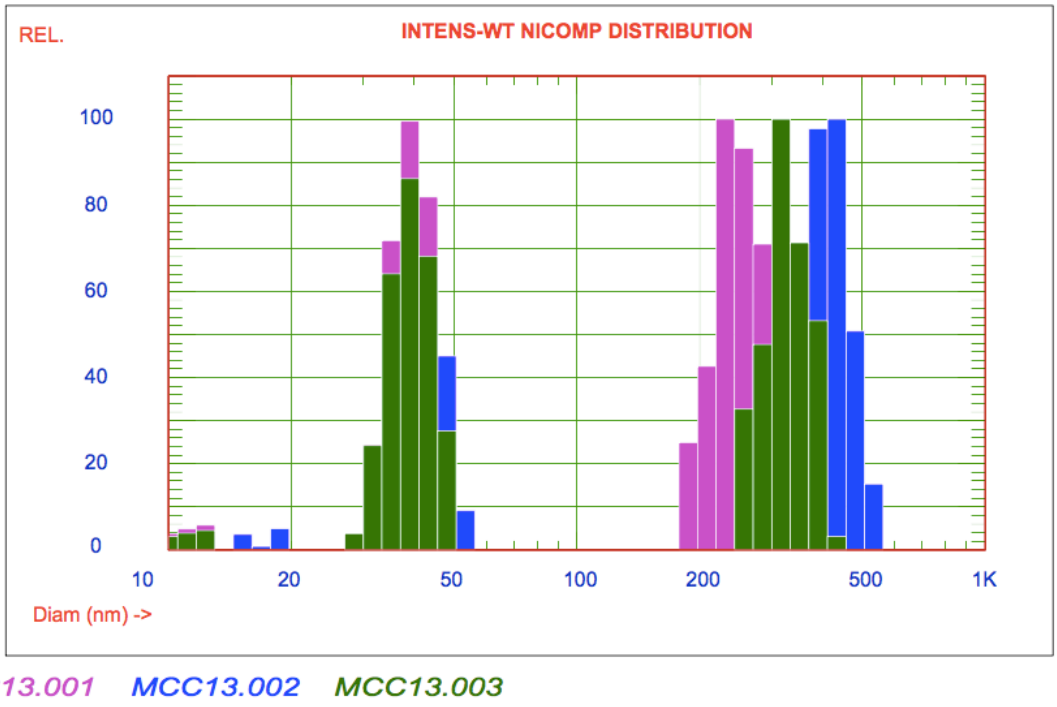

Figure 11. MCC13 extracellular vesicle size determination. Exosomes isolated from MCC13 cells were analysed using Nicomp Submicron Particle Sizer. The time of each run was adjusted so that ~1000 particles were measured. Two different populations of MCC13 exosomes were detected after three parallel runs. The first exosome population is narrowly distributed with a mean diameter of 39.4 nm ± 5 nm (12.69 %). The second peak shows a population with a mean diameter of 325.9 ± 41.6 nm (12.75 %).

For MCC26 cells, the Nicomp PSS detects two distinct exosome populations of 36.0 nm ± 4.5 nm (12.46 %) and 200.9 nm ± 22.5 nm (11.18 %) (Figure 12). At first glance it looks like there are three different exosome populations. However, the two first parallel runs show two distinct populations of exosomes of ~ 30 nm and ~75 nm respectively. These two first readings show a narrow distribution and overlap nicely. In the third read, however, a shift to the right with larger vesicles was observed. It is likely that these do not represent a real vesicle population and that the mean vesicle size and SD calculated by the Nicomp PSS is misleading.

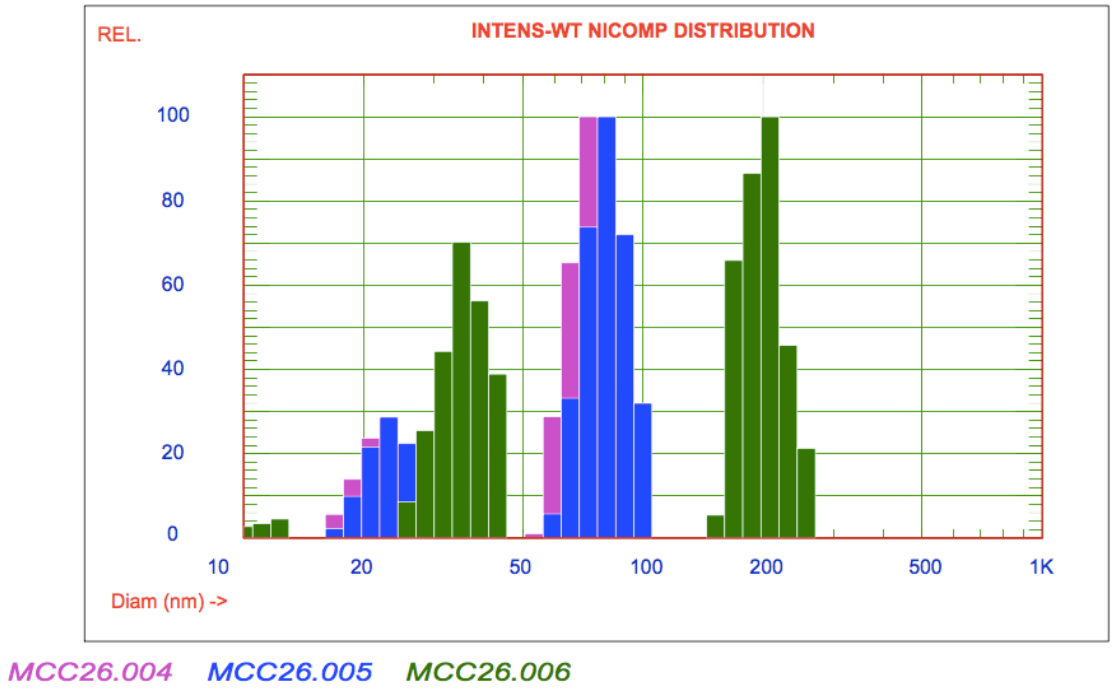

Figure 12. MCC26 extracellular vesicle size determination. Exosomes isolated from MCC26 cells were analysed using Nicomp Submicron Particle Sizer. The time of each run was adjusted so that ~1000 particles were measured. For MCC26 cells the Nicomp PSS detects two distinct exosome populations of 36.0 nm ± 4.5 nm (12.46 %) and 200.9 nm ± 22.5 nm (11.18 %) respectively after three parallel runs. The third read shows larger vesicles than the two preceding reads.

4.2. Western blot detected gelsolin, periostin and thrombospondin in exosomes of MCC cell lines

The proteins gelsolin, periostin and thrombospondin were previously detected by proteomic analyses of exosomes derived from the four MCC cell lines used in the study (Konstantinell et al., 2016). The role of exosomes derived from MCC tumour cells in the oncogenic process has not been studied, nor is it known whether MCPyV can affect the contents of such exosomes. Because these three proteins were most abundantly present in the exosomes of the four cell lines (Konstantinell et al., 2016) and have been shown to play a role in cancer (see section 1.8-1.10), studies with gelsolin, periostin and thrombospondin were pursued.

In order to verify the proteomic data and confirm the presence of the proteins of interest in the four MCPyV cell lines and their respective exosomes, western blot was undertaken. For western blot a signal corresponding to 93kDa was expected for periostin, while signals of

respectively 155kDa and 86 kDa were expected for thrombospondin and gelsolin using antibodies from Abcam (Table 4).

All three proteins were detected in exosomes isolated from MCC13, MCC26, MKL-1 and MKL-2 cells (Figures 13-15). Thrombospondin was also detected in the lysates of the four cell lines. However, neither gelsolin nor periostin seemed to be expressed at detectable levels in any of these cell lines. The experiment was repeated three times with similar results.

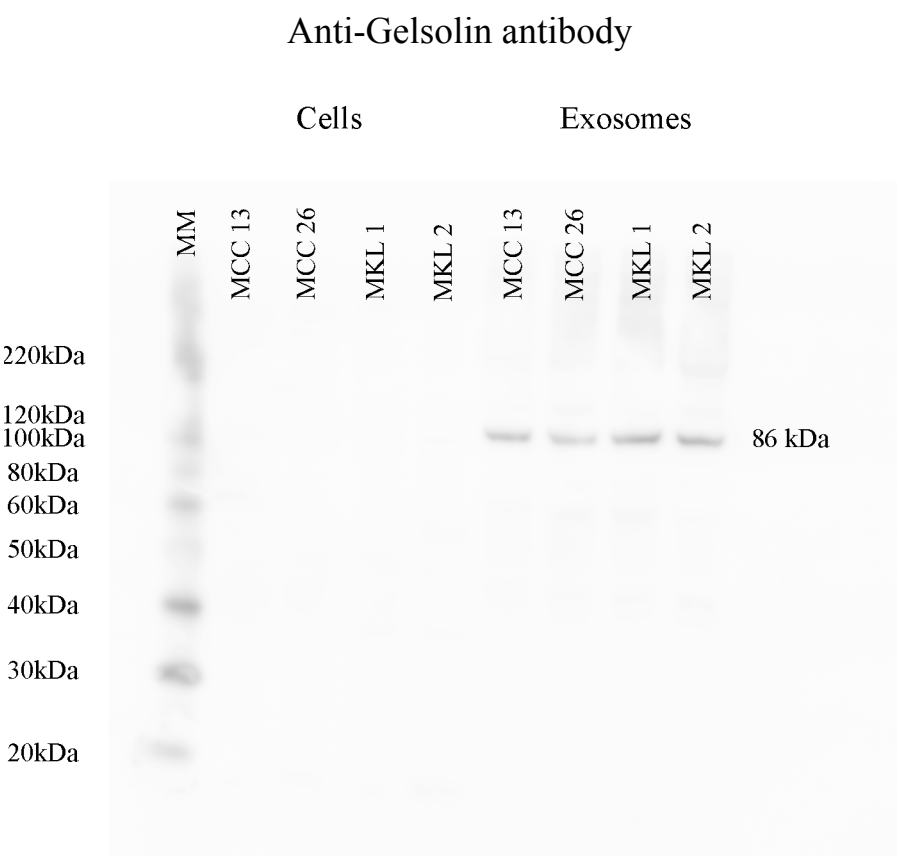

Figure 13. Gelosin (86 kDa) is detected in exosomes derived from MCPyV-positive (MKL-1 and MKL-2) and MCPyV-negative (MCC13 and MCC26) cell lines, but not in these cells. Western blot was performed with Anti-Gelsolin antibody from Abcam. Lane 1: magic marker indicating protein mass in kDa; lanes 2-5: cell lysates; lanes 6-9: exosomes derived from the cell lines.

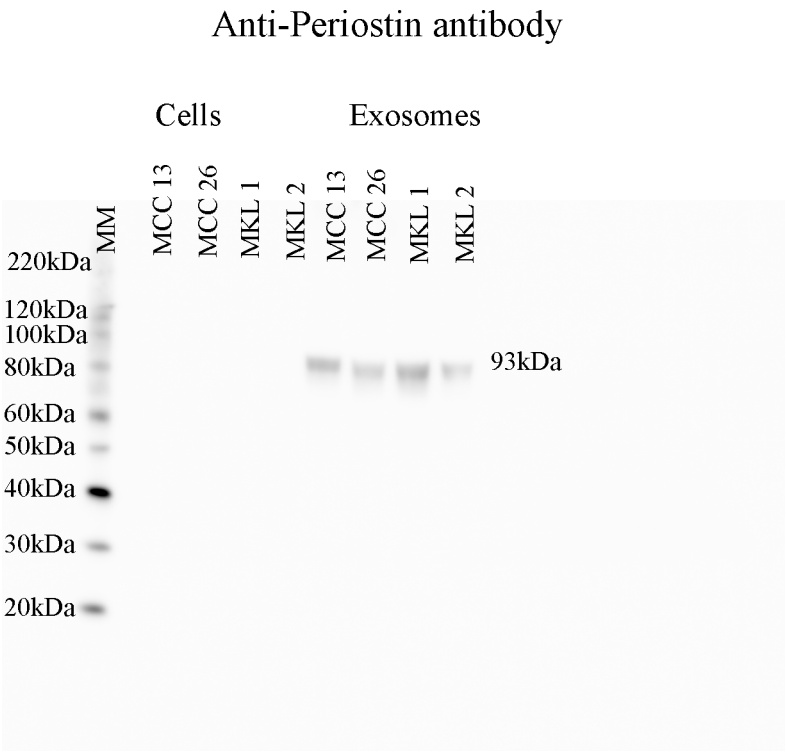

Figure 14. Periostin (93 kDa) is detected in exosomes derived from MCPyV-positive (MKL-1 and MKL-2) and MCPyV-negative (MCC13 and MCC26) cell lines, but not in these cells. Western blot was performed with Anti-Perisotin antibody from Abcam. Lane 1: magic marker indicating protein mass in kDa; lanes 2-5: cell lysates; lanes 6-9: exosomes derived from the cell lines.

Thrombospondin was detected in all MCC cell lines tested in addition to exosomes derived from the cells. One band of approximately 155 kDa (expected) and one band of approximately 120 kDa could be observed. For all cell lysates, an additional signal corresponding to an approximately 20 kDa polypeptide was detected (Figure 15). The bands from the wells containing isolated exosomes are stronger than the bands from the wells containing cell lysate. Since an equal amount of protein (30μg) was added to each well thrombospondin seems to be enriched in MCC exosomes. Furthermore, virus negative cell lines seem to express more thrombospondin compared to the virus positive MKL-1 and MKL-2 cells. Lowest relative thrombospondin levels were observed in MKL-2 cells. Western blot with CD63 was run as a technical control as is it known to be an exosomal marker (Lin, Li, Huang et al., 2015). However, the antibody showed high degree of unspecific binding, rendering it quite useless as a control (results not shown).

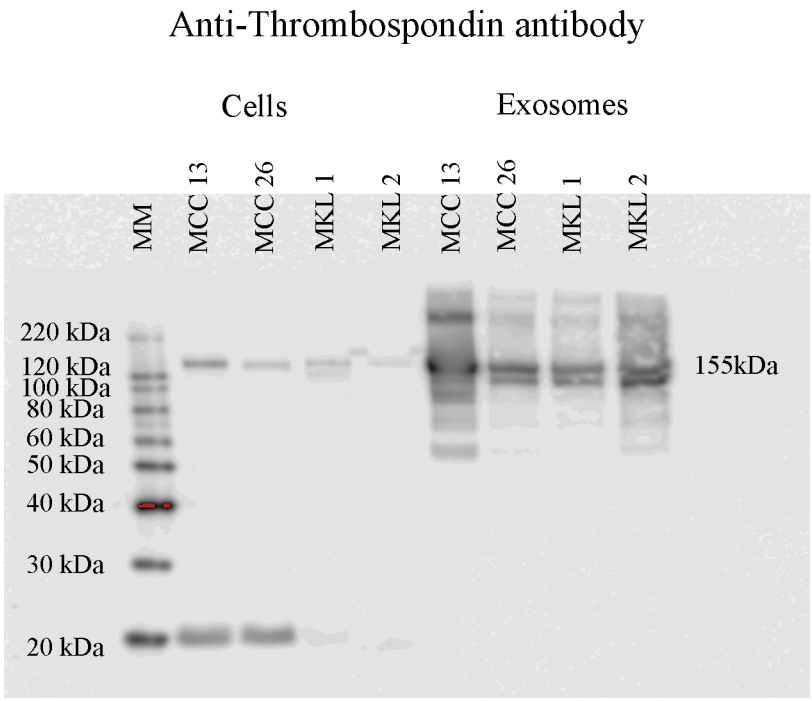

Figure 15. Thrombospondin is expressed in exosomes derived from MCPyV-positive (MKL-1 and MKL-2) and MCPyV-negative (MCC13 and MCC26) cell lines and in these cells. Western blot was performed with Anti-Thrombospondin antibody from Abcam. Lane 1: magic marker indicating protein mass in kDa; lanes 2-5: cell lysates; lanes 6-9: exosomes derived from the cell lines. Even though thrombospondin has a predicted protein mass of 129 kDa the expected fragment is 155 kDa due to glycosylation events (Abcam, 2017).

4.3. LT-ag protein was detected in MKL-1, but not in MKL-2 cells using Western blot

Western blot with antibodies directed against MCPyV LT-ag was also used to confirm that the virus positive cell lines MKL-1 and MKL-2 were actually virus positive and expressing LT-ag, and that the virus negative cell lines MCC13 and MCC26 did not express LT-ag. No bands corresponding to LT-ag were detected in the lysates of MCC13 and MCC26 cells, confirming that these cells are virus negative. A band of 50 kDa was detected in the well containing MKL-1. This corresponds with the expected size of truncated LT-ag expressed in MKL-1 (Shuda, Chang, & Moore, 2014). For MKL-2 a band of ~37 kDa corresponding to the truncated LT-ag expressed in this cell line was expected (Shuda et al., 2014). However, we failed to detect LT-ag expression in these cells with western blot (Figure 16).

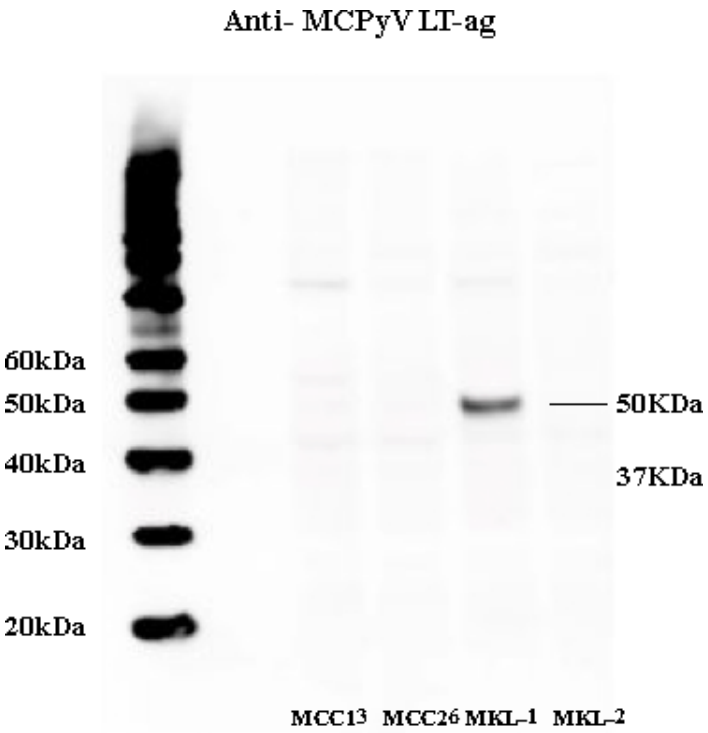

Figure 16. Detection of MCPyV LT-ag in MCC cells using western blot. MCPyV LT-ag (50 kDa) was detected in MKL-1, but no signal corresponding to the 37 kDa truncated LT-ag variant expressed in MKL-2 was observed. Western blot was performed with MCPyV large T antigen antibody from Santa Cruz Biotechnology. The left lane shows the protein ladder magic marker with protein fragments of known sizes (in kDa).

ERK-2, a 42 kDa protein kinase, was used as a loading control since the protein is relatively constant expressed in all cells and shows a clear gradual decrease in band strength following decreased protein load (Figure 17) (Dittmer & Dittmer, 2006). Since the bands obtained were of equal size (42 kDa) and strength, it indicates that equal amount of protein were added to each well.

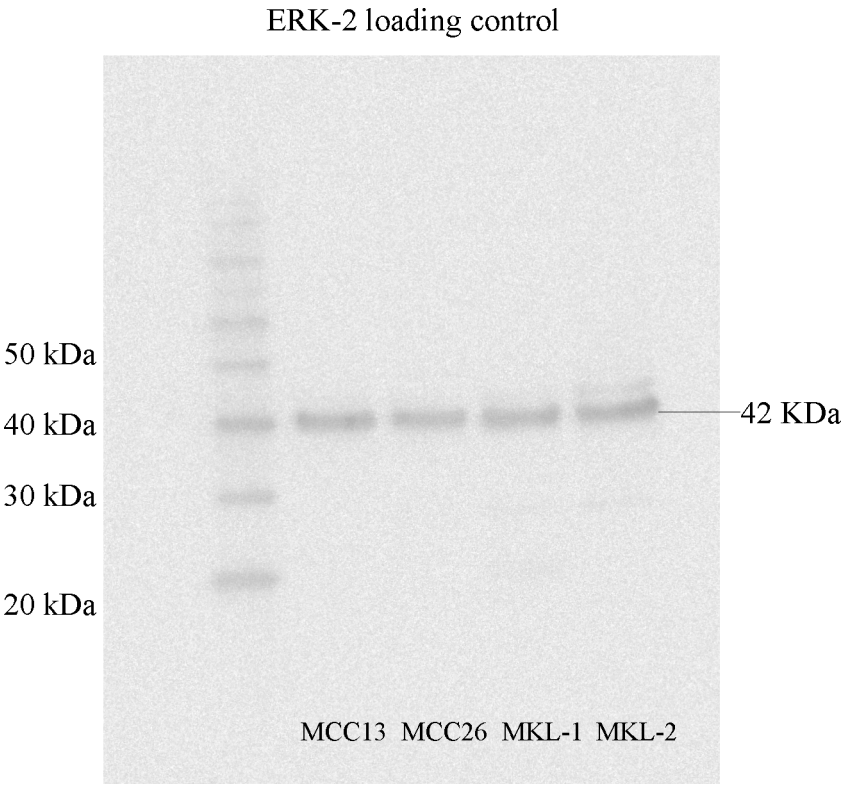

Figure 17. ERK-2 loading control. Four signals with similar intensity corresponding to 42 kDa were detected in the MCC cell lines used. Western blot was performed with ERK-2 antibody from Santa Cruz Biotechnology. The protein mass marker magic marker with 20 kDa, 30 kDa, 40 kDa and 50 kDa is shown to the left.

4.4. Periostin and thrombospondin were detected in MCC cell lines by RT-PCR

Since western blot only confirmed the presence of gelsolin and periostin in exosomes derived from MCC cells and weaker bands of thrombospondin were obtained in the wells containing MCC cell lysate, RT-PCR with specific primers was undertaken.

Total RNA was isolated from MCC13, MMC26, MKL-1 and MKL-2 cells and converted into cDNA. PCR with specific primers was performed, and the PCR products were analysed on a 1 % agarose gel in the presence of GelRed.

To check that the cDNA was free for contaminating genomic DNA, PCR was performed with primers complementary to the housekeeping gene *APRT*. These primers generate a 308 bp product for cDNA, while an 805 bp fragment is obtained with genomic DNA. Only the 308 bp fragment was obtained (Figure 18), suggesting that the cDNA prep did not contain contaminating genomic DNA.

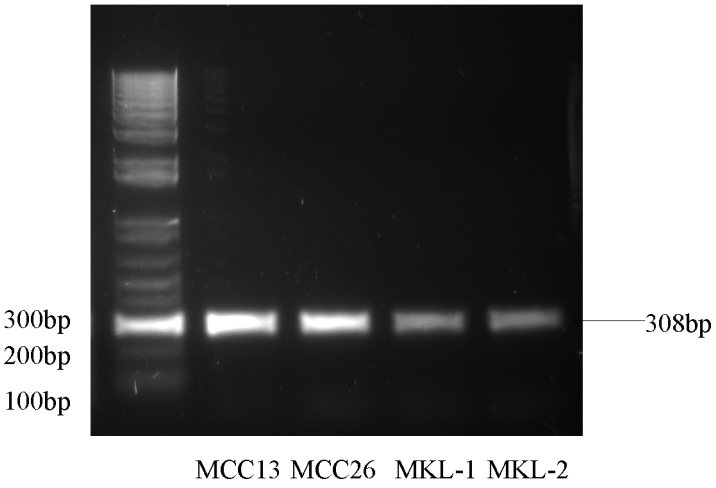

Figure 18. Detection of APRT transcripts in MCC cell lines by RT-PCR. Total RNA was purified from the four cell lines and converted to cDNA. Forty PCR cycles were run with APRT specific primers and the products were analysed on a 1 % agarose gel in the presence of GelRed. Left lane: 1kb+ size marker. The 100, 200 and 300 bp fragments are indicated. The expected APRT PCR product of 308 bp was detected in all cell lines examined.

The cDNA was then used to amplify the periostin and thrombospondin sequences in the MCC cell lines. Two isoforms of periostin with bands of 155 bp and 239 bp were detected in all MCC cell lines (Figure 19). This is in accordance with what Bai et al. found in their study when using the same primer pair (Bai, Nakamura, Zhou et al., 2010).

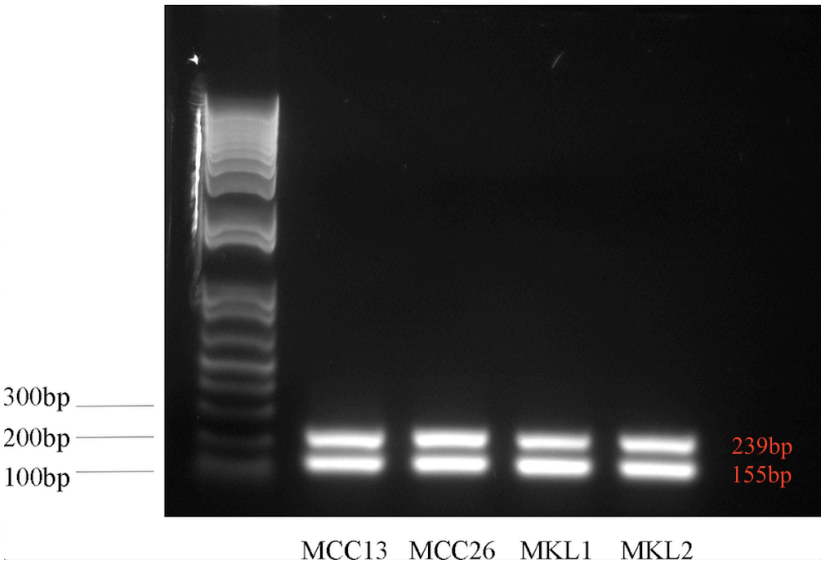

Figure 19. Detection of periostin transcripts in MCC cell lines using RT-PCR. The RT-PCR reaction confirmed that all MCC cell lines contained Periostin. The two bands in the picture (239 and 155 bps) were expected and are due to two different isoforms of periostin. The lane on the left contains the 1kb+ size marker. The bands of 100, 200 and 300 bps are indicated. Forty-five PCR cycles were run.

Thrombospondin (235bp) was detected in the virus positive cell line MKL-1 as well as both virus negative cell lines (Figure 20). Since the western blot analysis had already confirmed the presence of thrombospondin in all cell lines the experiment was not repeated.

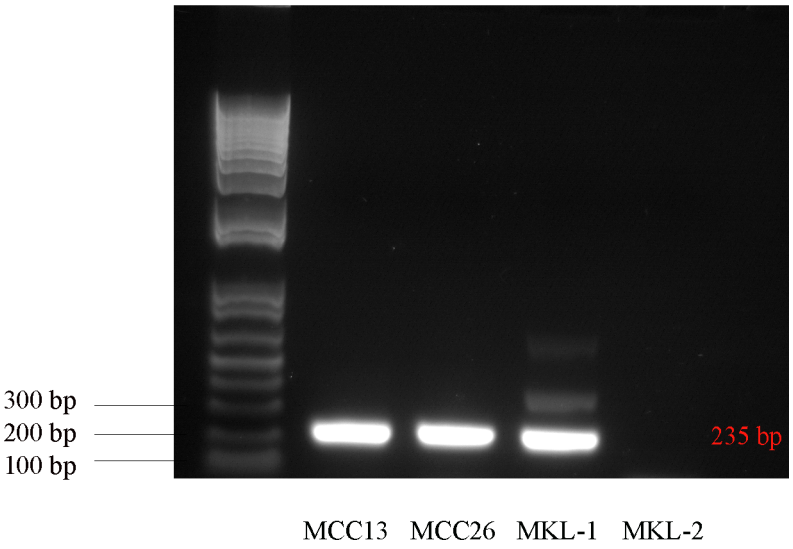

Figure 20. Detection of thrombospondin transcripts in MCC cell lines by RT-PCR. The presence of Thrombospondin (a band of 235 bp) was confirmed in all MCC cell lines except MKL-2. The lane on the left contains the 1kb+ size marker. The bands of 100, 200 and 300 bps are indicated. Forty-five PCR cycles were run.

The gelsolin sequence was not amplified by RT-PCR due to lack of time.

4.5. LT-ag mRNA was detected in virus positive MCC cell lines using RT-PCR

The cDNA was further used to detect LT-ag expression using specific primers in order to verify that the virus positive cell lines MKL-1 and MKL-2 were in fact virus positive (WB could only detect LT-ag in MKL-1 cells). The virus negative cell lines MCC13 and MCC26 were used as negative controls. LT-ag was detected in both MKL-1 and MKL-2 cells and not in the virus negative cell lines MCC13 and MCC26 (Figure 21). The somewhat stronger band in MKL-1 cells indicates a higher expression of LT-ag in MKL-1 cells than in MKL-2 cells (this could explain that LT-ag could only be detected in MKL-1 cells with western blot). Furthermore, the MKL-1 band is slightly smaller (394bp compared to 440bp) due to a deletion in the MKL-1 genome (Appendix 1). In conclusion, both MKL-1 and MKL-2 express LT-ag, although the expression levels seem to be lower in MKL-2 cells. This is in agreement with Guastafierro et al. who also found lower LT-ag expression levels in MKL-2 compared to MKL-1 (Guastafierro et al., 2013).

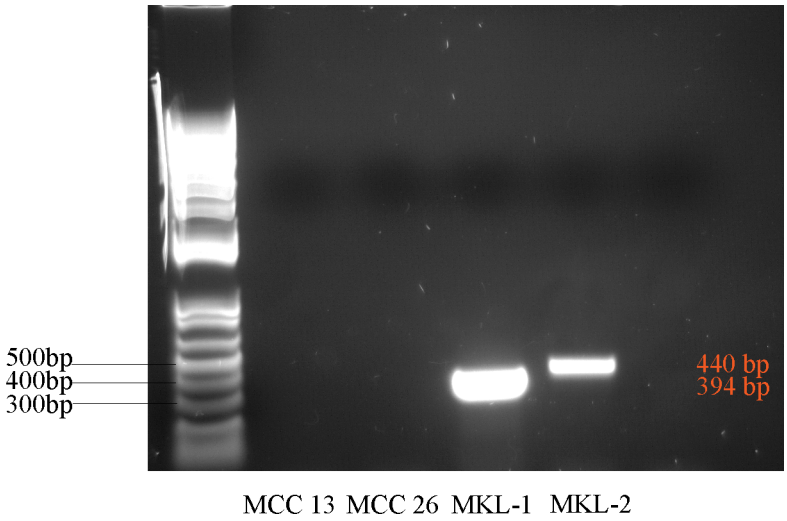

Figure 21. Detection of LT-ag transcripts in MCC cell lines by RT-PCR. LT-ag transcript was detected in the virus positive MCPyV cell lines MKL-1 and MKL-2 by RT-PCR. The lane on the left contains the 1kb+ size marker. The bands of 300, 400 and 500 bp are indicated. The expected sizes of PCR products for MKL-1 and MKL-2 of 394 and 440 bp, respectively were obtained. Forty-five RT-PCR cycles were run.

4.6. LT-ag, but not st-ag activates the gelsolin, periostin and thrombospondin promoters

LT-ag and st-ag of polyomaviruses have been shown to increase the expression of numerous cellular genes (Moens, Seternes, Johansen et al., 1997). This prompted us to test whether MCPyV LT-ag or/and st-ag had an effect on the expression of the *gelsolin, periostin* and *thrombospondin* genes. Transient transfection studies with a luciferase reported gene under control of the promoter of either one of these genes were performed in MCC13 cells. Cells were co-transfected with the empty expression vector pcDNA3.1 or with an expression plasmid for MCPyV LT-ag or/and st-ag.

Periostin and thrombospondin luciferase reporter constructs were obtained from other research groups (Landré et al., 2016; Yang et al., 2003). A luciferase reporter plasmid with the gelsolin promoter on the other hand was not available, and the gelsolin luciferase construct therefore had to be created before it could be used in transient transfection studies. The idea was to amplify the gelsolin promoter from human genomic DNA purified from blood by PCR, followed by TA-cloning into the TA vector pCR2.1 before cutting it out with the restriction enzymes *Nhe*I and *Xho*I, and inserting it in the *Nhe*I and *Xho*I restriction sites of pGL3 basic vector. The gelsolin promoter was attempted amplified with both Accustart

and Jumpstart PCR mixes, and two different PCR programmes with specially adjusted annealing temperatures and elongation times were run. However, the expected PCR fragment was not obtained probably due to high GC-content (298 bases out of 419; i.e. 71 %) of the gelsolin promoter. A last attempt to obtain the promoter was given using the Phusion® High-Fidelity DNA Polymerase, as this enzyme is recommended for difficult GC-rich constructs. Nevertheless, the desired band was not obtained and the gelsolin luciferase construct was finally ordered from GenScript. It should be noted that GenScript also had problems due to the promoters high GC-content. The promoter was attempted created several times, and in the end it had to be synthetized in different fragments and only one correct clone was obtained.

The effect of MCPyV LT-ag or st-ag alone, or the combined effect of LT-ag plus st-ag on the promoter activity of these three genes as measured in relative luciferase values is shown in Figures 22-24. MCC13 cells were transfected, as these are MCPyV negative.

Co-transfection with the gelsolin luciferase plasmid and MCPyV LT-ag expression vector showed a significant increase in promoter activity in all three experiments ($p=0.0001$, $p=0.001$ and $p=0.0059$ respectively) (Figure 22 A, B and C). When the data from the three experiments were combined (Figure 22 D) the effect of MCPyV LT-ag was found to be extremely significant in all three experiments ($p=0.0001$, $p=0.0001$ and $p=0.0002$). No significant effect was detected for either MCPyV st-ag alone or for MCPyV LT + st-ag combined, suggesting that st-ag inhibits LT-ag's stimulatory effect on the gelsolin promoter activity.

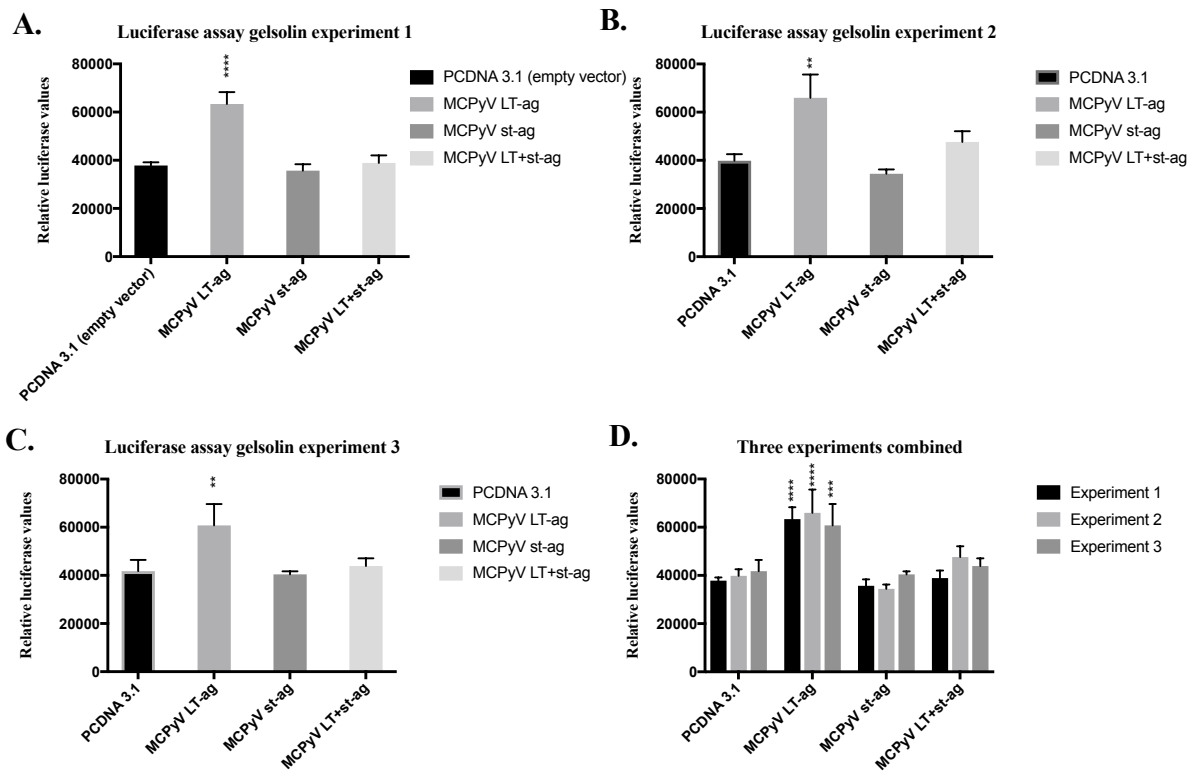

Figure 22. MCPyV LT-ag and st-ag's effect on gelsolin expression in MCC13 cells. MCC13 cells were co-transfected with the luciferase reporter plasmid containing the periostin promoter and either empty vector pcDNA3.1 or expression vector for MCPyV LT-ag or/and st-ag. Luciferase values were normalized to the protein concentration in each sample. The experiment was run in triplicates, and one bar represents the average relative luciferase value of three independent parallels. A, B and C shows the three parallel luciferase assays conducted and D shows the three experiments combined. Statistical significance is indicated by * above the bars (*= $p \leq 0.05$, statistically significant; ** = $p \leq 0.01$, very statistically significant; *** and **** = $p \leq 0.001$ and $p \leq 0.0001$, extremely statistically significant), and was calculated using one-way ANOVA for the individual experiments and two-way ANOVA for the combined experiments graph. The ANOVA was supplemented with Dunnet's post hoc test comparing each treatment to the empty vector pcDNA 3.1. **A.** In the first experiment LT-ag was extremely significantly different from the empty vector ($p=0.0001$). Neither st-ag nor LT + st-ag had a significant effect on the gelsolin promoter activity. **B.** In the second experiment LT-ag caused a very significant increase in gelsolin promoter activity ($p=0.001$). The combined effect of LT and st-ag and the effect of st-ag alone were not significant. **C.** In the third experiment the effect of LT-ag on the gelsolin promoter was found to be very significant ($p=0.0059$). Also here the effect of st-ag alone and the combined effect of st-ag and LT-ag were found to be insignificant. **D.** When the data from the three experiments were analysed together using a two-way ANOVA, the effect of MCPyV LT-ag was found to be extremely significant in all three experiments ($p=0.0001$, $p=0.0001$ and $p=0.0002$). No significant effect was detected for either MCPyV st-ag alone or for MCPyV LT+ st-ag combined.

MCC13 cells transiently transfected with the periostin luciferase plasmid and either MCPyV LT-ag or MCPyV LT + st-ag showed a significant increase in periostin promoter activity in the three parallel experiments conducted (p=0.0005, p=0.0346 and p=0.0107 for LT-ag and p=0.0344, p=0.0030 and p=0.0434 for LT + st-ag) (Figure 23 A, B and C). When combining the three experiments (Figure 23 D), LT-ag was found to have a very significant effect on promoter activity in experiment 1 (p=0.0011). In experiment 2, MCPyV LT-ag caused a significant increase (p=0.0353) and MCPyV LT + st-ag caused an extremely significant increase in promoter activity (p=0.0009). In the third experiment, LT-ag's effect on the periostin promoter was found to be extremely significant (p=0.0001) while the combined effect of st-ag and LT-ag was found to be very significant (p=0.0012).

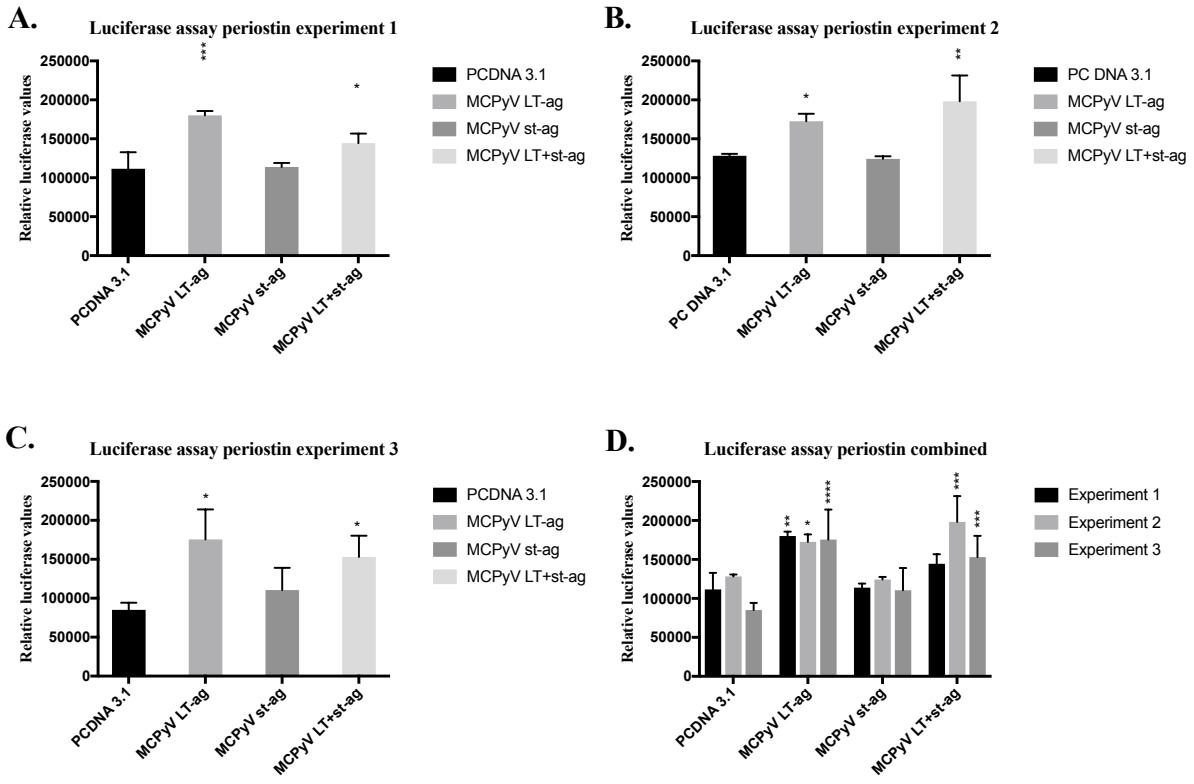

Figure 23. MCPyV LT-ag and st-ag's effect on periostin expression in MCC13 cells. Cells were co-transfected with the luciferase reporter plasmid containing the periostin promoter and either empty vector pcDNA3.1 or expression vector for MCPyV LT-ag or/and st-ag. Luciferase values were corrected for protein concentration in each sample and each bar represents the average of three independent parallels. A, B and C shows the three parallel luciferase assays conducted and D shows the three experiments combined. Statistical significance is indicated by * above the bars (*= $p \leq 0.05$, statistically significant; ** = $p \leq 0.01$, very statistically significant; *** and **** = $p \leq 0.001$ and $p \leq 0.0001$, extremely statistically significant), and was calculated using one-way

ANOVA for the individual experiments and two-way ANOVA for the combined experiments graph. The ANOVA was supplemented with Dunnet's post hoc test comparing each treatment to the empty vector pcDNA 3.1. **A.** In experiment 1 co-transfection with MCPyV LT-ag led to an extremely significant increase in periostin expression (p=0.0005), and transfection with both MCPyV LT- and st-ag also led to a significant increase in periostin expression (p=0.0344). **B.** Co-transfection with MCPyV LT-ag led to a significant increase in periostin expression (p=0.0346), and co-transfection with both MCPyV LT-ag and st-ag showed a very significant increase (p=0.0030) in the second experiment. **C.** In the third experiment both MCPyV LT-ag and MCPyV LT + st-ag led to a significant increase in periostin expression (p=0.0107 and p=0.0434). **D.** When using a two-way ANOVA accounting for different treatments and different experiments, the wells containing MCPyV LT-ag and periostin showed a very significant increase in experiment 1 (p=0.0011). In experiment 2, MCPyV LT-ag showed a significant increase (p=0.0353) while both LT-ag and st-ag led to an extremely significant increase in periostin expression (p=0.0009). In the third experiment MCPyV LT-ag's effect on periostin expression was found to be extremely significant (p=0.0001) and the combined effect of MCPyV LT- and st-ag was found to be very significant (p=0.0012). The effect of MCPyV st-ag alone showed no significant difference in periostin expression in any of the experiments.

MCC13 cells co-transfected with the thrombospondin luciferase plasmid and the expression vector for MCPyV LT-ag showed a significant increase of the thrombospondin promoter activity in all three experiments (p=0.0005, p=0.0346 and p=0.0107), while MCPyV st-ag showed no significant differences from the empty vector pcDNA 3.1 in any of the experiments. A significant stimulatory effect of combined expression of LT-ag pluss st-ag was measured on the thrombospondin promoter in the third experiment (p=0.0434). Since this difference was smaller than the one observed for LT-ag alone and no effect could be detected in experiment 1 and 2, the data suggests that st-ag impedes LT-ag's stimulatory effect (Figure 24 A, B and C). The three experiments combined showed an extremely statistically significant increase in thrombospondin expression following co-transfection with LT-ag in all experiments and LT-ag + st-ag in the third experiment (p=0.0001) (Figure 24 D).

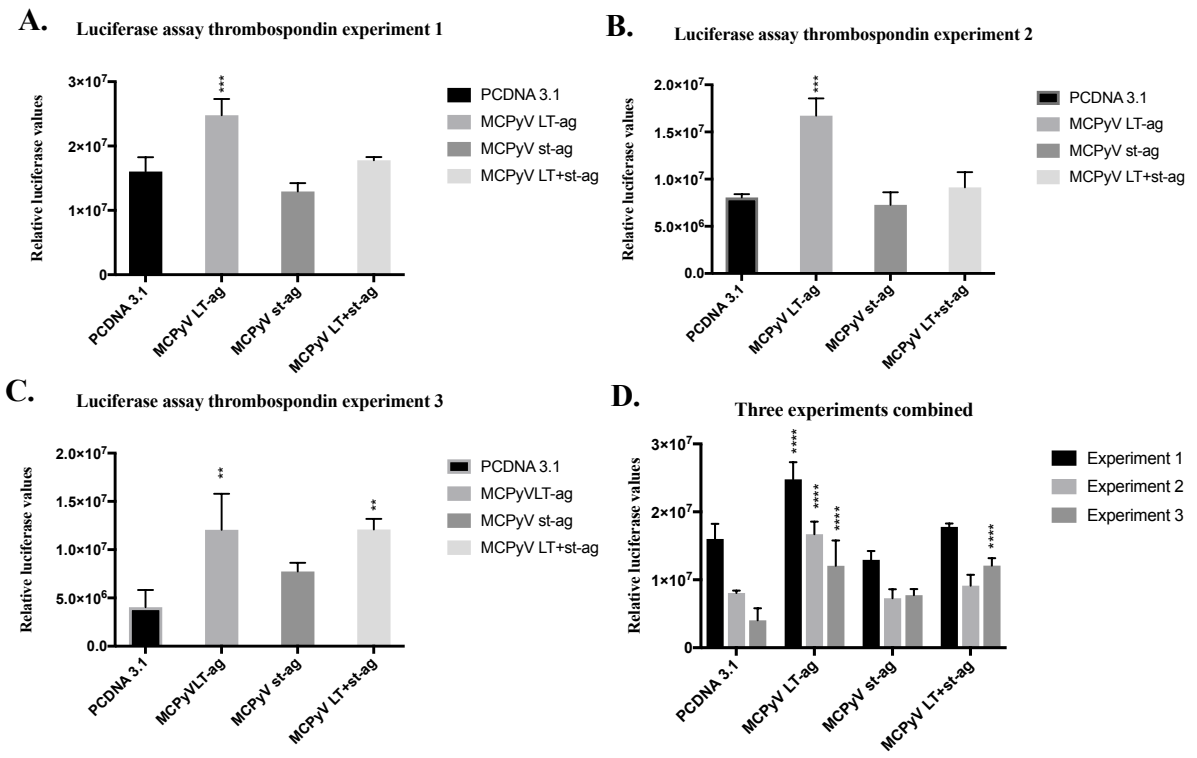

Figure 24. MCPyV LT-ag and st-ag's effect on thrombospondin expression in MCC13 cells. Cells were co-transfected with the luciferase reporter plasmid containing the thrombospondin promoter and either empty vector pcDNA3.1 or expression vector for MCPyV LT-ag or/and st-ag. Each bar represents the average of three independent parallels. Luciferase values were corrected for protein concentration in each sample. A, B and C shows the three parallel luciferase assays conducted and D shows the three experiments combined. Statistical significance is indicated by * above the bars (* = $p \leq 0.05$, statistically significant; ** = $p \leq 0.01$, very statistically significant; *** and **** = $p \leq 0.001$ and $p \leq 0.0001$, extremely statistically significant), and was calculated using one-way ANOVA for the individual experiments and two-way ANOVA for the combined experiments graph. The ANOVA was supplemented with Dunnet's post hoc test comparing each treatment to the empty vector pcDNA 3.1. **A.** In experiment 1, cells co-transfected with thrombospondin luciferase plasmid and the expression vector for MCPyV LT-ag showed an extremely significant increase of promoter activity (p=0.0005). No significant effect was detected for either st-ag or LT-ag + st-ag combined. **B.** In the second experiment LT-ag significantly increased thrombospondin promoter activity (p=0.0346). No stimulatory effect was detected for s t-ag or LT-ag + st-ag combined. **C.** In the third experiment a significant increase in thrombospondin promoter activity was detected when co-transfecting the cells with LT-ag (p=0.0107) and LT-ag + st-ag (p=0.0434). Co-transfected with MCPyV st-ag showed no significant differences from the empty vector pcDNA 3.1 on the thrombospondin promoter in any of the experiments. **D.** When the three experiments were combined LT-ag had an extremely significant increase in thrombospondin promoter activity in the three experiments (p=0.0001 for all 3). MCPyV LT-ag + st-ag showed an extremely significant increase in promoter activity in the third experiment (p=0.0001).

The co-transfection experiments in general showed that expression of MCPyV LT-ag with any of the luciferase reporter plasmids led to a significantly higher activity of the promoters, showed in higher relative luciferase values, as compared with the wells containing the empty vector pcDNA 3.1. MCPyV st-ag alone did not have a significant effect on promoter activity of any of the proteins (Figure 22, 23 and 24). Co-transfection with MCPyV LT-ag + st-ag and periostin also showed a significant increase in relative luciferase values compared to the empty vector. One out of three co-transfection experiments with thrombospondin and LT-ag + st-ag also showed a significant effect on the thrombospondin promoter. Nevertheless, this increase is in general less significant than the effect of MCPyV LT-ag alone.

4.7. Cell viability was not enhanced following exposure to recombinant gelsolin, periostin and thrombospondin proteins

To initiate the understanding of the biological relevance of exosomal proteins in MCC, we measured the effect of gelsolin, periostin and thrombospondin on MCC13 cell proliferation. MCC13 cells were incubated with increasing amounts of recombinant protein (0.1, 0.5 and 1 μg/μl) and proliferation was measured after 24, 48 and 72 hours using the MTT assay. Three parallel experiments were conducted.

In all the MTT assays conducted we experienced some problems growing the MCC13 cells treated with recombinant proteins in the 24 well plates. When studying the cells in the light microscope prior to assay start, it could be observed that the cells had changed morphology from their normal outstretched appearance and rounded up. Some cells had detached from the wells, especially in the lower right side of the 24-well plate, and may therefore have been washed off (results not shown).

The MTT assays conducted on serum starved MCC13 cells treated with increasing concentrations of recombinant gelsolin protein for different time points showed no significant differences in cell proliferation, as measured by the amount of formazan product produced, in experiment 1 and 3 for any of the protein concentrations (Figure 25 A and C). No cell proliferation was observed for the positive control, i.e. serum-treated cells in any of the experiments. However, a significant decrease in cell proliferation could be detected after 48 hours for the cells treated with 1 μg/μl recombinant gelsolin and for the positive control in

experiment 2 (Figure 25 B). Especially the latter is unexpected since normal cell medium supplemented with FBS was expected to induce proliferation in serum starved cells.

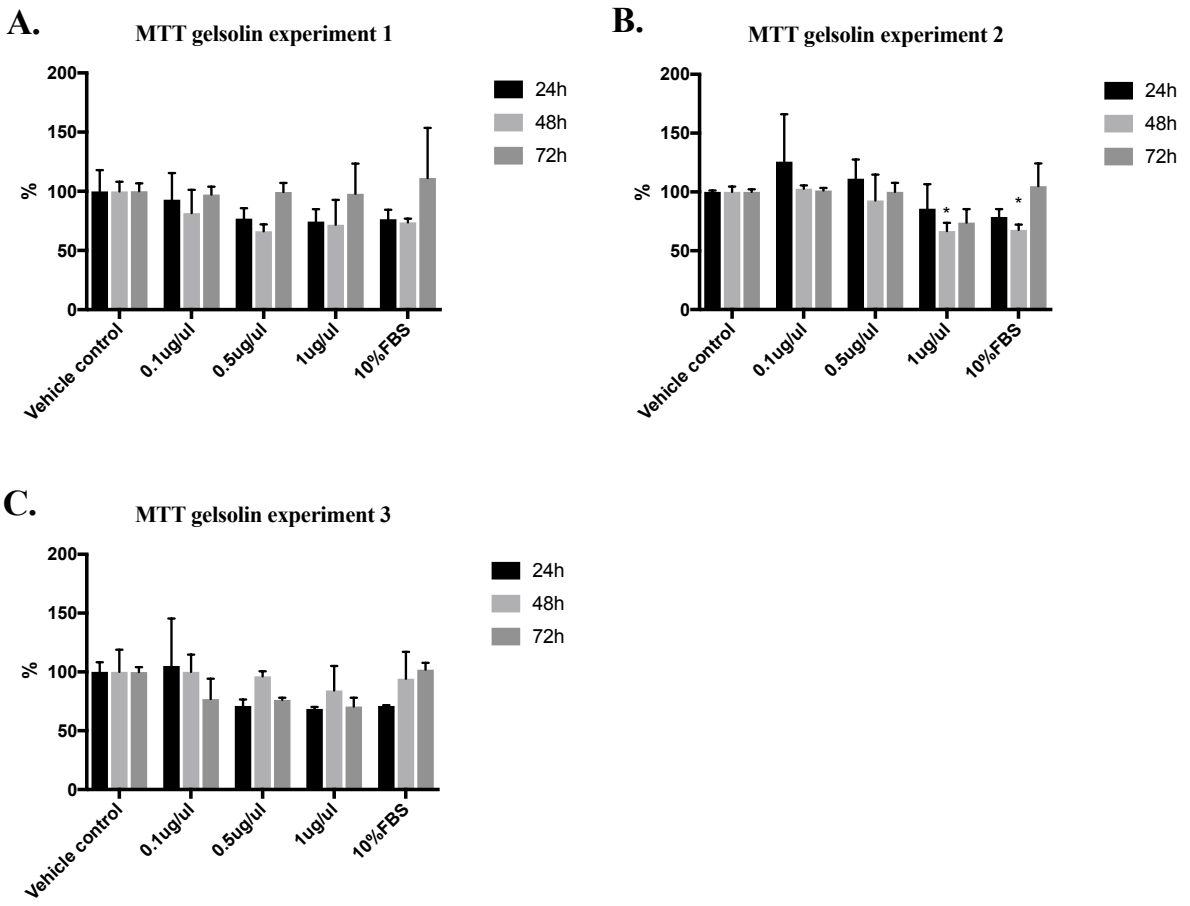

Figure 25. Proliferation of MCC13 cells in response to gelsolin. Starved MCC13 cells were treated with 0.1, 0.5 and 1μg/μl recombinant gelsolin protein, and the effect on cellular proliferation was measured using MTT-assay after 24, 48 and 72 hours respectively. Each treatment was compared pairwise to the vehicle control (Opti-MEM supplemented with 2 % PBS since the recombinant proteins were reconstituted in PBS) that was set as 100 %. Opti-MEM supplemented with 10 % FBS was used as a positive control. Two-way ANOVA followed up by Dunnet's post hoc test were used to analyse the data. Statistical significance is indicated by * above the bars (*= $p \leq 0.05$, statistically significant; ** = $p \leq 0.01$, very statistically significant; *** and **** = $p \leq 0.001$ and $p \leq 0.0001$, extremely statistically significant). Three parallel experiments were conducted (A, B and C). **A/C.** In experiment 1 and 3 no significant differences between the vehicle control and the different treatments could be detected. **B.** In the second experiment a significant decrease in cell proliferation was detected after 48 hours for both 1μg/μl gelsolin ($p=0.0424$) and the positive control ($p=0.0500$). Each bar represents the average of three independent parallels.

MCC13 cells treated with 0.1 μg/μl and 0.5 μg/μl recombinant periostin protein followed by MTT assay showed no significant difference to the vehicle control in any of the experiments (Figure 26). One μg/μl periostin showed a significant decrease in the formation of the crystalized formazan product in experiment 1 after 48 hours and in experiment 3 after 72 hours, indicating less viable cells. The positive control is significantly higher than the vehicle control in the second experiment after 72 hours. Even though no significant differences can be detected for the positive controls in experiment 1 and 3, an increasing trend in cell proliferation after 72 hours was observed (Figure 26).

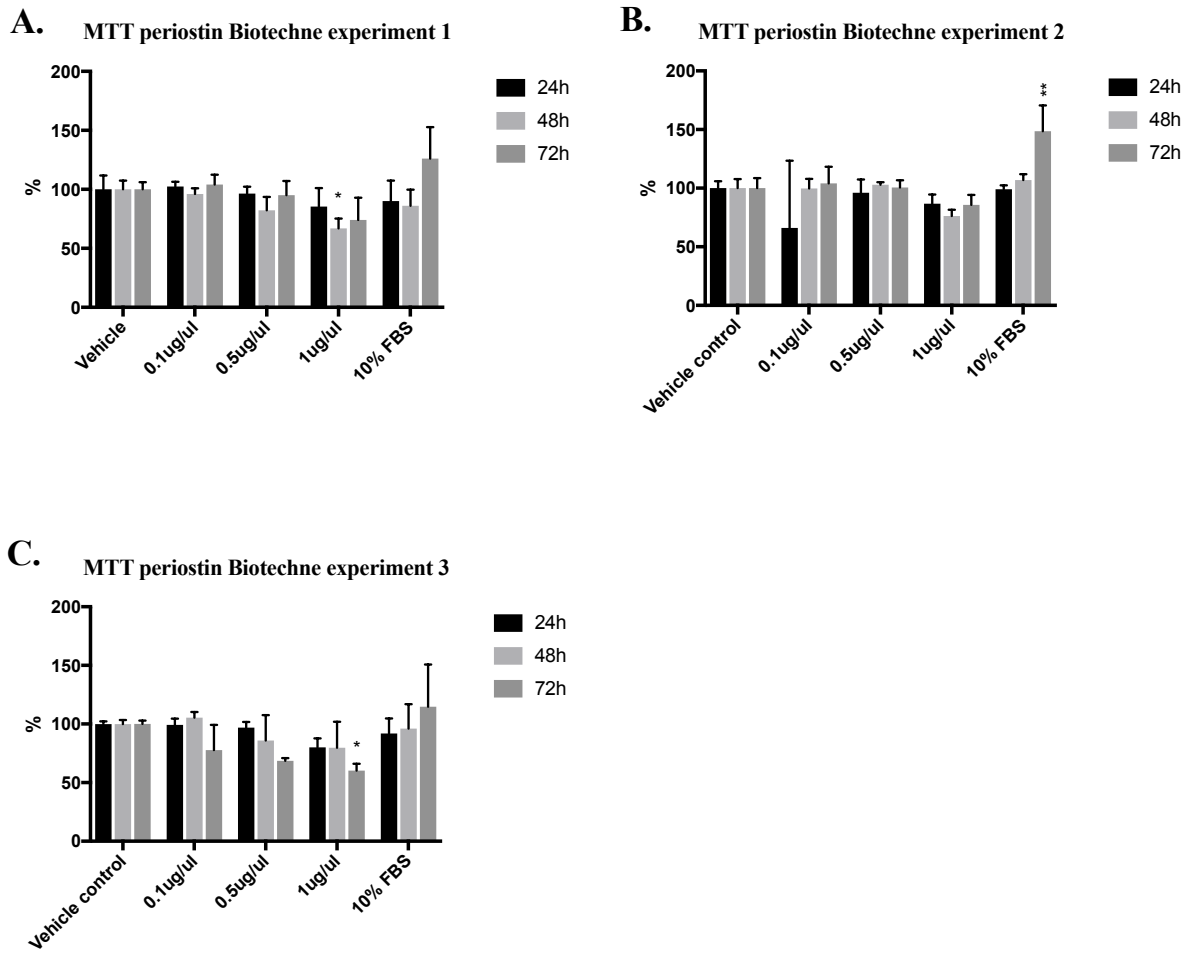

Figure 26 Proliferation of MCC13 cells in response to periostin. Serum starved MCC13 cells were treated with 0.1, 0.5 and 1μg/μl recombinant periostin protein, and the effect on cellular proliferation was measured using MTT-assay after 24, 48 and 72 hours respectively. Each treatment was compared pairwise to the vehicle control (Opti-MEM supplemented with 2 % PBS since the recombinant proteins were reconstituted in PBS) that was set as 100 %. Opti-MEM supplemented with 10 % FBS was used as a positive control. Two-way ANOVA followed

up by Dunnet's post hoc test were used to analyse the data. Statistical significance is indicated by * above the bars (* = p≤0.05, statistically significant; ** = p≤0.01, very statistically significant; *** and **** = p ≤0.001 and p≤0.0001, extremely statistically significant).Three parallel experiments were conducted (A, B and C). **A**. A significant decrease in cell viability or proliferation was measured after 48 hours for 1μg/μl (p=0.0138) in experiment 1. No significant difference from the vehicle control was detected for any of the other treatments. **B.** In the second experiment no significant differences could be detected between the vehicle control and periostin. **C.** In the third experiment, a significant decrease in formazan product produced relative to the vehicle control was detected for the wells containing 0.1 μg/μl periostin (p=0.0121). Each bar represents the average of three independent parallels.

In the first MTT assay conducted with various concentrations of recombinant thrombospondin, no significant differences in MTT conversion relative to the vehicle treated cells could be detected. In the second experiment a significant decrease in viable cells were detected after 24 hour incubation with 1μg/μl thrombospondin (p=0.0369). In the last assay conducted no significant differences could be detected between the vehicle control and increasing concentrations of thrombospondin at any of the time points measured. Serum treated cells showed a significant increase in viable cells relative to the vehicle control after 48 hours in experiment 1 and 2. An increasing trend could also be observed after 48 hours in the third experiment and after 72 hours in the two first experiments (Figure 27).

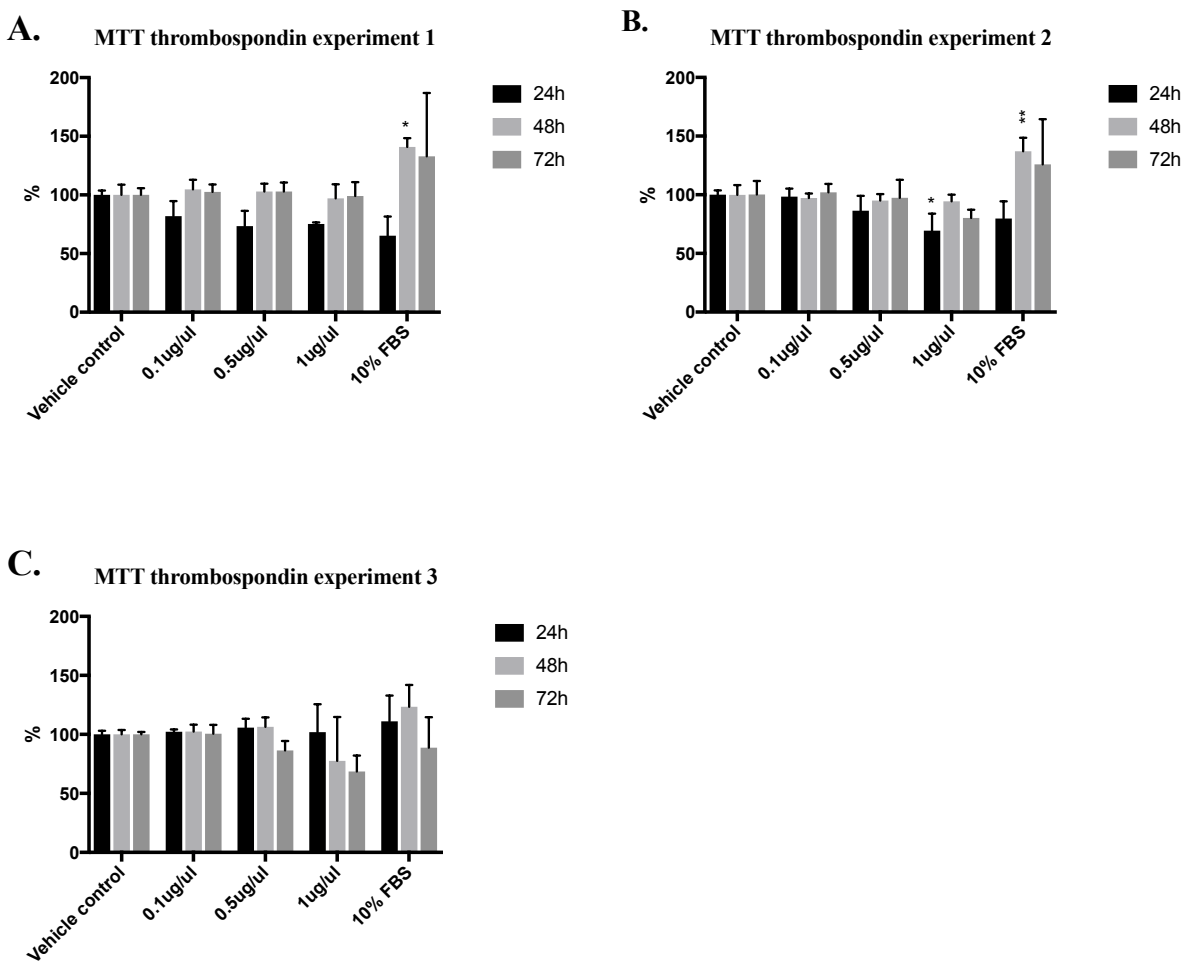

Figure 27. Proliferation of MCC13 cells in response to thrombospondin. Serum starved MCC13 cells were treated with 0.1, 0.5 and 1μg/μl recombinant thrombospondin protein, and the effect on cellular proliferation was measured using MTT-assay after 24, 48 and 72 hours respectively. Each treatment was compared pairwise to the vehicle control (Opti-MEM supplemented with 2 % PBS since the recombinant proteins were reconstituted in PBS) that was set as 100 %. Opti-MEM supplemented with 10 % FBS was used as a positive control. Two-way ANOVA followed up by Dunnet's post hoc test were used to analyse the data. Statistical significance is indicated by * above the bars (*= $p \leq 0.05$, statistically significant; ** = $p \leq 0.01$, very statistically significant; *** and **** = $p \leq 0.001$ and $p \leq 0.0001$, extremely statistically significant). Three parallel experiments were conducted (A, B and C). **A.** No significant differences between the vehicle control and cells treated with various amount of recombinant thrombospondin could be detected in the first experiment. **B.** In the second experiment a significant decrease in viable cells were detected after 24 hour incubation with 1μg/μl thrombospondin (p0.0369). **C.** No significant differences could be detected between the vehicle control and the increasing concentrations of thrombospondin at any of the time points measured. Each bar represents the average of three independent parallels.

Because of the troubles cultivating the cells with added recombinant protein in the 24 well plates, we wanted to try a different recombinant protein from a second supplier. Recombinant periostin protein was purchased from Novus, and three new parallel experiments were run. The results are depicted in Figure 28. Serum significantly stimulated proliferation after 48 and 72 hours in experiment 1 and 3, and after 72 hours in experiment 2 compared to vehicle-treated cells. A significant reduction in cell proliferation was measured with 0.1 µg/µl and 1 µg/µl periostin after 48 hours incubation in experiment 1 (p=0.0001) (Figure 28A), and 0.5 µg/µl and 1 µg/µl periostin after 48 hours in experiment 3 (p=0.0341 and p=0.0001) (Figure 28 C).

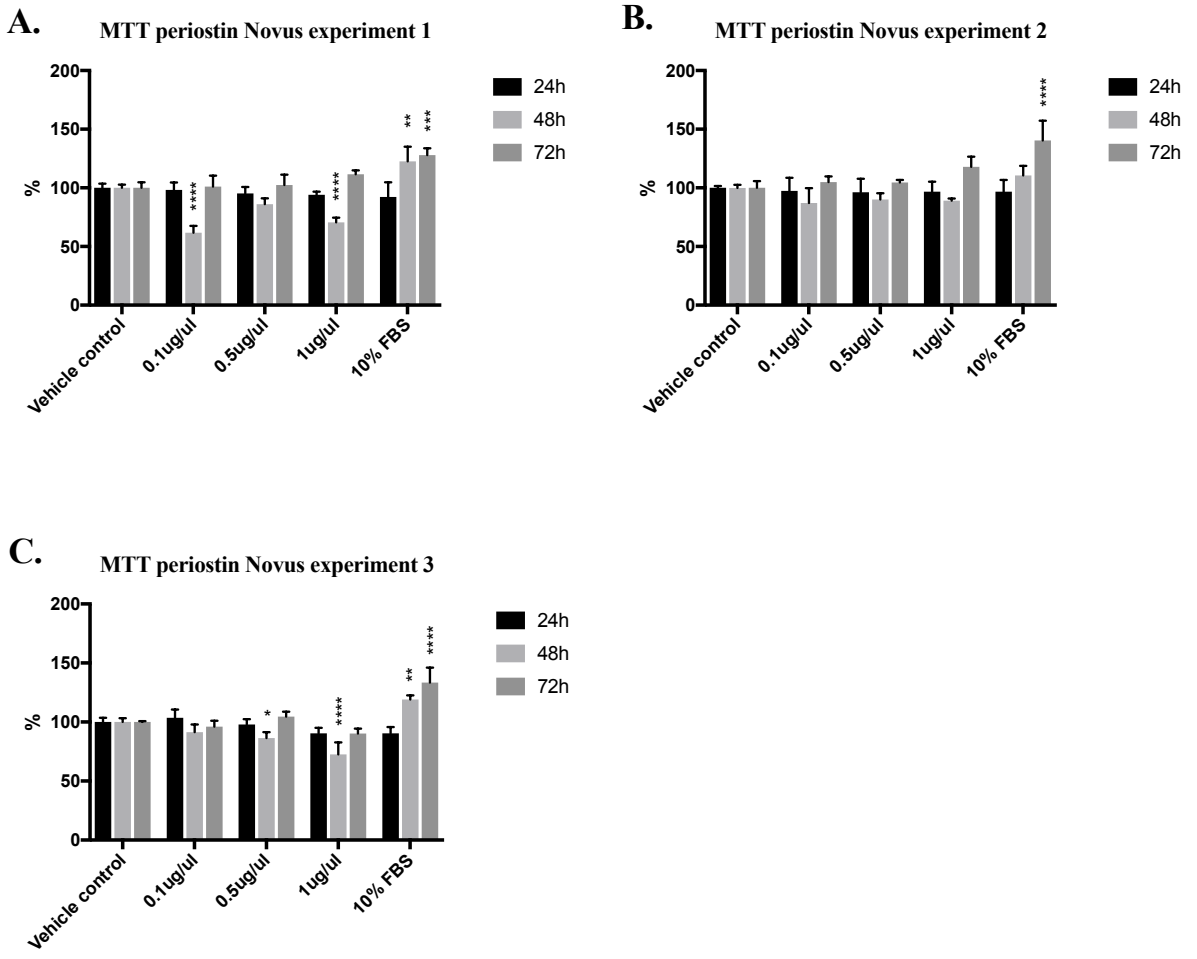

Figure 28. Proliferation of MCC13 cells in response to periostin from a different supplier. Serum starved MCC13 cells were treated with 0.1, 0.5 and 1µg/µl recombinant periostin protein from Novus, and the effect on cellular proliferation was measured using MTT-assay after 24, 48 and 72 hours respectively. Each treatment was compared pairwise to the vehicle control (Opti-MEM supplemented with 2 % PBS since the recombinant

proteins were reconstituted in PBS) that was set as 100 %. Normal cell medium RPMI-1640 supplemented with 10 % FBS was used as a positive control. Two-way ANOVA followed up by Dunnet's post hoc test were used to analyse the data. Statistical significance is indicated by * above the bars (*= $p \leq 0.05$, statistically significant; ** = $p \leq 0.01$, very statistically significant; *** and **** = $p \leq 0.001$ and $p \leq 0.0001$, extremely statistically significant). **A.** An extremely significant decrease ($p=0.0001$) in viable cells was detected after 48 hours for periostin concentrations of 0.1 μg/μl and 1.0 μg/μl respectively. **B.** No significant differences from the vehicle control could be detected for any protein concentrations added at any of the time points measured. **C.** In the third replicate of the experiment a significant decrease in formazan product was detected for 0.5 μg/μl ($p=0.0341$) and 1.0 μg/μl ($p= 0.0001$) periostin after 48 hours. Serum treated cells were significantly more viable than the vehicle control after 48 and 72 hours in experiment 1 ($p=0.0014$ and $p=0.001$) and experiment 3 ($p=0.0020$ and $p=0.0001$) and after 72 hours for experiment 2 ($p=0.0001$). Each bar represents the average of three independent parallels.

5. Discussion

5.1. Exosomes were successfully isolated from MCC cell lines

MCC exosomes were successfully isolated from MCC13, MCC26, MKL-1 and MKL-2 cells. This was confirmed as vesicles within the expected size range of 30-150 nm (Konstantinell et al., 2016) were detected using Submicron Particle Sizer 370. The PSS nicomp analysis in general detected two separate populations of vesicles. A population with relatively small vesicles (30 - 50 nm in mean diameter with SD around 10 %) was detected in all MCC cell lines. Since the populations of these small vesicles were narrowly distributed and overlapped nicely in at least run 1 and 2 they probably represent real populations of MCC exosomes. A second population with larger vesicles was also detected. At least for MKL-1 and MCC13 it is likely that the second population containing larger vesicles is caused by agglomeration of smaller vesicles since the exosome solution had been left in the tube for a while and had the opportunity to clump together, and because there were larger differences between the reads. For MCC26, two narrowly distributed populations of exosomes were detected of around 30 nm and 75 nm respectively in the two first runs. For exosomes isolated from MKL-2 cells the PSS failed to measure the second population, but a relatively narrowly distributed population of approximately 150 nm vesicles could be observed. These populations of larger vesicles detected in MCC26 and MKL-2 are probably also real, as they are within the expected size

range and narrowly distributed. Agglomeration of vesicles could possibly have been avoided by using higher concentrations of isolated exosomes, as the cycle time on the PSS is adjusted according to the amount of particles measured in the sample.

5.2. Gelsolin, periostin and thrombospondin transcripts were detected in MCC exosomes and cells using western blot and RT-PCR

Western blot detected gelsolin (86 kDa) and periostin (93 kDa) in MCC exosomes derived from the four cell lines used in the study, but not in the cells. The method identified thrombospondin (155 kDa) in both cell lysate and isolated exosomes, but the relative thrombospondin levels were much higher in the latter. Furthermore, obvious thrombospondin expression was detected in the virus negative cell lines MCC13 and MCC26 compared to the virus positive MKL-1 and MKL-2 cells. The lowest expression was observed in MKL-2 cells. For thrombospondin two additional bands of approximately 120 kDa and 20 kDa were also detected. The parallel bands of 155 kDa and 120 kDa may represent different isoforms of the protein, as two isoforms of thrombospondin-1 have been identified (Uniprot, 2017). The canonical thrombospondin-1 sequence has a length of 1.170 aa and a theoretical molecular mass of 129.383 kDa, and the second isotype has a length of 1.085 aa and a molecular mass of 120.148 kDa (Uniprot, 2017). The anti-thrombospondin antibody detects one of the homotrimeric repeats with a predicted band size of 129 kDa. However, the observed size of the band corresponds to 155 kDa, probably due to multiple glycosylation sites (Abcam, 2017). It is unknown how glycosylation events and other post-translational modifications affect the second isotype, but this could possibly explain the 120 kDa band observed. An alternative explanation is that the antibody detects the precursor and the mature protein. The signal peptide spans from aa 1-18 and is cleaved of to generate the mature thrombospondin-1 protein spanning from aa 19-1170 (Uniprot, 2017). Furthermore, thrombin digestion of thrombospondin creates bands of 155 kDa, 120 kDa, 20 kDa and 14 kDa respectively, when run on a non-reducing PAGE-gel (Huang, Detwiler, Milev et al., 1997). Konstantinell et al. detected thrombin in MCC exosomes from MCC13, MCC26, MKL-1 and MKL-2 cells by proteomics (Konstantinell et al., 2016). Furthermore, thrombin expression has been detected in several cancer tissues including small cell carcinoma of the lung, renal cell carcinoma, and malignant melanoma (Zacharski, Memoli, Morain et al., 1995). Therefore, digestion by thrombin could explain all three bands detected.

Immunoblotting is a semi quantitative method, meaning that it is possible to say something about the relative amount of protein but not an absolute quantity (Mahmood & Yang, 2012). Since the same amount of protein (30 μg, as detected by Direct Detect) was loaded from cell lysate and isolated exosomes on the PAGE gel, the strength of the bands is comparable. Nevertheless, the blot with the Exosomal marker CD63 could not rule out unequal loading volumes caused by e.g. pipetting errors or unequal blotting, or confirm that the exosome isolation was successful, as the antibody showed high degree of unspecific binding. Since the translation machinery converting mRNA to protein is located in the ribosomes of the cell (Alberts et al., 2008) and because of the proteomics data obtained in an earlier study in our research group, it was expected to detect the proteins in cell lysates. RT-PCR was undertaken with specific primers for periostin and thrombospondin to detect eventual mRNA transcripts. Gelsolin was not detected by RT-PCR due to lack of time despite of the inability to detect the protein in the cell lysate. Periostin mRNA was detected in all MCC cell lines, while thrombospondin transcripts were detected in the two virus negative cell lines and MKL-1, but not in MKL-2 cells. This is in accordance with what we observed in the western blot analysis; thrombospondin expression seemed to be higher in virus negative than virus positive cell lines, and MKL-2 showed the lowest relative thrombospondin expression among the MCC cell lines. The detection of periostin in MCC cell lines with RT-PCR but not with western blot can reflect posttranscriptional modification and degradation of mRNA in the cell before it is translated, or modification and programmed destruction of the proteins themselves (Vogel & Marcotte, 2012). Several studies have found a poor correlation between mRNA and protein expression levels (Abreu, Penalva, Marcotte et al., 2009). For example, a genome-wide study by Chen et al. looked at 98 genes in lung adenocarcinoma and found that only 21.4 % of the genes had a significant correlation between mRNA levels and protein expression (Chen, Gharib, Huang et al., 2002). Detection of mRNA transcripts but not proteins in the MCC cell lines may also indicate that the proteins are actively sorted into exosomes and released in the extracellular milieu. Cancer cells often release excessive amounts of exosomes with oncogenic proteins, miRNAs and mRNAs that can aid oncogenesis in recipient cells (Kahlert & Kalluri, 2013). It is currently not known how cancer cells sort exosome cargo, but mechanisms facilitating sorting of tumour suppressing elements into ILVs targeted for the lysosome and ILVs containing oncogenic elements to the plasma membrane probably exist (Soung et al., 2016). Finally, the inability to detect the proteins with western blot can reflect the sensitivity of the assay or poor quality of the antibodies.

5.3. Western blot and RT-PCR shows that LT-ag expression is higher in MKL-1 than in MKL-2 cells and confirms the lack of LT-ag in MCC13 and MCC26 cells

All virus positive MCC tumours contain integrated MCPyV that express a truncated LT-ag because of a nonsense mutation in the *LT-ag* gene (Feng et al., 2008). WB with specific antibodies directed towards MCPyV LT-ag was only able to detect the expected 50 kDa LT-ag form in MKL-1 cells, while the expected 37 kDa LT-ag was not detected in MKL-2 cells. A study by Shuda et al. shows that LT-ag expression varies considerably between the two MCC cell lines. In this study LT-ag expression was found to be noticeably lower in MKL-2 cells than in MKL-1 cells (Shuda et al., 2014). Therefore, the inability to detect LT-ag in MKL-2 cells by western blot in our study could be due to sensitivity of the assay. This assumption is supported by RT-PCR results confirming the presence of LT-ag mRNA in both virus positive cell lines. RT-PCR with LT-ag specific primers showed clear bands corresponding to the LT-ag transcripts of MKL-1 and MKL-2 (394bp compared to 440bp), respectively. Furthermore, the LT-ag band detected for MKL-1 cells was stronger than the band detected in MKL-2 cells, indicating higher level of LT-ag transcripts in MKL-1 cells compared to MKL-2 cells. However, it must be emphasised also here that RT-PCR detects mRNA that can be subject to further posttranscriptional regulation mechanisms. The mRNA detected can therefore not be directly translated into protein levels and biological effect (Koussounadis, Langdon, Um et al., 2015). The virus negative cell lines MCC13 and MCC26 were used as negative controls. LT-ag was not detected in the virus negative cell lines by either western blot or RT-PCR, confirming that these cell lines are virus negative.

5.4. MCPyV LT-ag, but not st-ag, significantly stimulates gelsolin, periostin and thrombospondin promoter activity in MCC13 cells

Our results showed that MCPyV LT-ag, but not st-ag stimulated gelsolin, periostin and thrombospondin promoter activity in MCC13 cells. LT-ag of polyomaviruses can induce promoter activity by either direct binding to tandem repeat 5'-G(A/G)GGC- 3' sequences, through direct interaction with general transcription factors such as TATA-binding protein (TBP) and TBP-associated factors (TAFs) and specific transcription factors (e.g. Sp1, AP1), and by activating signalling pathways that control the activity of transcription factors (Moens

et al., 1997; Peng & Acheson, 1998). The gelsolin promoter fragment used in these experiments contains four putative LT-ag binding motifs, but it remains to be proven that LT-ag actually binds these motifs. A study by Klawitz et al. found that LT-ag of polyomavirus SV40 bind to gelsolin, but the biological implications has not been investigated (Klawitz, Preuss, & Scheidtmann, 2001). No LT-ag binding sequences could be detected in the periostin or thrombospondin promoters used in the study (Appendix 4). St-ag showed no significant effect on the activity of these three promoters in MCC13 cells. In fact, the co-transfection with LT-ag + st-ag expression plasmids demonstrated that st-ag impedes LT-ag's stimulatory effect on the gelsolin promoter. Likewise, in the thrombospondin experiments MCPyV LT + st-ag showed no significant difference in experiment 1 and 2, but caused a significant increase in thrombospondin promoter activity in the third experiment. The significance detected here was lower than what could be detected for LT-ag alone. In the periostin experiments on the contrary, a significant up-regulation of the periostin promoter is found in all three experiments following co-transfection with MCPyV LT + st-ag. Knowing the oncogenic role of gelsolin, periostin and thrombospondin (see section 1.8-1.10), it can be speculated that MCPyV LT-ag potentiates tumorigenesis by increasing the expression of these proteins.

5.5. Increased cell proliferation was not measured after incubation with recombinant gelsolin, periostin thrombospondin proteins followed by MTT assay

When looking at the plates containing MCC13 cells and recombinant proteins in the microscope it was observed that the cells looked less outstretched and had detached from the bottom of the 24 well plate in a half moon pattern at the right side/bottom of the plates (results not shown). When repeating the experiment, extra caution was taken when adding or removing cell medium in order to not disturb or detach the cells. The plates were also placed in a different incubator and the water level in the incubator was controlled. Nevertheless, detached cells were observed also in the subsequent experiments. It is likely that these observations have affected the experiments, and that the results obtained does not really measure the respective proteins effect on cell proliferation, but rather how many cells have loosened from the 24 well plate and been washed away. This is supported by the fact that

serum treated cells did not differ significantly from the vehicle control in any of the gelsolin experiments or for periostin in experiment 1 and 3.

In general, incubation with increasing concentration of recombinant gelsolin did not result in significant differences in viable cells relative to the vehicle control, except for experiment 2 after 48 hours for the cells treated with 1 μg/μl recombinant gelsolin that showed a significant decrease in viable cells measured. Since gelsolin has been found to possess both pro-tumour (Shieh et al., 2006) and anti-tumour properties (Li et al., 2016) both increased and decreased proliferative abilities could be expected. However, since serum treated cells showed no significant increase relative to the vehicle treated cells it is likely that the observed differences are due to errors in the assay.

Serum starved MCC13 cells treated different concentrations of periostin showed no significant effect on cell proliferation except for a significant decrease in the amount of formazan product produced by cells treated with 1 μg/μl periostin in experiment 1 after 48 hours and in experiment 3 after 72 hours. This is opposite of what we expected based on the majority of the literature suggesting that periostin up-regulation in several cancers has been connected to increased cell motility, proliferation and invasiveness (Bao et al., 2004; Gillan et al., 2002; Hu et al., 2015; Kudo et al., 2006). This combined with the observations of detached cells before assay start gives reason to doubt the results.

For the MTT assays conducted with recombinant thrombospondin no significant differences compared with the vehicle control could be detected in either experiment 1 or 3 at any of the protein concentrations added at any of the time points measured. A significant decrease could be detected after 24 hours incubation with 1 μg/μl thrombospondin in experiment 2. Here the vehicle treated cells showed an increasing trend in viability after 48 and 72 hours incubation in all experiments, but the difference was only significant after 48 hours incubation time in experiment 1 and 2. Most evidence suggest that thrombospondin possesses anti-angiogenic properties and that increased thrombospondin expression is beneficial (Good et al., 1990; Rodriguez-Manzaneque et al., 2001). This is in line with what we see here. However, since it is uncertain whether the assay measures cell viability or cells washed away, the experiment must be repeated. Newer studies also suggest that thrombospondin can increase cancer cells invasive properties (Huang et al., 2017) and that increased expression have been observed in cancerous tissue (Borsotti et al., 2015).

When repeating the periostin experiment with recombinant protein from Novus the cells were also seeded out directly in Opti-MEM in order to omit disturbing the cells when changing to starvation medium at assay start. Normal cell medium supplemented with 10 % FBS was used as positive control instead of Opti-MEM with added serum. In this last experiment the serum threated cells were significantly more viable than the vehicle control, suggesting that this is a more comprehensible control. However, also here a significant reduction in cell proliferation was measured with 0.1 μg/μl and 1 μg/μl periostin after 48 hours incubation in experiment 1, and 0.5 μg/μl and 1 μg/μl periostin after 48 hours in experiment 3 despite most evidence suggesting that periostin induces cell proliferation and invasiveness.

5.6. Future perspectives

Further research is needed in order to elaborate on the role of LT-ag on gelsolin, periostin and thrombospondin expression. To confirm that LT-ag increases the expression of these proteins, the expression levels could be measured in virus-negative MCC cells transfected with LT-ag or/and st-ag by western blot. Alternatively, the levels of gelsolin, periostin and thrombospondin could be monitored in MCPyV-positive MCC cells depleted (e.g. by RNA interference) or knocked out (e.g. by CRISPR/CAS9) for LT-ag. Furthermore, it would be interesting to study the pathways and promoter elements involved in LT-ag-mediated activation of the promoters of these genes.

Since the MTT cell proliferation assay was inconclusive, this will have to be repeated. Alternatively, the role of gelsolin, periostin and thrombospondin in tumourigenic processes such as cell invasiveness and metastasis could be examined using cell migration assay, where the cells capacity to move through a membrane or to close a wound in a culture plate is measured (Justus, Leffler, Ruiz-Echevarria et al., 2014), and cell survival assays where apoptotic and anti-apoptotic processes are studied. Furthermore, the clonogenicity, i.e. the ability of a single cell to form a colony (Franken, Rodermond, Stap et al., 2006), of MCC cell lines could be determined using knockout (e.g. by CRISP/CAS9) or knockdown (e.g. by siRNA) of gelsolin, periostin and thrombospondin. Finally, it would be interesting to study the effect of MCC-derived exosomes on target cells (e.g. dermal fibroblasts because of their relevance as cancer-associated fibroblasts or other cells in the tumour microenvironment). Purified exosomes from virus-positive and virus-negative MCC cell lines could be added to

cultured human fibroblasts, and changes in phenotype and or chemo-resistance could be observed.

Bibliography

Abcam. (2017). Anti-Thrombospondin 1 antibody (ab85762). Retrieved 28.04, 2017, from http://www.abcam.com/thrombospondin-1-antibody-ab85762.html?productWallTab=Questions

Abreu, R. d. S., Penalva, L. O., Marcotte, E. M., & Vogel, C. (2009). Global signatures of protein and mRNA expression levels. *Molecular bioSystems, 5*(12), 1512-1526. doi: 10.1039/b908315d

Al-Nedawi, K., Meehan, B., Micallef, J., Lhotak, V., May, L., Guha, A., et al. (2008). Intercellular transfer of the oncogenic receptor EGFRvIII by microvesicles derived from tumour cells. *Nat Cell Biol, 10*(5), 619-624. doi: http://www.nature.com/ncb/journal/v10/n5/suppinfo/ncb1725_S1.html

Alberts, B., Johnson, A., Lewis, J., Raff, M., Roberts, K. a., & Walter, P. (2008). *The Molecular Biology of the Cell* (Fifth edition ed.). New York, USA.: Garland Sciences Taylor and Francis Group.

Albores-Saavedra, J., Batich, K., Chable-Montero, F., Sagy, N., Schwartz, A. M., & Henson, D. E. (2010). Merkel cell carcinoma demographics, morphology, and survival based on 3870 cases: a population based study. *J Cutan Pathol, 37*(1), 20-27. doi: 10.1111/j.1600-0560.2009.01370.x

ANALYSTA. (2017). Particle Sizing Systems NICOMP 370 DLS. Retrieved 07.05, 2017, from http://www.anasysta.com/englisch/content/Gebrauchtgeraeteflyer_EN.pdf

Asch, H. L., Head, K., Dong, Y., Natoli, F., Winston, J. S., Connolly, J. L., et al. (1996). Widespread Loss of Gelsolin in Breast Cancers of Humans, Mice, and Rats. *Cancer Research, 56*(21), 4841-4845.

Azmi, A. S., Bao, B., & Sarkar, F. H. (2013). Exosomes in Cancer Development, Metastasis and Drug Resistance: A Comprehensive Review. *Cancer metastasis reviews, 32*(0), 10.1007/s10555-10013-19441-10559. doi: 10.1007/s10555-013-9441-9

Bai, Y., Nakamura, M., Zhou, G., Li, Y., Liu, Z., Ozaki, T., et al. (2010). Novel isoforms of periostin expressed in the human thyroid. *Jpn Clin Med, 1*, 13-20. doi: 10.4137/jcm.s5899

Bao, S., Ouyang, G., Bai, X., Huang, Z., Ma, C., Liu, M., et al. (2004). Periostin potently promotes metastatic growth of colon cancer by augmenting cell survival via the Akt/PKB pathway. *Cancer Cell, 5*(4), 329-339.

Baril, P., Gangeswaran, R., Mahon, P. C., Caulee, K., Kocher, H. M., Harada, T., et al. (2007). Periostin promotes invasiveness and resistance of pancreatic cancer cells to hypoxia-induced cell death: role of the beta4 integrin and the PI3k pathway. *Oncogene, 26*(14), 2082-2094. doi: 10.1038/sj.onc.1210009

Beach, A., Zhang, H.-G., Ratajczak, M. Z., & Kakar, S. S. (2014). Exosomes: an overview of biogenesis, composition and role in ovarian cancer. *Journal of Ovarian Research, 7*, 14-14. doi: 10.1186/1757-2215-7-14

Birnboim, H. C., & Doly, J. (1979). A rapid alkaline extraction procedure for screening recombinant plasmid DNA. *Nucleic Acids Research, 7*(6), 1513-1523.

Bland, J. M., & Altman, D. G. (1995). Multiple significance tests: the Bonferroni method. *Bmj, 310*(6973), 170.

Borsotti, P., Ghilardi, C., Ostano, P., Silini, A., Dossi, R., Pinessi, D., et al. (2015). Thrombospondin-1 is part of a Slug-independent motility and metastatic program in cutaneous melanoma, in association with VEGFR-1 and FGF-2. *Pigment Cell Melanoma Res, 28*(1), 73-81. doi: 10.1111/pcmr.12319

Buck, C. B., Van Doorslaer, K., Peretti, A., Geoghegan, E. M., Tisza, M. J., An, P., et al. (2016). The Ancient Evolutionary History of Polyomaviruses. *PLoS Pathog, 12*(4), e1005574. doi: 10.1371/journal.ppat.1005574

Calvignac-Spencer, S., Feltkamp, M. C., Daugherty, M. D., Moens, U., Ramqvist, T., Johne, R., et al. (2016). A taxonomy update for the family Polyomaviridae. *Arch Virol, 161*(6), 1739-1750. doi: 10.1007/s00705-016-2794-y

Campbell, S. C., Volpert, O. V., Ivanovich, M., & Bouck, N. P. (1998). Molecular mediators of angiogenesis in bladder cancer. *Cancer Res, 58*(6), 1298-1304.

Carter, J. J., Daugherty, M. D., Qi, X., Bheda-Malge, A., Wipf, G. C., Robinson, K., et al. (2013). Identification of an overprinting gene in Merkel cell polyomavirus provides evolutionary insight into the birth of viral genes. *Proc Natl Acad Sci U S A, 110*(31), 12744-12749. doi: 10.1073/pnas.1303526110

Chang, Y., & Moore, P. S. (2012). Merkel Cell Carcinoma: A Virus-Induced Human Cancer. *Annual review of pathology, 7*, 123-144. doi: 10.1146/annurev-pathol-011110-130227

Chaput, N., Flament, C., Viaud, S., Taieb, J., Roux, S., Spatz, A., et al. (2006). Dendritic cell derived-exosomes: biology and clinical implementations. *J Leukoc Biol, 80*(3), 471-478. doi: 10.1189/jlb.0206094

Chen, G., Gharib, T. G., Huang, C. C., Taylor, J. M., Misek, D. E., Kardia, S. L., et al. (2002). Discordant protein and mRNA expression in lung adenocarcinomas. *Mol Cell Proteomics, 1*(4), 304-313.

Cheng, J., DeCaprio, J. A., Fluck, M. M., & Schaffhausen, B. S. (2009). Cellular transformation by Simian Virus 40 and Murine Polyoma Virus T antigens. *Semin Cancer Biol, 19*(4), 218-228. doi: 10.1016/j.semcancer.2009.03.002

Dai, S., Wei, D., Wu, Z., Zhou, X., Wei, X., Huang, H., et al. (2008). Phase I Clinical Trial of Autologous Ascites-derived Exosomes Combined With GM-CSF for Colorectal Cancer. *Molecular Therapy, 16*(4), 782-790. doi: http://dx.doi.org/10.1038/mt.2008.1

De Toro, J., Herschlik, L., Waldner, C., & Mongini, C. (2015). Emerging Roles of Exosomes in Normal and Pathological Conditions: New Insights for Diagnosis and Therapeutic Applications. *Frontiers in Immunology, 6*, 203. doi: 10.3389/fimmu.2015.00203

DeCaprio, J. A., & Garcea, R. L. (2013). A cornucopia of human polyomaviruses. *Nat Rev Microbiol, 11*(4), 264-276. doi: 10.1038/nrmicro2992

Dittmer, A., & Dittmer, J. (2006). Beta-actin is not a reliable loading control in Western blot analysis. *Electrophoresis, 27*(14), 2844-2845. doi: 10.1002/elps.200500785

Eaton, S. L., Hurtado, M. L., Oldknow, K. J., Graham, L. C., Marchant, T. W., Gillingwater, T. H., et al. (2014). A Guide to Modern Quantitative Fluorescent Western Blotting with Troubleshooting Strategies. *Journal of Visualized Experiments : JoVE*(93), 52099. doi: 10.3791/52099

Erkan, M., Kleeff, J., Gorbachevski, A., Reiser, C., Mitkus, T., Esposito, I., et al. (2007). Periostin creates a tumor-supportive microenvironment in the pancreas by sustaining fibrogenic stellate cell activity. *Gastroenterology, 132*(4), 1447-1464. doi: 10.1053/j.gastro.2007.01.031

Escudier, B., Dorval, T., Chaput, N., Andre, F., Caby, M. P., Novault, S., et al. (2005). Vaccination of metastatic melanoma patients with autologous dendritic cell (DC) derived-exosomes: results of thefirst phase I clinical trial. *J Transl Med, 3*(1), 10. doi: 10.1186/1479-5876-3-10

Feng, H., Shuda, M., Chang, Y., & Moore, P. S. (2008). Clonal integration of a polyomavirus in human Merkel cell carcinoma. *Science, 319*(5866), 1096-1100. doi: 10.1126/science.1152586

Franken, N. A. P., Rodermond, H. M., Stap, J., Haveman, J., & van Bree, C. (2006). Clonogenic assay of cells in vitro. *Nat. Protocols, 1*(5), 2315-2319.

Freze Baez, C., Cirauqui Diaz, N., Baeta Cavalcanti, S. M., & Brandao Varella, R. (2014). Genetic and structural analysis of Merkel cell polyomavirus large T antigen from diverse biological samples. *Intervirology, 57*(6), 331-336. doi: 10.1159/000363241

Fukuda, K., Sugihara, E., Ohta, S., Izuhara, K., Funakoshi, T., Amagai, M., et al. (2015). Periostin Is a Key Niche Component for Wound Metastasis of Melanoma. *PLoS One, 10*(6), e0129704. doi: 10.1371/journal.pone.0129704

Gillan, L., Matei, D., Fishman, D. A., Gerbin, C. S., Karlan, B. Y., & Chang, D. D. (2002). Periostin secreted by epithelial ovarian carcinoma is a ligand for alpha(V)beta(3) and alpha(V)beta(5) integrins and promotes cell motility. *Cancer Res, 62*(18), 5358-5364.

Goddard, J. C., Sutton, C. D., Jones, J. L., O'Byrne, K. J., & Kockelbergh, R. C. (2002). Reduced thrombospondin-1 at presentation predicts disease progression in superficial bladder cancer. *Eur Urol, 42*(5), 464-468.

Good, D. J., Polverini, P. J., Rastinejad, F., Le Beau, M. M., Lemons, R. S., Frazier, W. A., et al. (1990). A tumor suppressor-dependent inhibitor of angiogenesis is immunologically and functionally indistinguishable from a fragment of thrombospondin. *Proc Natl Acad Sci U S A, 87*(17), 6624-6628.

Gopal, S. K., Greening, D. W., Hanssen, E. G., Zhu, H. J., Simpson, R. J., & Mathias, R. A. (2016). Oncogenic epithelial cell-derived exosomes containing Rac1 and PAK2 induce angiogenesis in recipient endothelial cells. *Oncotarget, 7*(15), 19709-19722. doi: 10.18632/oncotarget.7573

Greco, V., Hannus, M., & Eaton, S. (2001). Argosomes: A Potential Vehicle for the Spread of Morphogens through Epithelia. *Cell, 106*(5), 633-645. doi: http://dx.doi.org/10.1016/S0092-8674(01)00484-6

Grim, M., & Halata, Z. (2000). Developmental origin of avian Merkel cells. *Anat Embryol (Berl), 202*(5), 401-410.

Gross, J. C., Chaudhary, V., Bartscherer, K., & Boutros, M. (2012). Active Wnt proteins are secreted on exosomes. *Nat Cell Biol, 14*(10), 1036-1045. doi: http://www.nature.com/ncb/journal/v14/n10/abs/ncb2574.html - supplementary-information

Grossfeld, G. D., Ginsberg, D. A., Stein, J. P., Bochner, B. H., Esrig, D., Groshen, S., et al. (1997). Thrombospondin-1 expression in bladder cancer: association with p53 alterations, tumor angiogenesis, and tumor progression. *J Natl Cancer Inst, 89*(3), 219-227.

Guastafierro, A., Feng, H., Thant, M., Kirkwood, J. M., Chang, Y., Moore, P. S., et al. (2013). Characterization of an early passage Merkel cell polyomavirus-positive Merkel cell carcinoma cell line, MS-1, and its growth in NOD scid gamma mice. *J Virol Methods, 187*(1), 6-14. doi: 10.1016/j.jviromet.2012.10.001

Gupta, K., Gupta, P., Wild, R., Ramakrishnan, S., & Hebbel, R. P. (1999). Binding and displacement of vascular endothelial growth factor (VEGF) by thrombospondin: effect on human microvascular endothelial cell proliferation and angiogenesis. *Angiogenesis, 3*(2), 147-158.

Halata, Z., Grim, M., & Bauman, K. I. (2003). Friedrich Sigmund Merkel and his "Merkel cell", morphology, development, and physiology: review and new results. *Anat Rec A Discov Mol Cell Evol Biol, 271*(1), 225-239. doi: 10.1002/ar.a.10029

Halata, Z., Grim, M., & Christ, B. (1990). Origin of spinal cord meninges, sheaths of peripheral nerves, and cutaneous receptors including Merkel cells. An experimental and ultrastructural study with avian chimeras. *Anat Embryol (Berl), 182*(6), 529-537.

Harrison, C. J., Meinke, G., Kwun, H. J., Rogalin, H., Phelan, P. J., Bullock, P. A., et al. (2011). Asymmetric Assembly of Merkel Cell Polyomavirus Large T-antigen Origin

Binding Domains at the Viral Origin. *Journal of molecular biology, 409*(4), 529-542. doi: 10.1016/j.jmb.2011.03.051
Helbæk, M. (2001). Statistikk for kjemikere. *Tapir Akademisk Forlag*.
Hewson, C., & Morris, K. V. (2016). Form and Function of Exosome-Associated Long Non-coding RNAs in Cancer. *Curr Top Microbiol Immunol, 394*, 41-56. doi: 10.1007/82_2015_486
Heymann, W. R. (2008). Merkel cell carcinoma: Insights into pathogenesis. *Journal of the American Academy of Dermatology, 59*(3), 503-504. doi: 10.1016/j.jaad.2008.02.027
Hood, J. L., San, R. S., & Wickline, S. A. (2011). Exosomes released by melanoma cells prepare sentinel lymph nodes for tumor metastasis. *Cancer Res, 71*(11), 3792-3801. doi: 10.1158/0008-5472.can-10-4455
Hoshino, A., Costa-Silva, B., Shen, T.-L., Rodrigues, G., Hashimoto, A., Tesic Mark, M., et al. (2015). Tumour exosome integrins determine organotropic metastasis. *Nature, 527*(7578), 329-335. doi: 10.1038/nature15756
Houben, R., Shuda, M., Weinkam, R., Schrama, D., Feng, H., Chang, Y., et al. (2010). Merkel cell polyomavirus-infected Merkel cell carcinoma cells require expression of viral T antigens. *J Virol, 84*(14), 7064-7072. doi: 10.1128/jvi.02400-09
Hu, Q., Tong, S., Zhao, X., Ding, W., Gou, Y., Xu, K., et al. (2015). Periostin Mediates TGF-beta-Induced Epithelial Mesenchymal Transition in Prostate Cancer Cells. *Cell Physiol Biochem, 36*(2), 799-809. doi: 10.1159/000430139
Huang, E. M., Detwiler, T. C., Milev, Y., & Essex, D. W. (1997). Thiol-disulfide isomerization in thrombospondin: effects of conformation and protein disulfide isomerase. *Blood, 89*(9), 3205-3212.
Huang, T., Wang, L., Liu, D., Li, P., Xiong, H., Zhuang, L., et al. (2017). FGF7/FGFR2 signal promotes invasion and migration in human gastric cancer through upregulation of thrombospondin-1. *Int J Oncol, 50*(5), 1501-1512. doi: 10.3892/ijo.2017.3927
Huber, V., Fais, S., Iero, M., Lugini, L., Canese, P., Squarcina, P., et al. (2005). Human colorectal cancer cells induce T-cell death through release of proapoptotic microvesicles: role in immune escape. *Gastroenterology, 128*(7), 1796-1804.
Johnston, C., Martin, B., Fichant, G., Polard, P., & Claverys, J. P. (2014). Bacterial transformation: distribution, shared mechanisms and divergent control. *Nat Rev Microbiol, 12*(3), 181-196. doi: 10.1038/nrmicro3199
Johnstone, R. M., Bianchini, A., & Teng, K. (1989). Reticulocyte maturation and exosome release: transferrin receptor containing exosomes shows multiple plasma membrane functions. *Blood, 74*(5), 1844-1851.
Justus, C. R., Leffler, N., Ruiz-Echevarria, M., & Yang, L. V. (2014). In vitro Cell Migration and Invasion Assays. *Journal of Visualized Experiments : JoVE*(88), 51046. doi: 10.3791/51046
Kahlert, C., & Kalluri, R. (2013). Exosomes in Tumor Microenvironment Influence Cancer Progression and Metastasis. *Journal of molecular medicine (Berlin, Germany), 91*(4), 431-437. doi: 10.1007/s00109-013-1020-6
Karlsson, J. O., Ostwald, K., Kabjorn, C., & Andersson, M. (1994). A method for protein assay in Laemmli buffer. *Anal Biochem, 219*(1), 144-146. doi: 10.1006/abio.1994.1243
Kim, T. K., & Eberwine, J. H. (2010). Mammalian cell transfection: the present and the future. *Analytical and Bioanalytical Chemistry, 397*(8), 3173-3178. doi: 10.1007/s00216-010-3821-6
Klawitz, I., Preuss, U., & Scheidtmann, K. H. (2001). Interaction of SV40 large T antigen with components of the nucleo/cytoskeleton. *Int J Oncol, 19*(6), 1325-1332.

Konstantinell, A., Bruun, J. A., Olsen, R., Aspar, A., Skalko-Basnet, N., Sveinbjornsson, B., et al. (2016). Secretomic analysis of extracellular vesicles originating from polyomavirus-negative and polyomavirus-positive Merkel cell carcinoma cell lines. *Proteomics, 16*(19), 2587-2591. doi: 10.1002/pmic.201600223

Kosaka, N., Iguchi, H., Hagiwara, K., Yoshioka, Y., Takeshita, F., & Ochiya, T. (2013). Neutral Sphingomyelinase 2 (nSMase2)-dependent Exosomal Transfer of Angiogenic MicroRNAs Regulate Cancer Cell Metastasis. *The Journal of Biological Chemistry, 288*(15), 10849-10859. doi: 10.1074/jbc.M112.446831

Kosaka, N., Yoshioka, Y., Fujita, Y., & Ochiya, T. (2016). Versatile roles of extracellular vesicles in cancer. *J Clin Invest, 126*(4), 1163-1172. doi: 10.1172/jci81130

Koussounadis, A., Langdon, S. P., Um, I. H., Harrison, D. J., & Smith, V. A. (2015). Relationship between differentially expressed mRNA and mRNA-protein correlations in a xenograft model system. *Scientific Reports, 5*, 10775. doi: 10.1038/srep10775

Kudo, Y., Ogawa, I., Kitajima, S., Kitagawa, M., Kawai, H., Gaffney, P. M., et al. (2006). Periostin promotes invasion and anchorage-independent growth in the metastatic process of head and neck cancer. *Cancer Res, 66*(14), 6928-6935. doi: 10.1158/0008-5472.can-05-4540

Kunigelis, K. E., & Graner, M. W. (2015). The Dichotomy of Tumor Exosomes (TEX) in Cancer Immunity: Is It All in the ConTEXt? *Vaccines, 3*(4), 1019-1051. doi: 10.3390/vaccines3041019

Kwun, H. J., Shuda, M., Feng, H., Camacho, C. J., Moore, P. S., & Chang, Y. (2013). Merkel Cell Polyomavirus Small T Antigen Controls Viral Replication and Oncoprotein Expression by Targeting the Cellular Ubiquitin Ligase SCF(Fbw7). *Cell Host Microbe, 14*(2), 125-135. doi: 10.1016/j.chom.2013.06.008

Landré, V., Antonov, A., Knight, R., & Melino, G. (2016). p73 promotes glioblastoma cell invasion by directly activating POSTN (periostin) expression. *Oncotarget, 7*(11), 11785-11802. doi: 10.18632/oncotarget.7600

Lawler, J. W., Slayter, H. S., & Coligan, J. (1978). Isolation and characterization of a high molecular weight glycoprotein from human blood platelets. *Journal of Biological Chemistry, 253*(23), 8609-8616.

Lawler, P. R., & Lawler, J. (2012). Molecular Basis for the Regulation of Angiogenesis by Thrombospondin-1 and -2. *Cold Spring Harbor Perspectives in Medicine, 2*(5), a006627. doi: 10.1101/cshperspect.a006627

Lemos, B., & Nghiem, P. (2007). Merkel cell carcinoma: more deaths but still no pathway to blame. *J Invest Dermatol, 127*(9), 2100-2103. doi: 10.1038/sj.jid.5700925

Leonard, J. H., Dash, P., Holland, P., Kearsley, J. H., & Bell, J. R. (1995). Characterisation of four Merkel cell carcinoma adherent cell lines. *Int J Cancer, 60*(1), 100-107.

Leonard, J. H., Ramsay, J. R., Kearsley, J. H., & Birrell, G. W. (1995). Radiation sensitivity of Merkel cell carcinoma cell lines. *Int J Radiat Oncol Biol Phys, 32*(5), 1401-1407. doi: 10.1016/0360-3016(94)00610-w

Leonard, J. H., Williams, G., Walters, M. K., Nancarrow, D. J., & Rabbitts, P. H. (1996). Deletion mapping of the short arm of chromosome 3 in Merkel cell carcinoma. *Genes Chromosomes Cancer, 15*(2), 102-107. doi: 10.1002/(sici)1098-2264(199602)15:2<102::aid-gcc4>3.0.co;2-7

Li, G. H., Arora, P. D., Chen, Y., McCulloch, C. A., & Liu, P. (2012). Multifunctional roles of gelsolin in health and diseases. *Med Res Rev, 32*(5), 999-1025. doi: 10.1002/med.20231

Li, W.-X., Yang, M.-X., Hong, X.-Q., Dong, T.-G., Yi, T., Lin, S.-L., et al. (2016). Overexpression of gelsolin reduces the proliferation and invasion of colon carcinoma cells. *Molecular Medicine Reports, 14*(4), 3059-3065. doi: 10.3892/mmr.2016.5652

Lin, J., Li, J., Huang, B., Liu, J., Chen, X., Chen, X. M., et al. (2015). Exosomes: novel biomarkers for clinical diagnosis. *ScientificWorldJournal, 2015*, 657086. doi: 10.1155/2015/657086
Liu, A. Y., Zheng, H., & Ouyang, G. (2014). Periostin, a multifunctional matricellular protein in inflammatory and tumor microenvironments. *Matrix Biology, 37*, 150-156. doi: http://dx.doi.org/10.1016/j.matbio.2014.04.007
Liu, C., Yu, S., Zinn, K., Wang, J., Zhang, L., Jia, Y., et al. (2006). Murine mammary carcinoma exosomes promote tumor growth by suppression of NK cell function. *J Immunol, 176*(3), 1375-1385.
Liu, W., Yang, R., Payne, A. S., Schowalter, R. M., Spurgeon, M. E., Lambert, P. F., et al. (2016). Identifying the Target Cells and Mechanisms of Merkel Cell Polyomavirus Infection. *Cell Host Microbe, 19*(6), 775-787. doi: 10.1016/j.chom.2016.04.024
Lonza. (2012). MycoAlertTM PLUS Mycoplasma detection kit. Walkersville, MD 21793-0127 USA.
Lowry, R. (2008). One way ANOVA–independent samples. *Vassar. edu.* Retrieved 24.04, 2017, from http://vassarstats.net/textbook/ch14pt2.html
Luga, V., Zhang, L., Viloria-Petit, Alicia M., Ogunjimi, Abiodun A., Inanlou, Mohammad R., Chiu, E., et al. (2012). Exosomes Mediate Stromal Mobilization of Autocrine Wnt-PCP Signaling in Breast Cancer Cell Migration. *Cell, 151*(7), 1542-1556. doi: http://dx.doi.org/10.1016/j.cell.2012.11.024
Lundholm, M., Schröder, M., Nagaeva, O., Baranov, V., Widmark, A., Mincheva-Nilsson, L., et al. (2014). Prostate Tumor-Derived Exosomes Down-Regulate NKG2D Expression on Natural Killer Cells and CD8+ T Cells: Mechanism of Immune Evasion. *PLoS One, 9*(9), e108925. doi: 10.1371/journal.pone.0108925
Lv, L. H., Wan, Y. L., Lin, Y., Zhang, W., Yang, M., Li, G. L., et al. (2012). Anticancer drugs cause release of exosomes with heat shock proteins from human hepatocellular carcinoma cells that elicit effective natural killer cell antitumor responses in vitro. *J Biol Chem, 287*(19), 15874-15885. doi: 10.1074/jbc.M112.340588
Macherey Nagel. (2014). Plasmid DNA purification- user manual, NucleoBond® Xtra Midi. [Rev. 12]. *March 2014 / Rev. 12*.
Madigan, M. T., Martinko, J. M., Stahl, D. A., & Clark, D. P. (2012). *Brock- Biology of microorganisms* (Thirteenth edition ed.). San Francisco: Pearson Education.
Mahmood, T., & Yang, P.-C. (2012). Western Blot: Technique, Theory, and Trouble Shooting. *North American Journal of Medical Sciences, 4*(9), 429-434. doi: 10.4103/1947-2714.100998
Mannherz, H. G., Mazur, A. J., & Jockusch, B. (2010). Repolymerization of actin from actin:thymosin beta4 complex induced by diaphanous related formins and gelsolin. *Ann N Y Acad Sci, 1194*, 36-43. doi: 10.1111/j.1749-6632.2010.05467.x
Margosio, B., Rusnati, M., Bonezzi, K., Cordes, B.-l. A., Annis, D. S., Urbinati, C., et al. (2008). Fibroblast growth factor-2 binding to the thrombospondin-1 type III repeats, a novel antiangiogenic domain. *The International Journal of Biochemistry & Cell Biology, 40*(4), 700-709. doi: http://doi.org/10.1016/j.biocel.2007.10.002
Maricich, S. M., Wellnitz, S. A., Nelson, A. M., Lesniak, D. R., Gerling, G. J., Lumpkin, E. A., et al. (2009). Merkel cells are essential for light-touch responses. *Science, 324*(5934), 1580-1582. doi: 10.1126/science.1172890
Mathivanan, S., Ji, H., & Simpson, R. J. (2010). Exosomes: Extracellular organelles important in intercellular communication. *Journal of Proteomics, 73*(10), 1907-1920. doi: http://dx.doi.org/10.1016/j.jprot.2010.06.006
McHugh, M. L. (2011). Multiple comparison analysis testing in ANOVA. *Biochem Med (Zagreb), 21*(3), 203-209.

Meckes, D. G. (2015). Exosomal Communication Goes Viral. *Journal of Virology, 89*(10), 5200-5203. doi: 10.1128/JVI.02470-14
Meckes, D. G., Jr., Gunawardena, H. P., Dekroon, R. M., Heaton, P. R., Edwards, R. H., Ozgur, S., et al. (2013). Modulation of B-cell exosome proteins by gamma herpesvirus infection. *Proc Natl Acad Sci U S A, 110*(31), E2925-2933. doi: 10.1073/pnas.1303906110
Meckes, D. G., Jr., Shair, K. H., Marquitz, A. R., Kung, C. P., Edwards, R. H., & Raab-Traub, N. (2010). Human tumor virus utilizes exosomes for intercellular communication. *Proc Natl Acad Sci U S A, 107*(47), 20370-20375. doi: 10.1073/pnas.1014194107
Melo, S. A., Sugimoto, H., O'Connell, J. T., Kato, N., Villanueva, A., Vidal, A., et al. (2014). Cancer Exosomes Perform Cell-Independent MicroRNA Biogenesis and Promote Tumorigenesis. *Cancer cell, 26*(5), 707-721. doi: 10.1016/j.ccell.2014.09.005
Mirochnik, Y., Kwiatek, A., & Volpert, O. V. (2008). Thrombospondin and apoptosis: molecular mechanisms and use for design of complementation treatments. *Current drug targets, 9*(10), 851-862.
Moens, U., & Johannessen, M. (2008). Human polyomaviruses and cancer: expanding repertoire. *J Dtsch Dermatol Ges, 6*(9), 704-708. doi: 10.1111/j.1610-0387.2008.06810.x
Moens, U., Rasheed, K., Abdulsalam, I., & Sveinbjornsson, B. (2015). The role of Merkel cell polyomavirus and other human polyomaviruses in emerging hallmarks of cancer. *Viruses, 7*(4), 1871-1901. doi: 10.3390/v7041871
Moens, U., Seternes, O. M., Johansen, B., & Rekvig, O. P. (1997). Mechanisms of transcriptional regulation of cellular genes by SV40 large T- and small T-antigens. *Virus Genes, 15*(2), 135-154.
Moens, U., Van Ghelue, M., & Johannessen, M. (2007). Oncogenic potentials of the human polyomavirus regulatory proteins. *Cellular and Molecular Life Sciences, 64*(13), 1656-1678. doi: 10.1007/s00018-007-7020-3
Moll, I., Kuhn, C., & Moll, R. (1995). Cytokeratin 20 is a general marker of cutaneous Merkel cells while certain neuronal proteins are absent. *J Invest Dermatol, 104*(6), 910-915.
Morra, L., Rechsteiner, M., Casagrande, S., von Teichman, A., Schraml, P., Moch, H., et al. (2012). Characterization of periostin isoform pattern in non-small cell lung cancer. *Lung Cancer, 76*(2), 183-190. doi: http://doi.org/10.1016/j.lungcan.2011.10.013
Morrison, K. M., Miesegaes, G. R., Lumpkin, E. A., & Maricich, S. M. (2009). Mammalian Merkel cells are descended from the epidermal lineage. *Developmental biology, 336*(1), 76-83. doi: 10.1016/j.ydbio.2009.09.032
Mosher, D. F., Johansson, M. W., Gillis, M. E., & Annis, D. S. (2015). Periostin and TGF-β-induced Protein: Two Peas in a Pod? *Critical reviews in biochemistry and molecular biology, 50*(5), 427-439. doi: 10.3109/10409238.2015.1069791
Nag, S., Larsson, M., Robinson, R. C., & Burtnick, L. D. (2013). Gelsolin: the tail of a molecular gymnast. *Cytoskeleton (Hoboken), 70*(7), 360-384. doi: 10.1002/cm.21117
Naito, Y., Yoshioka, Y., Yamamoto, Y., & Ochiya, T. (2017). How cancer cells dictate their microenvironment: present roles of extracellular vesicles. *Cellular and Molecular Life Sciences, 74*(4), 697-713. doi: 10.1007/s00018-016-2346-3
Nelson, D. L., & Cox, M. M. (2013). *Lehninger Principles of Biochemistry* (sixth ed.). Houndmills, Basingstoke, England: Macmillan Higher Education.
Nghiem, P. T., Bhatia, S., Lipson, E. J., Kudchadkar, R. R., Miller, N. J., Annamalai, L., et al. (2016). PD-1 Blockade with Pembrolizumab in Advanced Merkel-Cell Carcinoma. *N Engl J Med, 374*(26), 2542-2552. doi: 10.1056/NEJMoa1603702

Ni, X. G., Zhou, L., Wang, G. Q., Liu, S. M., Bai, X. F., Liu, F., et al. (2008). The ubiquitin-proteasome pathway mediates gelsolin protein downregulation in pancreatic cancer. *Mol Med, 14*(9-10), 582-589. doi: 10.2119/2008-00020.Ni

Nikfarjam, L., & Farzaneh, P. (2012). Prevention and Detection of Mycoplasma Contamination in Cell Culture. *Cell Journal (Yakhteh), 13*(4), 203-212.

Nolan, T., Hands, R. E., & Bustin, S. A. (2006). Quantification of mRNA using real-time RT-PCR. *Nature protocols, 1*(3), 1559-1582.

Particle Sizing Systems. (2016). DLS. Retrieved 16.02., 2017, from http://pssnicomp.com/glossary/dls/

Peng, Y. C., & Acheson, N. H. (1998). Polyomavirus large T antigen binds cooperatively to its multiple binding sites in the viral origin of DNA replication. *J Virol, 72*(9), 7330-7340.

Perez-Janices, N., Blanco-Luquin, I., Tuñón, M. T., Barba-Ramos, E., Ibáñez, B., Zazpe-Cenoz, I., et al. (2015). EPB41L3, TSP-1 and RASSF2 as new clinically relevant prognostic biomarkers in diffuse gliomas. *Oncotarget, 6*(1), 368-380.

Pfaffl, M. W. (2004). Quantification strategies in real-time PCR. In Bustin S.A. (Ed.), *A-Z of quantitative PCR* (pp. 87 - 112). La Jolla, CA, USA: International University Line (IUL).

Pilzer, D., & Fishelson, Z. (2005). Mortalin/GRP75 promotes release of membrane vesicles from immune attacked cells and protection from complement-mediated lysis. *Int Immunol 17* (9), 1239-1248. . doi: doi: 10.1093/intimm/dxh300

Promega. (2017). pGL3 Luciferase Reporter Vectors: Promega Corporation, an affiliate of Promega Biotech AB.

Qiagen. (2014). RNeasy® Plus Mini Handbook For purification of total RNA from animal cells and easy-to-lyse animal tissues using gDNA Eliminator columns (Vol. 12/2014). USA.

Raposo, G., Nijman, H. W., Stoorvogel, W., Liejendekker, R., Harding, C. V., Melief, C. J., et al. (1996). B lymphocytes secrete antigen-presenting vesicles. *J Exp Med, 183*(3), 1161-1172.

Ren, B., Song, K., Parangi, S., Jin, T., Ye, M., Humphreys, R., et al. (2009). A Double Hit to Kill Tumor and Endothelial Cells by TRAIL and Antiangiogenic 3TSR. *Cancer Res, 69*(9), 3856-3865. doi: 10.1158/0008-5472.CAN-08-2940

Richards, K. F., Guastafierro, A., Shuda, M., Toptan, T., Moore, P. S., & Chang, Y. (2015). Merkel cell polyomavirus T antigens promote cell proliferation and inflammatory cytokine gene expression. *J Gen Virol, 96*(12), 3532-3544. doi: 10.1099/jgv.0.000287

Riss, T. L., Moravec, R. A., Niles, A. L., Duellman, S., Benink, H. A., Worzella, T. J., et al. (2004). Cell Viability Assays. In G. S. Sittampalam, N. P. Coussens, K. Brimacombe, A. Grossman, M. Arkin, D. Auld, C. Austin, B. Bejcek, M. Glicksman, J. Inglese, P. W. Iversen, Z. Li, J. McGee, O. McManus, L. Minor, A. Napper, J. M. Peltier, T. Riss, O. J. Trask, Jr., & J. Weidner (Eds.), *Assay Guidance Manual*. Bethesda (MD): Eli Lilly & Company and the National Center for Advancing Translational Sciences.

Rodriguez-Manzaneque, J. C., Lane, T. F., Ortega, M. A., Hynes, R. O., Lawler, J., & Iruela-Arispe, M. L. (2001). Thrombospondin-1 suppresses spontaneous tumor growth and inhibits activation of matrix metalloproteinase-9 and mobilization of vascular endothelial growth factor. *Proc Natl Acad Sci U S A, 98*(22), 12485-12490. doi: 10.1073/pnas.171460498

Ruan, K., Bao, S., & Ouyang, G. (2009). The multifaceted role of periostin in tumorigenesis. *Cellular and Molecular Life Sciences, 66*(14), 2219. doi: 10.1007/s00018-009-0013-7

Sambrooke, J., & Russel, D. W. (2001). *Molecular Cloning; a laboratory manual* (Third ed. Vol. 1). USA: Cold Spring Harbor Laboratory Press.

Saribas, A. S., Coric, P., Hamazaspyan, A., Davis, W., Axman, R., White, M. K., et al. (2016). Emerging From the Unknown: Structural and Functional Features of Agnoprotein of Polyomaviruses. *J Cell Physiol, 231*(10), 2115-2127. doi: 10.1002/jcp.25329

Sasaki, H., Sato, Y., Kondo, S., Fukai, I., Kiriyama, M., Yamakawa, Y., et al. (2002). Expression of the periostin mRNA level in neuroblastoma. *J Pediatr Surg, 37*(9), 1293-1297.

Schmitt, M., Wieland, U., Kreuter, A., & Pawlita, M. (2012). C-terminal deletions of Merkel cell polyomavirus large T-antigen, a highly specific surrogate marker for virally induced malignancy. *Int J Cancer, 131*(12), 2863-2868. doi: 10.1002/ijc.27607

Seo, G. J., Chen, C. J., & Sullivan, C. S. (2009). Merkel cell polyomavirus encodes a microRNA with the ability to autoregulate viral gene expression. *Virology, 383*(2), 183-187. doi: 10.1016/j.virol.2008.11.001

Shao, R., Bao, S., Bai, X., Blanchette, C., Anderson, R. M., Dang, T., et al. (2004). Acquired Expression of Periostin by Human Breast Cancers Promotes Tumor Angiogenesis through Up-Regulation of Vascular Endothelial Growth Factor Receptor 2 Expression. *Molecular and Cellular Biology, 24*(9), 3992-4003. doi: 10.1128/MCB.24.9.3992-4003.2004

Shieh, D.-B., Chen, I. W., Wei, T.-Y., Shao, C.-Y., Chang, H.-J., Chung, C.-H., et al. (2006). Tissue expression of gelsolin in oral carcinogenesis progression and its clinicopathological implications. *Oral Oncology, 42*(6), 599-606. doi: 10.1016/j.oraloncology.2005.10.021

Shieh, D. B., Godleski, J., Herndon, J. E., Azuma, T., Mercer, H., Sugarbaker, D. J., et al. (1999). Cell motility as a prognostic factor in stage I nonsmall cell lung carcinoma. *Cancer, 85*(1), 47-57.

Shuda, M., Chang, Y., & Moore, P. S. (2014). Merkel cell polyomavirus-positive Merkel cell carcinoma requires viral small T-antigen for cell proliferation. *J Invest Dermatol, 134*(5), 1479-1481. doi: 10.1038/jid.2013.483

Shuda, M., Feng, H., Kwun, H. J., Rosen, S. T., Gjoerup, O., Moore, P. S., et al. (2008). T antigen mutations are a human tumor-specific signature for Merkel cell polyomavirus. *Proc Natl Acad Sci U S A, 105*(42), 16272-16277. doi: 10.1073/pnas.0806526105

Shuda, M., Guastafierro, A., Geng, X., Shuda, Y., Ostrowski, S. M., Lukianov, S., et al. (2015). Merkel Cell Polyomavirus Small T Antigen Induces Cancer and Embryonic Merkel Cell Proliferation in a Transgenic Mouse Model. *PLoS One, 10*(11), e0142329. doi: 10.1371/journal.pone.0142329

Shuda, M., Kwun, H. J., Feng, H., Chang, Y., & Moore, P. S. (2011). Human Merkel cell polyomavirus small T antigen is an oncoprotein targeting the 4E-BP1 translation regulator. *The Journal of Clinical Investigation, 121*(9), 3623-3634. doi: 10.1172/JCI46323

Soldevilla, B., Rodriguez, M., San Millan, C., Garcia, V., Fernandez-Perianez, R., Gil-Calderon, B., et al. (2014). Tumor-derived exosomes are enriched in DeltaNp73, which promotes oncogenic potential in acceptor cells and correlates with patient survival. *Hum Mol Genet, 23*(2), 467-478. doi: 10.1093/hmg/ddt437

Soto-Pantoja, D. R., Sipes, J. M., Morris, N., Emmenaker, N. J., & Roberts, D. D. (2015). Thrombospondin-1 regulates energy metabolism to increase carcinogenesis in an in vivo model of colorectal cancer: AACR.

Soung, Y. H., Nguyen, T., Cao, H., Lee, J., & Chung, J. (2016). Emerging roles of exosomes in cancer invasion and metastasis. *BMB Rep, 49*(1), 18-25.

Spurgeon, M. E., Cheng, J., Bronson, R. T., Lambert, P. F., & DeCaprio, J. A. (2015). Tumorigenic activity of merkel cell polyomavirus T antigens expressed in the

stratified epithelium of mice. *Cancer Res, 75*(6), 1068-1079. doi: 10.1158/0008-5472.can-14-2425
System Biosciences. (2013). ExoQuick-TCTM Exosome Precipitation Solution, User manual.
Szeder, V., Grim, M., Halata, Z., & Sieber-Blum, M. (2003). Neural crest origin of mammalian Merkel cells. *Developmental biology, 253*(2), 258-263. doi: http://dx.doi.org/10.1016/S0012-1606(02)00015-5
Takeshita, S., Kikuno, R., Tezuka, K., & Amann, E. (1993). Osteoblast-specific factor 2: cloning of a putative bone adhesion protein with homology with the insect protein fasciclin I. *Biochem J, 294 (Pt 1)*, 271-278.
Theiss, J. M., Günther, T., Alawi, M., Neumann, F., Tessmer, U., Fischer, N., et al. (2015). A Comprehensive Analysis of Replicating Merkel Cell Polyomavirus Genomes Delineates the Viral Transcription Program and Suggests a Role for mcv-miR-M1 in Episomal Persistence. *PLoS Pathogens, 11*(7), e1004974. doi: 10.1371/journal.ppat.1004974
Thery, C., Duban, L., Segura, E., Veron, P., Lantz, O., & Amigorena, S. (2002). Indirect activation of naive CD4+ T cells by dendritic cell-derived exosomes. *Nat Immunol, 3*(12), 1156-1162.
Thery, C., Ostrowski, M., & Segura, E. (2009). Membrane vesicles as conveyors of immune responses. *Nat Rev Immunol, 9*(8), 581-593.
Thor, A. D., Edgerton, S. M., Liu, S., Moore, D. H., & Kwiatkowski, D. J. (2001). Gelsolin as a Negative Prognostic Factor and Effector of Motility in erbB-2-positive Epidermal Growth Factor Receptor-positive Breast Cancers. *Clinical Cancer Research, 7*(8), 2415-2424.
Toker, C. (1972). Trabecular carcinoma of the skin. *Arch Dermatol, 105*(1), 107-110.
Uniprot. (2017). UniProtKB - P07996 (TSP1_HUMAN). Retrieved 28.04, 2017, from http://www.uniprot.org/uniprot/P07996 - sequences
Van Ghelue, M., & Moens, U. (2011). Merkel Cell Polyomavirus: A Causal Factor in Merkel Cell Carcinoma. In Prof. Caterina La Porta (Ed.), *Skin Cancers - Risk Factors, Prevention and Therapy (chapter 5)*. Tromsø, Norway: INTECH, Chapters published November 14, 2011 under CC BY 3.0 license.
Van Keymeulen, A., Mascre, G., Youseff, K. K., Harel, I., Michaux, C., De Geest, N., et al. (2009). Epidermal progenitors give rise to Merkel cells during embryonic development and adult homeostasis. *The Journal of Cell Biology, 187*(1), 91-100. doi: 10.1083/jcb.200907080
Veitch, N. C. (2004). Horseradish peroxidase: a modern view of a classic enzyme. *Phytochemistry, 65*(3), 249-259.
Verhaegen, M. E., Mangelberger, D., Harms, P. W., Vozheiko, T. D., Weick, J. W., Wilbert, D. M., et al. (2015). Merkel cell polyomavirus small T antigen is oncogenic in transgenic mice. *J Invest Dermatol, 135*(5), 1415-1424. doi: 10.1038/jid.2014.446
Vincent-Schneider, H., Stumptner-Cuvelette, P., Lankar, D., Pain, S., Raposo, G., Benaroch, P., et al. (2002). Exosomes bearing HLA-DR1 molecules need dendritic cells to efficiently stimulate specific T cells. *Int Immunol, 14*(7), 713-722.
Vogel, C., & Marcotte, E. M. (2012). Insights into the regulation of protein abundance from proteomic and transcriptomic analyses. *Nature reviews. Genetics, 13*(4), 227-232. doi: 10.1038/nrg3185
Volpert, O. V., Zaichuk, T., Zhou, W., Reiher, F., Ferguson, T. A., Stuart, P. M., et al. (2002). Inducer-stimulated Fas targets activated endothelium for destruction by anti-angiogenic thrombospondin-1 and pigment epithelium-derived factor. *Nat Med, 8*(4), 349-357. doi: 10.1038/nm0402-349

Vousden, K. H., & Lane, D. P. (2007). p53 in health and disease. *Nat Rev Mol Cell Biol, 8*(4), 275-283. doi: 10.1038/nrm2147

Wang, S., Herndon, M. E., Ranganathan, S., Godyna, S., Lawler, J., Argraves, W. S., et al. (2004). Internalization but not binding of thrombospondin-1 to low density lipoprotein receptor-related protein-1 requires heparan sulfate proteoglycans. *J Cell Biochem, 91*(4), 766-776. doi: 10.1002/jcb.10781

Wang, Z., Xiong, S., Mao, Y., Chen, M., Ma, X., Zhou, X., et al. (2016). Periostin promotes immunosuppressive premetastatic niche formation to facilitate breast tumour metastasis. *The Journal of Pathology, 239*(4), 484-495. doi: 10.1002/path.4747

Webber, J., Steadman, R., Mason, M. D., Tabi, Z., & Clayton, A. (2010). Cancer exosomes trigger fibroblast to myofibroblast differentiation. *Cancer Res, 70*(23), 9621-9630. doi: 10.1158/0008-5472.can-10-1722

Wendler, F., Favicchio, R., Simon, T., Alifrangis, C., Stebbing, J., & Giamas, G. (2017). Extracellular vesicles swarm the cancer microenvironment: from tumor-stroma communication to drug intervention. *Oncogene, 36*(7), 877-884. doi: 10.1038/onc.2016.253

Wendzicki, J. A., Moore, P. S., & Chang, Y. (2015). Large T and small T antigens of Merkel cell polyomavirus. *Curr Opin Virol, 11*, 38-43. doi: 10.1016/j.coviro.2015.01.009

Woo, S.-H., Stumpfova, M., Jensen, U. B., Lumpkin, E. A., & Owens, D. M. (2010). Identification of epidermal progenitors for the Merkel cell lineage. *Development, 137*(23), 3965-3971. doi: 10.1242/dev.055970

Wu, H. A. N., Chen, L., Xie, J. U. N., Li, R. A. N., Li, G.-N., Chen, Q.-H., et al. (2016). Periostin expression induced by oxidative stress contributes to myocardial fibrosis in a rat model of high salt-induced hypertension. *Molecular Medicine Reports, 14*(1), 776-782. doi: 10.3892/mmr.2016.5308

Wu, T., Luo, Q., & Ouyang, G. (2015). Periostin: a potent chemotactic factor for recruiting tumor-associated macrophage. *Protein & Cell, 6*(4), 235-237. doi: 10.1007/s13238-015-0141-9

Wu, Z., Zeng, Q., Cao, K., & Sun, Y. (2016). Exosomes: small vesicles with big roles in hepatocellular carcinoma. *Oncotarget, 7*(37), 60687-60697. doi: 10.18632/oncotarget.10807

Yang, C., Kim, S. H., Bianco, N. R., & Robbins, P. D. (2011). Tumor-derived exosomes confer antigen-specific immunosuppression in a murine delayed-type hypersensitivity model. *PLoS One, 6*(8), e22517. doi: 10.1371/journal.pone.0022517

Yang, Q. W., Liu, S., Tian, Y., Salwen, H. R., Chlenski, A., Weinstein, J., et al. (2003). Methylation-associated silencing of the thrombospondin-1 gene in human neuroblastoma. *Cancer Res, 63*(19), 6299-6310.

Yu, S., Cao, H., Shen, B., & Feng, J. (2015). Tumor-derived exosomes in cancer progression and treatment failure. *Oncotarget, 6*(35), 37151-37168. doi: 10.18632/oncotarget.6022

Yu, S., Liu, C., Su, K., Wang, J., Liu, Y., Zhang, L., et al. (2007). Tumor exosomes inhibit differentiation of bone marrow dendritic cells. *J Immunol, 178*(11), 6867-6875.

Zacharski, L. R., Memoli, V. A., Morain, W. D., Schlaeppi, J. M., & Rousseau, S. M. (1995). Cellular localization of enzymatically active thrombin in intact human tissues by hirudin binding. *Thromb Haemost, 73*(5), 793-797.

Zeelenberg, I. S., Ostrowski, M., Krumeich, S., Bobrie, A., Jancic, C., Boissonnas, A., et al. (2008). Targeting tumor antigens to secreted membrane vesicles in vivo induces efficient antitumor immune responses. *Cancer Res, 68*(4), 1228-1235. doi: 10.1158/0008-5472.can-07-3163

Zhang, H.-G., & Grizzle, W. E. (2014). Exosomes: A Novel Pathway of Local and Distant Intercellular Communication that Facilitates the Growth and Metastasis of Neoplastic

Lesions. *The American Journal of Pathology, 184*(1), 28-41. doi: 10.1016/j.ajpath.2013.09.027

Zhang, X., Yuan, X., Shi, H., Wu, L., Qian, H., & Xu, W. (2015). Exosomes in cancer: small particle, big player. *Journal of Hematology & Oncology, 8*, 83. doi: 10.1186/s13045-015-0181-x

Zhuang, G., Wu, X., Jiang, Z., Kasman, I., Yao, J., Guan, Y., et al. (2012). Tumour-secreted miR-9 promotes endothelial cell migration and angiogenesis by activating the JAK-STAT pathway. *Embo j, 31*(17), 3513-3523. doi: 10.1038/emboj.2012.183

Zhuo, J., Tan, E. H., Yan, B., Tochhawng, L., Jayapal, M., Koh, S., et al. (2012). Gelsolin Induces Colorectal Tumor Cell Invasion via Modulation of the Urokinase-Type Plasminogen Activator Cascade. *PLoS One, 7*(8), e43594. doi: 10.1371/journal.pone.0043594

Zitvogel, L., Regnault, A., Lozier, A., Wolfers, J., Flament, C., Tenza, D., et al. (1998). Eradication of established murine tumors using a novel cell-free vaccine: dendritic cell derived exosomes. *Nat Med, 4*(5), 594-600.

Appendices

Appendix 1. Alignment of MKL-1 and MKL-2 genomes

The LT-ag coding sequence (exons) is highlighted in grey. The deleted sequences in MKL-1 LT-ag compared to MKL-2 LT-ag is shown by a stippled line. Stars indicate equal bases in the two sequences. The start codon of LT-ag is shown in green and the stop codon in red. The primers used in PCR are shown in light blue. Notice that there is one mismatch in the forward primer. MKL-1 encodes a 440 bp LT-ag, while MKL-2 LT-ag spans 394 bp.

```
MKL-1       ------------------------------------------GGGGCTCCTAGCCTCC
MKL-2       TTGGCTGCCTAGGTGACTTTTTTTTTTCAAGTTGGCAGAGGCTTGGGGCTCCTAGCCTCC
                                                      ****************

MKL-1       GAGGCCTCTGGAAAAAAAAGAGAGAGGCCTCTGAGGCTTAAGAGGCTTAATTAGCAAAAA
MKL-2       GAGGCCTCTGGAAAAAAAAGAGAGAGGCCTCTGAGGCTTAAGAGGCTTAATTAGCAAAAA
            ************************************************************

MKL-1       AGGCAGTATCTAAGGGCAGATCCCAAGGGCGGGAAACTGCAGTATAAAAACCACTCCTTA
MKL-2       AGGCAGTATCTAAGGGCAGATCCCAAGGGCGGGAAACTGCAGTATAAAAACCACTCCTTA
            ************************************************************

MKL-1       GTGAGGTGGCTCATTTGCTCCTCTGCTCTTTCTGCAAACTCCTTCTGCATATAGACAAGA
MKL-2       GTGAGGTAGCTCATTTGCTCCTCTGCTCTTTCTGCAAACTCCTTCTGCATATAGACAAGA
            ******* ****************************************************

MKL-1       TGGATTTAGTCCTAAATAGGAAAGAAAGAGAGGCTCTCTGCAAGCTTTTAGAGATTGCTC
MKL-2       TGGATTTAGTCCTAAATAGGAAAGAAAGAGAGGCTCTCTGCAAGCTTTTAGAGATTTCTC
            ********************************************************** ***

MKL-1       CTAATTGTTATGGCAACATCCCTCTGATGAAAGCTGCTTTCAAAAGAAGCTGCTTAAAGC
MKL-2       CTAATTGTTATGGCAACATCCCTCTGATGAAAGCTGCTTTCAAAAGAAGCTGCTTAAAGC
            ************************************************************

MKL-1       ATCACCCTGATAAAGGGGGAAATCCTGTTATAATGATGGAATTGAACACCCTTTGGAGCA
MKL-2       ATCACCCTGATAAAGGGGGAAATCCTGTTATAATGATGGAATTGAACACCCTTTGGAGCA
            ************************************************************

MKL-1       AATTCCAGCAAAATATCCACAAGCTCAGAAGTGACTTCTCTATGTTTGATGAGGTCAGTA
```

```
MKL-2       AATTCCAGCAAAATATCCACAAGCTCAGAAGTGACTTCTCTATGTTTGATGAGGTCAGTA
            ************************************************************

MKL-1       CAAAATTTCCTTGGGAAGAATATGGAACTTTAAAGGATTATATGCAAAGTGGATATAATG
MKL-2       CAAAATTTCCTTGGGAAGAATATGGAACTTTAAAGGATTATATGCAAAGTGGATATAATG
            ************************************************************

MKL-1       CTAGATTTTGCAGAGGTCCTGGGTGCATGCTTAAGCAACTTAGAGATTCTAAGTGCGCTT
MKL-2       CTAGATTTTGCAGAGGTCCTGGGTGCATGCTTAAGCAACTTAGAGATTCTAAGTGCGCTT
            ************************************************************

MKL-1       GTATTAGCTGTAAGTTGTCTCGCCAGCATTGTAGTCTAAAAACTTTAAAGCAAAAAAACT
MKL-2       GTATTAGCTGTAAGTTGTCTCGCCAGCATTGTAGTCTAAAAACTTTAAAGCAAAAAAACT
            ************************************************************

MKL-1       GTCTGACGTGGGGAGAGTGTTTTTGCTATCAGTGCTTTATTCTTTGGTTTGGATTTCCTC
MKL-2       GTCTGACGTGGGGAGAGTGTTTTTGCTATCAGTGCTTTATTCTTTGGTTTGGATTTCCTC
            ************************************************************

MKL-1       CTACTTGGGAAAGTTTTGACTGGTGGCAAAAAACTTTAGAAGAAACTGACTACTGCTTAC
MKL-2       CTACTTGGGAAAGTTTTGACTGGTGGCAAAAAACTTTAGAAGAAACTGACTACTGCTTAC
            ************************************************************

MKL-1       TGCATCTGCACCTTTTCTAGACTCCTACTTCCTTCCTCTGTAAGTATTAGATATGGAAAA
MKL-2       TGCATCTGCACCTTTTCTAGACTCCTACTTCCTTCCTCTGTAAGTATTAGATATGGAAAA
            ************************************************************

MKL-1       GTCTATAAGGCAAAATATCAAAGAAAGGTTATTTATGACAGATTTTCTGTACTTTCCCAT
MKL-2       GTCTATAAGGCAAAATATCAAAGAAAGGTTATTTATGACAGATTTTCTGTACTTTCCCAT
            ************************************************************

MKL-1       CTAGGTTGACGAGGCCCCTATATATGGGACCACTAAATTCAAAGAATGGTGGAGATCAGG
MKL-2       CTAGGTTGACGAGGCCCCTATATATGGGACCACTAAATTCAAAGAATGGTGGAGATCAGG
            ************************************************************

MKL-1       AGGATTCAGCTTCGGGAAGGCATACGAATATGGGCCCAATCCACACGGGACCAACTCAAG
MKL-2       AGGATTCAGCTTCGGGAAGGCATACGAATATGGGCCCAATCCACACGGGACCAACTCAAG
            ************************************************************

MKL-1       ATCCAGAAAGCCTTCCTCCAATGCATCCAGGGGAGCCCCCAGTGGAAGCTCACCACCCCA
MKL-2       ATCCAGAAAGCCTTCCTCCAATGCATCCAGGGGAGCCCCCAGTGGAAGCTCACCACCCCA
            ************************************************************
```

```
MKL-1       CAGCCAGAGCTCTTCCTCTGGGTATGGGTCCTTCTCAGCGTCCCAGGCTTCAGACTCCCA
MKL-2       CAGCCAGAGCTCTTCCTCTGGGTATGGGTCCTTCTCAGCGTCCCAGGCTTCAGACTCCCA
            ************************************************************

MKL-1       GTCCAGAGGACCCGATATACCTCCCGAACACCATGAGGAACCCACCTCATCCTCTGGATC
MKL-2       GTCCAGAGGACCCGATATACCTCCCGAACACCATGAGGAACCCACCTCATCCTCTGGATC
            ************************************************************

MKL-1       CAGTAGCAGAGAGGAGACCACCAATTCAGGAAGAGAATCCAGCACACCCAATGGAACCAG
MKL-2       CAGTAGCAGAGAGGAGACCACCAATTCAGGAAGAGAATCCAGCACACCCAATGGAACCAG
            ************************************************************

MKL-1       TGTACCTAGAAATTCTTCCAGAACGGATGGCACCTGGGAGGATCTCTTCTGCGATGAATC
MKL-2       TGTACCTAGAAATTCTTCCAGAACGGATGGCACCTGGGAGGATCTCTTCTGCGATGAATC
            ************************************************************

MKL-1       ACTTTCCTCCCCTGAGCCTCCCTCGTCCTCTGAGGAGCCTGAGGAGCCCCCCTCCTCAAG
MKL-2       ACTTTCCTCCCCTGAGCCTCCCTCGTCCTCTGAGGAGCCTGAGGAGCCCCCCTCCTCAAG
            ************************************************************

MKL-1       AAGCTCGCCCCGGCAGCCCCCGTCTTCCTCTGCCGAGGAGGCCTCGTCATCTCAGTTTAC
MKL-2       AAGCTCGCCCCGGCAGCCCCCGTCTTCCTCTGCCGAGGAGGCCTCGTCATCTCAGTTTAC
            ************************************************************

MKL-1       AGATGAGGAATACAGATCCTCCTCCTTCACCACCCCGAAGACCCCTCCTCCATTCTCAAG
MKL-2       AGATGAGGAATACAGATTCTCCTCCTTCACCACCCCGAAGACCCCTCCTGCATTCTAAAG
            ***************** ****************************** ****** ***

MKL-1       AAAGCGAAAATTTGGGGGGTCCCGAAGCTCTGCAAGCTCTGCTAGTTCAGCAAGTTTTAC
MKL-2       AAAGCGAAAATTTGGGGGGTCCCGAAGCTCTGCAAGCTGTGCTAGTTTAGCAAGTTTTAT
            ************************************ ******** **********

MKL-1       AAGCACTCCACCAAAGCCAAAAAAGAACAGAGAAACTCCTGTTCCTACTGATTTTCCTAT
MKL-2       AAGCACTCCACCAAAGCCAAAAAAGAATAGAGAAACTCCTGTTCCTACTGATTTTCCTAT
            ************************** ********************************

MKL-1       TGATCTTTCTGATTATCTTAGCCATGCTGTATATA-------------------------
MKL-2       TGATCTTTCTGATTATCTTAGCCATGCTGTATATAGTAATAAAACAGTAAGTTGTTTTGC
            ***********************************

MKL-1       ----------------------AGCTATAGAGTTATATGATAAGATTGAGAAATTTAAAGT
MKL-2       CATTTATACTACTTCTGATAAAGCTATAGAGTTATATGATAAGATTGAGAAATTTAAAGT
```

```
                                    ****************************************

MKL-1       TGATTTTAAAAGCAGGCATGCCTGTGAATTAGGATGTATTTTATTGTTTATAACTTTATC

MKL-2       TGATTTTAAAAGCAGGCATGCCTGTGAATTAGGATGTATTTTATTGTTTATAACTTTATG

            ************************************************************

MKL-1       AAAGCATAGAGTATCTGCTATTAAGAATTTTTGCTCTACCTTCTGCACTATAAGCTTTTT

MKL-2       AAAGCATAGAGTATCTGCTATTAAGAATTTTTGCTGTACCTTCTGCACTATAAGCTTTTT

            ********************************** ************************

MKL-1       AATTTGTAAAGGAGTGAATAAGATGCCTGAAATGTATAATAATTTATGCAAGCCCCCTTA

MKL-2       AATTTGTAAAGGAGTGAATAAGATGCCTGAAATGTATAATAATTTATGCAAGCCCCCTTA

            ************************************************************

MKL-1       CAAATTACTGCAAGAGAATAAGCCACTGCTCAATTATGAATTTCAAGAAAAAGAAAAAGA

MKL-2       CAAATTACTGCAAGAGAATAAGCCACTGCTCAATTATGAATTTGAAGAAAAAGAAAAAGA

            ******************************************** ***************

MKL-1       GGCCAGCTGTAATTGGAATTTAGTTGCTGAATTTGCTTGTGAATATGAGCTAGACGACCA

MKL-2       GGCCAGCTGTAATTGGAATTTAGTTGCTGAATTTGCTTGTGAATATGAGCTAGACGACCA

            ******************************************************************

MKL-1       CTTTATTATCTTAGCCCATTATCTAGACTTTGCAAAACCATTTCCTTGCCAAAAGTGTGA

MKL-2       CTTTATTATCTTAGCCCATTATCTAGACTTTGCAAAACCATTTCCTTGCCAAAAGTGTGA

            ************************************************************

MKL-1       AAACAGATCTCGCCTCAAACCTCACAAGGCTCATGAGGCTCATCATTCTAATGCTAAGCT

MKL-2       AAACAGATCTTGCCTCAAACCTCACAAGGCTCATGAGGCTCATCATTCTAATGCTAAGCT

            ********** ***************************************************

MKL-1       ATTTTATGAATCTAAATCTCAGAAAACCATTTGCCAACAAGCCGCAGACACTGTTCTAGC

MKL-2       ATTTTATGAATCTAAATCTCAGAAAACCATTTGCCAACAAGCCGCAGACACTGTTCTAGC

            ************************************************************

MKL-1       CAAAAGGAGGTTAGAGATGCTGGAAATGACCAGGACAGAAATGCTATGTAAGAAGTTTAA

MKL-2       CAAAAGGAGGTTAGAGATGCTGGAAATGACCAGGACAGAAATGCTATGTAAGAAGTTTAA

            ************************************************************

MKL-1       GAAGCACCTAGAGAGATTAAGAGATTTAGATACAATAGATCTACTGTATTATATGGGTGG

MKL-2       GAAGCACCTAGAGAGATTAAGAGATTTAGATACAATAGATCTACTGTATTATATGGGTGG

            ************************************************************

MKL-1       TGTGGCCTGGTACTGCTGCTTATTTGAAGAGTTTGAAAAGAAGCTGCAGAAAATTATTCA
```

```
MKL-2       TGTGGCCTGGTACTGCTGCTTATTTGAAGAGTTTGAAAAGAAGCTGCAGAAAATTATTCA

            ************************************************************

MKL-1       ATTATTAACAGAGAATATACCTAAGTATAGAAACATTTGGTTTAAAGGGCCTATTAACAG

MKL-2       ATTATTAACAGAGAATATACCTAAGTATAGAAACATTTGGTTTAAAGGGCCTATTAACAG

            ************************************************************

MKL-1       TGGAAAAACAAGCTTTGCTGCAGCCTTAATAGATTTGCTAGAAGGGAAGGCCTTGAATAT

MKL-2       TGGAAAAACAAGCTTTGCTGCAGCCTTAATAGATTTGCTAGAAGGGAAGGCCTTGAATAT

            ************************************************************

MKL-1       AAACTGTCCATCTGATAAACTGCCTTTTGAACTAGGATGTGCTCTGGATAAATTTATGGT

MKL-2       AAACTGTCCATCTGATAAACTTCCTTTTGAACTAGGATGTGCTTTGGATAAATTTATGGT

            ******************** ********************* ****************

MKL-1       TGTTTTTGAGGATGTGAAAGGGCAAAATAGCCTAAATAAAGATCTGCAACCAGGGCAAGG

MKL-2       TGTTTTTGAGGATGTGAAAGGGCAAAATAGCCTAAATAAAGATCTGCAACCAGGGCAAGG

            ************************************************************

MKL-1       AATAAATAACCTTGATAACTTAAGAGATCATCTAGATGGTGCTGTAGCTGTAAGCTTAGA

MKL-2       AATAAATAACCTTGATAACTTAAGAGATCATCTAGATGGTGCTGTAGCTGTAAGCTTAGA

            ************************************************************

MKL-1       GAAGAAGCATGTGAATAAAAAGCATCAGATTTTTCCTCCTTGTATTGTTACTGCTAATGA

MKL-2       GAAGAAGCATGTGAATAAAAAGCATCAGATTTTTCCTCCTTGTATTGTTACTGCTAATGA

            ************************************************************

MKL-1       TTATTTTATTCCCAAAACATTAATAGCAAGATTTAGTTATACTTTACACTTTTCCCCAAA

MKL-2       TTATTTTATTCCCAAAACATTAATAGCAAGATTTAGTTATACTTTACACTTTTCCCCAAA

            ************************************************************

MKL-1       GGCAAATCTAAGAGATTCCCTGGATCAGAACATGGAAATAAGAAAAAGAAGAATTCTTCA

MKL-2       GGCAAATCTAAGAGATTCCCTGGATCAGAACATGGAAATAAGAAAAAGAAGAATTCTTCA

            ************************************************************

MKL-1       AAGTGGAACCACTTTATTGCTTTGTCTTATTTGGTGCTTGCCTGATACAACCTTTAAGCC

MKL-2       AAGTGGAACCACTTTATTGCTTTGTCTTATTTGGTGCTTGCCTGATACAACCTTTAAGCC

            ************************************************************

MKL-1       TTGCTTACAAGAAGAAATTAAAAACTGGAAGCAAATTTTACAGAGTGAAATATCATATGG

MKL-2       TTGCTTACAAGAAGAAATTAAAAACTGGAAGCAAATTTTACAGAGTGAAATATCATATGG

            ************************************************************
```

```
MKL-1       TAAATTTTGTCAAATGATAGAAAATGTAGAAGCTGGTCAGGACCCTCTGCTCAATATTCT
MKL-2       TAAATTTTGTCAAATGATAGAAAATGTAGAAGCTGGTCAGGACCCTCTGCTCAATATTCT
            ************************************************************

MKL-1       TATTGAGGAAGAGGGCCCTGAGGAAACTGAAGAAACCCAAGATTCTGGTACTTTTTCTCA
MKL-2       TATTGAGGAAGAGGGCCCTGAGGAAACTGAAGAAACCCAAGATTCTGGTACTTTTTCTCA
            ************************************************************

MKL-1       ATAAAGGCATCTGCTTCATATTTCCTGTGTTTGTTTTTCTGGGGCCTACTTAACTGAATA
MKL-2       ATAA--ACATCTGCTTCATATTTCCTGTGTTTGTTTTTCTGGGGCCTACTTAACTGAATA
            ****   ***************************************************

MKL-1       GGAATGCATGAAATAATTCTCATAATTCTTGTGTTTGGCTTTCTTTTTGAGAGGCCTTTT
MKL-2       GGAATGCATGAAATAATTCTCATAATTCTTGTGTTTGGCTTTCTTTTTGAGAGGCCTTTT
            ************************************************************

MKL-1       GAGGTCCTTTCAGTGGCGCCTTGCCCTTATCCTGCTGATTACTTTGGAATGTTACTGCTG
MKL-2       GAGGTCCTTTCAGTGGCGCCTTGCCCTTATCCTGCTGATTACTTTGGAATGTTACTGCTG
            ************************************************************

MKL-1       CTGGGGCAACAGAGGGCTTTGGGTAAACAGTTTTCTCCTGCCCAAATTTATCTAAAAATC
MKL-2       CTGGGGCAACAGAGGGCTTTGGGTAAACAGTTTTCTCCTGCCCAAATTTATCTAAAAATC
            ************************************************************

MKL-1       TGACAATATCAGGATCACCAGGTAATTGTTCTGACCCCTCATATATTCTAACCTCTTCTA
MKL-2       TGACAATATCAGGATCACCAGGTAATTGTTCTGACCCCTCATATATTCTAACCTCTTCTA
            ************************************************************

MKL-1       CCTGATTATCTTTTCCTTCCATAGGTTGGCCTGACACTTTTGGCATTAAGTTGCTGAAGA
MKL-2       CCTGATTATCTTTTCCTTCCATAGGTTGGCCTGACACTTTTGGCATTAAGTTGCTGAAGA
            ************************************************************

MKL-1       GTGAGTTTATTAAATTAACTACTGGGTAGGGGTTTTTCACCCATCTTTTTCTCAAAGTAA
MKL-2       GTGAGTTTATTAAATTAACTACTGGGTAGGGGTTTTTCACCCATCTTTTTCTCAAAGTAA
            ************************************************************

MKL-1       CATTAAAATATCTAGGCAACCCATGAAGAGCCATTTTTCCACTGGTTTTAAACAGAAACC
MKL-2       CATTAAAATATCTAGGCAACCCATGAAGAGCCATTTTTCCACTGGTTTTAAACAGAAACC
            ************************************************************

MKL-1       CCACTATGTCTGCACAGCTAATAAATAGGCCATCTCCTTTGCATAGAGGGCCCACTCCAT
MKL-2       CCACTATGTCTGCACAGCTAATAAATAGGCCATCTCCTTTGCATAGAGGGCCCACTCCAT
```

```
          ************************************************************

MKL-1     TCTCATCTAAAAGGACAGTAGTTAGAGTATTACTAAATTGAAGAACTGTAGGAGTCTGAG

MKL-2     TCTCATCTAAAAGGACAGTAGTTAGAGTATTACTAAATTGAAGAACTGTAGGAGTCTGAG

          ************************************************************

MKL-1     AGCCTGTCTGAATAGACCCATAGTATCTACTGTTTTCATTTTTAGAAGGATCAGGACACC

MKL-2     AGCCTGTCTGAATAGACCCATAGTATCTACTGTTTTCATTTTTAGAAGGATCAGGACACC

          ************************************************************

MKL-1     ATACTTCTATAGGATAATTTCCATCTTTATCTAATTTTGCTTTAGCTTGTGGATCTAGGC

MKL-2     ATACTTCTATAGGATAATTTCCATCTTTATCTAATTTTGCTTTAGCTTGTGGATCTAGGC

          ************************************************************

MKL-1     CCTGATTTTTAGGTGTCATTTTTCTTCCCAATACAGTTTCAATTGTAATAGGCCCACCAT

MKL-2     CCTGATTTTTAGGTGTCATTTTTCTTCCCAATACAGTTTCAATTGTAATAGGCCCACCAT

          ************************************************************

MKL-1     TTGTAGTTTTTGGATACTCAGTCTGGTAATCTAAAACTAGGCCTTGCAAATCCAGAGGTT

MKL-2     TTGTAGTTTTTGGATACTCAGTCTGGTAATCTAAAACTAGGCCTTGCAAATCCAGAGGTT

          ************************************************************

MKL-1     CTCCCCCAATGGCAAACATATGGTAATTTACTCCTGACACAGGAATACCAGCACCATAAT

MKL-2     CTCCCCCAATGGCAAACATATGGTAATTTACCCCTGACACAGGAATACCAGCACCATAAT

          ****************************** ****************************

MKL-1     CATGAACTCTTTTCATGTCCCAATAATGAACATTAATTAAAGAACTTATTCCAACTACTT

MKL-2     CATGAACTCTTTTCATGTCCCAATAATGAACATTAATTAAAGAACTTATTCCAACTACTT

          ************************************************************

MKL-1     CTGTTTTAACAGATATTGCCTCCCACATCTGCAATGTGTCACAGGTAATATCCTCATTTA

MKL-2     CTGTTTTAACAGATATTGCCTCCCACATCTGCAATGTGTCACAGGTAATATCCTCATTTA

          ************************************************************

MKL-1     GCATTGGCAGAGACACTCTTGCCACACTGTAAGCTGGCAAATTTTCCTTGATGGGCTGAT

MKL-2     GCATTGGCAGAGACACTCTTGCCACACTGTAAGCTGGCAAATTTTCCTTGATGGGCTGAT

          ************************************************************

MKL-1     CTGGAGATGATCCCTTTGGCTGCAGGTCATAAGTATAAGTATACCAGTTTGAAGTAGTAG

MKL-2     CTGGAGATGATCCCTTTGGCTGCAGGTCATAAGTATAAGTATACCAGTTTGAAGTAGTAG

          ************************************************************

MKL-1     GAAGATCAGGGGAATTAACTCCCATTCTTGGATTCAAATACAACTCAATTTGGGTAATGC
```

```
MKL-2       GAAGATCAGGGGAATTAACTCCCATTCTTGGATTCAAATACAACTCAATTTGGGTAATGC
            ************************************************************

MKL-1       TATCTTCTCCAGTAACCACAGATAATACTTCCACTCCTCCTTTAACAAGCAGTTTTGGAA
MKL-2       TATCTTCTCCAGTAACCACAGATAATACTTCCACTCCTCCTTTAACAAGCAGTTTTGGAA
            ************************************************************

MKL-1       CTGAGGCAACATTAGGGCAGCATCCCGGCTTAGGTATACATTGCCTTTTGGGTGTTTTAC
MKL-2       CTGAGGCAACATTAGGGCAGCATCCCGGCTTAGGTATACATTGCCTTTTGGGTGTTTTAC
            ************************************************************

MKL-1       AGGTGGATGATGCTTTTCTTTTTGGTGCCATCTTCAATTACTTGTAATTCAGGAGAAATA
MKL-2       AGGTGGATGATGCTTTTCTTTTTGGTGCCATCTTCAATTACTTGTAATTCAGGAGAAATA
            ************************************************************

MKL-1       TATCCACTAAGGCCTAGTACCAGAGGAAGAAGCCAATCTGGAGTTTGCTGCTGCAGAGTT
MKL-2       TATCCACTAAGGCCTAGCACCAGAGGAAGAAGCCAATCTGGAGTTTGCTGCTGCAGAGTT
            **************** ****************************************

MKL-1       CCTCCTATATGTTCAGGAATTAATATAGCCTCTCCTGATAAAAGGCCCTGATTCTGAGAA
MKL-2       CCTCCTATATGTTCAGGAATTAATATAGCCTCTCCTGATAAAAGGCCCTGATTCTGAGAA
            ************************************************************

MKL-1       GCAGTTGTCTGAAAGACCCACCGGCTATTTAGTATCAGATTCACTAGGTTTGATTGTATC
MKL-2       GCAGTTGTCTGAAAGACCCACCGGCTATTTAGTATCAGATTCACTAGGTTTGATTGTATC
            ************************************************************

MKL-1       TGCAGCCTAGAGGTAGGAGATAAAGAATTAAAAATATCTTGCCCCACAGAATGCAGCAAG
MKL-2       TGCAGCCTAGAGGTAGGAGATAAAGAATTAAAAATATCTTGCCCCACAGAATGCAGCAAG
            ************************************************************

MKL-1       CTATTTTCCCACTGCAGAGGATCTAGGCTAAAGGCCATAAGTGCATGCCTCAAAACCTCA
MKL-2       CTATTTTCCCACTGCAGAGGATCTAGGCTAAAGGCCATAAGTGCATGCCTCAAAACCTCA
            ************************************************************

MKL-1       TTACTACCTACCCACGAAACATCCCTCTTTACAAGTGACACTTGCTCGCGTGACAACCTC
MKL-2       TTACTACCTACCCACGAAACATCCCTCTTTACAAGTGACACTTGCTCGCGTGACAACCTC
            ************************************************************

MKL-1       ACCCCCACAGTTATTAGAGAGCCTATACCACTAACAGTTTGGAGAATGAAGCCATAAGTT
MKL-2       ACCCCCACAGTT------------------------------------------------
            ************
```

```
MKL-1      AAACCTTGGTTAACCAAAGAAGCCACTAATGAGAAATTTGAAAACTGTTCAGCTGTGAAC

MKL-2      ------------------------------------------------------------

MKL-1      CCAAGTTGAGCTAAAGCCTCAATGCCAGAAATACCCTCAATTGTCATTAAACTGGAGATC

MKL-2      ------------------------------------------------------------

MKL-1      TCTGCTTCCAAAGCTGCTAAAGCTTCTCCTGTAAGAATAGCTTCCAAAGTTACTCCTGTG

MKL-2      ------------------------------------------------------------

MKL-1      GTGGCACTTAGTTCAGTAGCAATTTCACCAATATTGGCCAGCAGTGTGATGATGCCCCCC

MKL-2      ------------------------------------------------------------

MKL-1      ATCCTGAAAAATAAATAAGGATACTTACTCTTTTAATGTCCTCCTCCCTTTGTAAGAGAA

MKL-2      ------------------------------------------------------------

MKL-1      AAAAAAGCCTCCGGGCCTCCCTTGTTGAAAAAAAGTTAAGAGTCTTCCGTCTCCCTCCCA

MKL-2      ------------------------------------------------------------

MKL-1      AACAGAAAGAAAAAAAGTTTTGTTTATCAGTCAAACTCCGCCTCTCCAGGAAATGAGTCA

MKL-2      ------------------------------------------------------------

MKL-1      ATGCCAGAAACCCTGCAGCAATAAAAGTTCAATCATGTAACCACAACTTGGCTGCCTAGG

MKL-2      ------------------------------------------------------------

MKL-1      TGACTTTTTTTTTTCAAGTTGGCAGAGGCTT

MKL-2      --------------------------------
```

Appendix 2. ANOVA tables generated from luciferase assays with gelsolin, periostin and thrombospondin promoters

Table 20. One-way ANOVA table generated for gelsolin luciferase assay experiment 1. The table indicates that there are significant differences within the dataset and a Dunnet's post hoc analysis was therefore undertaken.

Table Analyzed	Experiment 1				
Data sets analyzed	A : PCDNA 3.1 (empty vector)	B : MCPyV LT-ag	C : MCPyV st-ag	D : MCPyV LT+st-ag	
ANOVA summary					
F	47.33				
P value	<0.0001				
P value summary	****				
Significant diff. among means (P < 0.05)?	Yes				
R square	0.9467				
Brown-Forsythe test					
F (DFn, DFd)	0.458 (3, 8)				
P value	0.7191				
P value summary	ns				
Are SDs significantly different (P < 0.05)?	No				
Bartlett's test					
Bartlett's statistic (corrected)					
P value					
P value summary					
Are SDs significantly different (P < 0.05)?					
ANOVA table	SS	DF	MS	F (DFn, DFd)	P value
Treatment (between columns)	1523253994	3	507751331	F (3, 8) = 47.33	P<0.0001
Residual (within columns)	85827257	8	10728407		
Total	1609081251	11			
Data summary					
Number of treatments (columns)	4				
Number of values (total)	12				

Table 21. One-way ANOVA table generated for gelsolin luciferase assay experiment 2. The table indicates that there are significant differences within the dataset and a Dunnet's post hoc analysis was therefore undertaken.

Table Analyzed	Experiment 2				
Data sets analyzed	A : PCDNA 3.1	B : MCPyV LT-ag	C : MCPyV st-ag	D : MCPyV LT+st-ag	
ANOVA summary					
F	18.5				
P value	0.0006				
P value summary	***				
Significant diff. among means (P < 0.05)?	Yes				
R square	0.874				
Brown-Forsythe test					
F (DFn, DFd)	1.17 (3, 8)				
P value	0.3798				
P value summary	ns				
Are SDs significantly different (P < 0.05)?	No				
Bartlett's test					
Bartlett's statistic (corrected)					
P value					
P value summary					
Are SDs significantly different (P < 0.05)?					
ANOVA table	SS	DF	MS	F (DFn, DFd)	P value
Treatment (between columns)	1707662914	3	569220971	F (3, 8) = 18.5	P=0.0006
Residual (within columns)	246156451	8	30769556		
Total	1953819366	11			
Data summary					
Number of treatments (columns)	4				
Number of values (total)	12				

Table 22. One-way ANOVA table generated for gelsolin luciferase assay experiment 3. The table indicates that there are significant differences within the dataset and a Dunnet's post hoc analysis was therefore performed.

Table Analyzed	Experiment 3				
Data sets analyzed	A : PCDNA 3.1	B : MCPyV LT-ag	C : MCPyV st-ag	D : MCPyV LT+st-ag	
ANOVA summary					
F	9.613				
P value	0.0050				
P value summary	**				
Significant diff. among means (P < 0.05)?	Yes				
R square	0.7828				
Brown-Forsythe test					
F (DFn, DFd)	1.214 (3, 8)				
P value	0.3656				
P value summary	ns				
Are SDs significantly different (P < 0.05)?	No				
Bartlett's test					
Bartlett's statistic (corrected)					
P value					
P value summary					
Are SDs significantly different (P < 0.05)?					
ANOVA table	SS	DF	MS	F (DFn, DFd)	P value
Treatment (between columns)	809746799	3	269915600	F (3, 8) = 9.613	P=0.0050
Residual (within columns)	224633544	8	28079193		
Total	1034380343	11			
Data summary					
Number of treatments (columns)	4				
Number of values (total)	12				

Table 23. Two-way ANOVA table generated for the combined gelsolin luciferase assay experiments. The table indicates that there are significant differences within the dataset and a Dunnet's post hoc analysis was therefore undertaken. Column factor = treatment, row factor = experiment.

Table Analyzed	Three experiments combined				
Two-way ANOVA	Ordinary				
Alpha	0.05				
Source of Variation	% of total variation	P value	P value summary	Significant?	
Interaction	3.674	0.3252	ns	No	
Row Factor	1.449	0.2527	ns	No	
Column Factor	82.95	<0.0001	****	Yes	
ANOVA table	SS	DF	MS	F (DFn, DFd)	P value
Interaction	171369299	6	28561550	F (6, 24) = 1.232	P=0.3252
Row Factor	67602652	2	33801326	F (2, 24) = 1.457	P=0.2527
Column Factor	3869294408	3	1289764803	F (3, 24) = 55.61	P<0.0001
Residual	556617253	24	23192386		
Number of missing values	0				

Table 24. One-way ANOVA table generated for periostin luciferase assay experiment 1. The table indicates that there are significant differences within the dataset and a Dunnet's post hoc analysis was therefore applied to the dataset.

Table Analyzed	Experiment 1				
Data sets analyzed	A : PCDNA 3.1	B : MCPyV LT-ag	C : MCPyV st-ag	D : MCPyV LT+st-ag	
ANOVA summary					
F	18.83				
P value	0.0006				
P value summary	***				
Significant diff. among means (P < 0.05)?	Yes				
R square	0.876				
Brown-Forsythe test					
F (DFn, DFd)	0.9089 (3, 8)				
P value	0.4785				
P value summary	ns				
Are SDs significantly different (P < 0.05)?	No				
Bartlett's test					
Bartlett's statistic (corrected)					
P value					
P value summary					
Are SDs significantly different (P < 0.05)?					
ANOVA table	SS	DF	MS	F (DFn, DFd)	P value
Treatment (between columns)	9290313989	3	3096771330	F (3, 8) = 18.83	P=0.0006
Residual (within columns)	1315430011	8	164428751		
Total	10605744000	11			
Data summary					
Number of treatments (columns)	4				
Number of values (total)	12				

Table 25. One-way ANOVA table generated for periostin luciferase assay experiment 2. The table indicates that there are significant differences within the dataset and a Dunnet's post hoc analysis was therefore undertaken.

Table Analyzed	Experiment 2				
Data sets analyzed	A : PC DNA 3.1	B : MCPyV LT-ag	C : MCPyV st-ag	D : MCPyV LT+st-ag	
ANOVA summary					
F	12.69				
P value	0.0021				
P value summary	**				
Significant diff. among means (P < 0.05)?	Yes				
R square	0.8264				
Brown-Forsythe test					
F (DFn, DFd)	2.097 (3, 8)				
P value	0.1790				
P value summary	ns				
Are SDs significantly different (P < 0.05)?	No				
Bartlett's test					
Bartlett's statistic (corrected)					
P value					
P value summary					
Are SDs significantly different (P < 0.05)?					
ANOVA table	SS	DF	MS	F (DFn, DFd)	P value
Treatment (between columns)	11522649295	3	3840883098	F (3, 8) = 12.69	P=0.0021
Residual (within columns)	2420869696	8	302608712		
Total	13943518991	11			
Data summary					
Number of treatments (columns)	4				
Number of values (total)	12				

Table 26. One-way ANOVA table generated for periostin luciferase assay experiment 3. The table indicates that there are significant differences within the dataset and a Dunnet´s post hoc analysis was therefore performed.

Table Analyzed	Experiment 3				
Data sets analyzed	A : PCDNA 3.1	B : MCPyV LT-ag	C : MCPyV st-ag	D : MCPyV LT+st-ag	
ANOVA summary					
F	6.376				
P value	0.0163				
P value summary	*				
Significant diff. among means (P < 0.05)?	Yes				
R square	0.7051				
Brown-Forsythe test					
F (DFn, DFd)	0.2333 (3, 8)				
P value	0.8707				
P value summary	ns				
Are SDs significantly different (P < 0.05)?	No				
Bartlett's test					
Bartlett's statistic (corrected)					
P value					
P value summary					
Are SDs significantly different (P < 0.05)?					
ANOVA table	SS	DF	MS	F (DFn, DFd)	P value
Treatment (between columns)	14989091515	3	4996363838	F (3, 8) = 6.376	P=0.0163
Residual (within columns)	6268951333	8	783618917		
Total	21258042848	11			
Data summary					
Number of treatments (columns)	4				
Number of values (total)	12				

Table 27. Two-way ANOVA table generated for the combined periostin luciferase assay experiments. The table indicates that there are significant differences within the dataset and a Dunnet's post hoc analysis was therefore undertaken. Column factor = treatments, row factor = experiments.

Table Analyzed	3experiments combined				
Two-way ANOVA	Ordinary				
Alpha	0.05				
Source of Variation	% of total variation	P value	P value summary	Significant?	
Interaction	8.564	0.1634	ns	No	
Row Factor	7.947	0.0184	*	Yes	
Column Factor	63.38	<0.0001	****	Yes	
ANOVA table	SS	DF	MS	F (DFn, DFd)	P value
Interaction	4261454222	6	710242370	F (6, 24) = 1.704	P=0.1634
Row Factor	3954593595	2	1977296797	F (2, 24) = 4.743	P=0.0184
Column Factor	31540600577	3	10513533526	F (3, 24) = 25.22	P<0.0001
Residual	10005251041	24	416885460		
Number of missing values	0				

Table 28. One-way ANOVA table generated for thrombospondin luciferase assay experiment 1. The table indicates that there are significant differences within the dataset and a Dunnet's post hoc analysis was therefore applied.

Table Analyzed	Experiment 1				
Data sets analyzed	A : PCDNA 3.1	B : MCPyV LT-ag	C : MCPyV st-ag	D : MCPyV LT+st-ag	
ANOVA summary					
F	22.77				
P value	0.0003				
P value summary	***				
Significant diff. among means (P < 0.05)?	Yes				
R square	0.8952				
Brown-Forsythe test					
F (DFn, DFd)	0.492 (3, 8)				
P value	0.6976				
P value summary	ns				
Are SDs significantly different (P < 0.05)?	No				
Bartlett's test					
Bartlett's statistic (corrected)					
P value					
P value summary					
Are SDs significantly different (P < 0.05)?					
ANOVA table	SS	DF	MS	F (DFn, DFd)	P value
Treatment (between columns)	2.271e+014	3	75694708209089	F (3, 8) = 22.77	P=0.0003
Residual (within columns)	26591818441671	8	3323977305209		
Total	2.537e+014	11			
Data summary					
Number of treatments (columns)	4				
Number of values (total)	12				

Table 29. One-way ANOVA table generated for thrombospondin luciferase assay experiment 2. The table indicates that there are significant differences within the dataset and a Dunnet´s post hoc analysis was therefore undertaken.

Table Analyzed	Experiment 2				
Data sets analyzed	A : PCDNA 3.1	B : MCPyV LT-ag	C : MCPyV st-ag	D : MCPyV LT+st-ag	
ANOVA summary					
F	28.97				
P value	0.0001				
P value summary	***				
Significant diff. among means (P < 0.05)?	Yes				
R square	0.9157				
Brown-Forsythe test					
F (DFn, DFd)	0.5814 (3, 8)				
P value	0.6436				
P value summary	ns				
Are SDs significantly different (P < 0.05)?	No				
Bartlett's test					
Bartlett's statistic (corrected)					
P value					
P value summary					
Are SDs significantly different (P < 0.05)?					
ANOVA table	SS	DF	MS	F (DFn, DFd)	P value
Treatment (between columns)	1.703e+014	3	56757257573372	F (3, 8) = 28.97	P=0.0001
Residual (within columns)	15675922136521	8	1959490267065		
Total	1.859e+014	11			
Data summary					
Number of treatments (columns)	4				
Number of values (total)	12				

Table 30. One-way ANOVA table generated for thrombospondin luciferase assay experiment 3. The table indicates that there are significant differences within the dataset and a Dunnet's post hoc analysis was therefore undertaken.

Table Analyzed	Experiment 3				
Data sets analyzed	A : PCDNA 3.1	B : MCPyVLT-ag	C : MCPyV st-ag	D : MCPyV LT+st-ag	
ANOVA summary					
F	9.402				
P value	0.0053				
P value summary	**				
Significant diff. among means (P < 0.05)?	Yes				
R square	0.779				
Brown-Forsythe test					
F (DFn, DFd)	0.4186 (3, 8)				
P value	0.7446				
P value summary	ns				
Are SDs significantly different (P < 0.05)?	No				
Bartlett's test					
Bartlett's statistic (corrected)					
P value					
P value summary					
Are SDs significantly different (P < 0.05)?					
ANOVA table	SS	DF	MS	F (DFn, DFd)	P value
Treatment (between columns)	1.35e+014	3	45013361957769	F (3, 8) = 9.402	P=0.0053
Residual (within columns)	38302337641333	8	4787792205167		
Total	1.733e+014	11			
Data summary					
Number of treatments (columns)	4				
Number of values (total)	12				

Table 31. Two-way ANOVA table generated for the combined thrombospondin luciferase assay experiments. The table indicates that there are significant differences within the dataset and a Dunnet's post hoc analysis was therefore undertaken. Column factor = treatments, row factor = experiments.

Table Analyzed	Three experiments combined				
Two-way ANOVA	Ordinary				
Alpha	0.05				
Source of Variation	% of total variation	P value	P value summary	Significant?	
Interaction	7.988	0.0029	**	Yes	
Row Factor	47.47	<0.0001	****	Yes	
Column Factor	37.63	<0.0001	****	Yes	
ANOVA table	SS	DF	MS	F (DFn, DFd)	P value
Interaction	93222691212458	6	15537115202076	F (6, 24) = 4.628	P=0.0029
Row Factor	5.54e+014	2	2.77e+014	F (2, 24) = 82.51	P<0.0001
Column Factor	4.392e+014	3	1.464e+014	F (3, 24) = 43.61	P<0.0001
Residual	80570078219529	24	3357086592480		
Number of missing values	0				

Appendix 3. Two-way ANOVA tables generated from MTT experiments with recombinant gelsolin, thrombospondin and periostin from two different suppliers.

Table 32. ANOVA table generated for MTT gelsolin experiment 1. The table indicates significant differences within the dataset and therefore Dunnet's post hoc test was performed. Column factor = treatment, row factor = incubation time.

Table Analyzed	Exp 1				
Two-way ANOVA	Ordinary				
Alpha	0.05				
Source of Variation	% of total variation	P value	P value summary	Significant?	
Interaction	10.67	0.6418	ns	No	
Row Factor	23.77	0.0038	**	Yes	
Column Factor	12.72	0.1539	ns	No	
ANOVA table	SS	DF	MS	F (DFn, DFd)	P value
Interaction	1856	8	232	F (8, 30) = 0.7575	P=0.6418
Row Factor	4134	2	2067	F (2, 30) = 6.748	P=0.0038
Column Factor	2212	4	553.1	F (4, 30) = 1.805	P=0.1539
Residual	9190	30	306.3		
Number of missing values	0				

Table 33. ANOVA table generated for MTT gelsolin experiment 2. The table indicates significant differences within the dataset and therefore Dunnet's post hoc test was performed. Column factor = treatment, row factor = incubation time.

Table Analyzed	Exp 2				
Two-way ANOVA	Ordinary				
Alpha	0.05				
Source of Variation	% of total variation	P value	P value summary	Significant?	
Interaction	15.03	0.2058	ns	No	
Row Factor	8.722	0.0453	*	Yes	
Column Factor	38.17	0.0003	***	Yes	
ANOVA table	SS	DF	MS	F (DFn, DFd)	P value
Interaction	2792	8	349	F (8, 30) = 1.48	P=0.2058
Row Factor	1620	2	810.1	F (2, 30) = 3.436	P=0.0453
Column Factor	7091	4	1773	F (4, 30) = 7.52	P=0.0003
Residual	7072	30	235.7		
Number of missing values	0				

Table 34. ANOVA table generated for MTT gelsolin experiment 3. The table indicates significant differences within the dataset and therefore Dunnet's post hoc test was performed. Column factor = treatment, row factor = incubation time.

Table Analyzed	Exp 3				
Two-way ANOVA	Ordinary				
Alpha	0.05				
Source of Variation	% of total variation	P value	P value summary	Significant?	
Interaction	20.65	0.1605	ns	No	
Row Factor	7.714	0.1058	ns	No	
Column Factor	23.87	0.0137	*	Yes	
ANOVA table	SS	DF	MS	F (DFn, DFd)	P value
Interaction	3189	8	398.7	F (8, 30) = 1.621	P=0.1605
Row Factor	1191	2	595.7	F (2, 30) = 2.423	P=0.1058
Column Factor	3687	4	921.9	F (4, 30) = 3.749	P=0.0137
Residual	7377	30	245.9		
Number of missing values	0				

Table 35. ANOVA table generated for MTT periostin Biotechne experiment 1. The table indicates significant differences within the dataset and therefore Dunnet's post hoc test was performed. Column factor = incubation time, row factor = treatment.

Table Analyzed	Exp 1				
Two-way ANOVA	Ordinary				
Alpha	0.05				
Source of Variation	% of total variation	P value	P value summary	Significant?	
Interaction	18.81	0.1049	ns	No	
Row Factor	32.52	0.0007	***	Yes	
Column Factor	10.69	0.0243	*	Yes	
ANOVA table	SS	DF	MS	F (DFn, DFd)	P value
Interaction	2492	8	311.4	F (8, 30) = 1.858	P=0.1049
Row Factor	4307	4	1077	F (4, 30) = 6.422	P=0.0007
Column Factor	1415	2	707.7	F (2, 30) = 4.221	P=0.0243
Residual	5030	30	167.7		
Number of missing values	0				

Table 36. ANOVA table generated for MTT periostin Biotechne experiment 2. The table indicates significant differences within the dataset and therefore Dunnet's post hoc test was performed. Column factor = incubation time row factor = treatment.

Table Analyzed	Exp 2				
Two-way ANOVA	Ordinary				
Alpha	0.05				
Source of Variation	% of total variation	P value	P value summary	Significant?	
Interaction	20.4	0.0987	ns	No	
Row Factor	28.1	0.0026	**	Yes	
Column Factor	11.06	0.0266	*	Yes	
ANOVA table	SS	DF	MS	F (DFn, DFd)	P value
Interaction	4612	8	576.5	F (8, 30) = 1.891	P=0.0987
Row Factor	6353	4	1588	F (4, 30) = 5.211	P=0.0026
Column Factor	2500	2	1250	F (2, 30) = 4.101	P=0.0266
Residual	9143	30	304.8		
Number of missing values	0				

Table 37. ANOVA table generated for MTT periostin Biotechne experiment 3. The table indicates significant differences within the dataset and therefore Dunnet's post hoc test was performed. Column factor = incubation time, row factor = treatment.

Table Analyzed	Exp 3				
Two-way ANOVA	Ordinary				
Alpha	0.05				
Source of Variation	% of total variation	P value	P value summary	Significant?	
Interaction	20.38	0.1265	ns	No	
Row Factor	30.7	0.0024	**	Yes	
Column Factor	5.337	0.1768	ns	No	
ANOVA table	SS	DF	MS	F (DFn, DFd)	P value
Interaction	3288	8	411	F (8, 30) = 1.754	P=0.1265
Row Factor	4954	4	1238	F (4, 30) = 5.284	P=0.0024
Column Factor	861	2	430.5	F (2, 30) = 1.837	P=0.1768
Residual	7031	30	234.4		
Number of missing values	0				

Table 38. ANOVA table generated for MTT thrombospondin experiment 1. The table indicates significant differences within the dataset and therefore Dunnet's post hoc test was performed. Column factor = incubation time, row factor = treatment.

Table Analyzed	Exp 1				
Two-way ANOVA	Ordinary				
Alpha	0.05				
Source of Variation	% of total variation	P value	P value summary	Significant?	
Interaction	22.08	0.0331	*	Yes	
Row Factor	11.08	0.0631	ns	No	
Column Factor	33.64	<0.0001	****	Yes	
ANOVA table	SS	DF	MS	F (DFn, DFd)	P value
Interaction	5586	8	698.2	F (8, 30) = 2.495	P=0.0331
Row Factor	2804	4	700.9	F (4, 30) = 2.504	P=0.0631
Column Factor	8509	2	4255	F (2, 30) = 15.2	P<0.0001
Residual	8396	30	279.9		
Number of missing values	0				

Table 39. ANOVA table generated for MTT thrombospondin experiment 2. The table indicates significant differences within the dataset and therefore Dunnet's post hoc test was performed. . Column factor = incubation time, row factor = treatment.

Table Analyzed	Exp 2				
Two-way ANOVA	Ordinary				
Alpha	0.05				
Source of Variation	% of total variation	P value	P value summary	Significant?	
Interaction	22.84	0.0259	*	Yes	
Row Factor	29.29	0.0005	***	Yes	
Column Factor	15.31	0.0031	**	Yes	
ANOVA table	SS	DF	MS	F (DFn, DFd)	P value
Interaction	4017	8	502.1	F (8, 30) = 2.631	P=0.0259
Row Factor	5152	4	1288	F (4, 30) = 6.747	P=0.0005
Column Factor	2692	2	1346	F (2, 30) = 7.052	P=0.0031
Residual	5727	30	190.9		
Number of missing values	0				

Table 40. ANOVA table generated for MTT thrombospondin experiment 3. The table indicates significant differences within the dataset and therefore Dunnet's post hoc test was performed. Column factor = incubation time, row factor = treatment.

Table Analyzed	Exp 3				
Two-way ANOVA	Ordinary				
Alpha	0.05				
Source of Variation	% of total variation	P value	P value summary	Significant?	
Interaction	15.35	0.3720	ns	No	
Row Factor	20.4	0.0338	*	Yes	
Column Factor	13.34	0.0305	*	Yes	
ANOVA table	SS	DF	MS	F (DFn, DFd)	P value
Interaction	2368	8	296	F (8, 30) = 1.13	P=0.3720
Row Factor	3147	4	786.9	F (4, 30) = 3.005	P=0.0338
Column Factor	2059	2	1029	F (2, 30) = 3.931	P=0.0305
Residual	7855	30	261.8		
Number of missing values	0				

Table 41. ANOVA table generated for MTT periostin Novus experiment 1. The table indicates significant differences within the dataset and therefore Dunnet's post hoc test was performed. Column factor = incubation time, row factor = treatment.

Table Analyzed	Exp 1				
Two-way ANOVA	Ordinary				
Alpha	0.05				
Source of Variation	% of total variation	P value	P value summary	Significant?	
Interaction	36.29	<0.0001	****	Yes	
Row Factor	29.25	<0.0001	****	Yes	
Column Factor	23.7	<0.0001	****	Yes	
ANOVA table	SS	DF	MS	F (DFn, DFd)	P value
Interaction	4869	8	608.6	F (8, 30) = 12.64	P<0.0001
Row Factor	3925	4	981.3	F (4, 30) = 20.38	P<0.0001
Column Factor	3179	2	1590	F (2, 30) = 33.02	P<0.0001
Residual	1444	30	48.14		
Number of missing values	0				

Table 42. ANOVA table generated for MTT periostin Novus experiment 2. The table indicates significant differences within the dataset and therefore Dunnet's post hoc test was performed. Column factor = incubation time, row factor = treatment.

Table Analyzed	Exp 2				
Two-way ANOVA	Ordinary				
Alpha	0.05				
Source of Variation	% of total variation	P value	P value summary	Significant?	
Interaction	22.23	0.0048	**	Yes	
Row Factor	23.86	0.0002	***	Yes	
Column Factor	30.75	<0.0001	****	Yes	
ANOVA table	SS	DF	MS	F (DFn, DFd)	P value
Interaction	2141	8	267.7	F (8, 30) = 3.6	P=0.0048
Row Factor	2298	4	574.5	F (4, 30) = 7.727	P=0.0002
Column Factor	2962	2	1481	F (2, 30) = 19.92	P<0.0001
Residual	2231	30	74.35		
Number of missing values	0				

Table 43. ANOVA table generated for MTT periostin Novus experiment 3. The table indicates significant differences within the dataset and therefore Dunnet's post hoc test was performed. Column factor = incubation time, row factor = treatment.

Table Analyzed	Exp 3				
Two-way ANOVA	Ordinary				
Alpha	0.05				
Source of Variation	% of total variation	P value	P value summary	Significant?	
Interaction	34.4	<0.0001	****	Yes	
Row Factor	43.58	<0.0001	****	Yes	
Column Factor	10.43	<0.0001	****	Yes	
ANOVA table	SS	DF	MS	F (DFn, DFd)	P value
Interaction	3251	8	406.4	F (8, 30) = 11.13	P<0.0001
Row Factor	4119	4	1030	F (4, 30) = 28.2	P<0.0001
Column Factor	986.1	2	493	F (2, 30) = 13.5	P<0.0001
Residual	1095	30	36.51		
Number of missing values	0				

Appendix 4. Putative LT-ag binding sites

Putative LT-ag binding sites in the gelsolin promoter

The putative LT-ag binding sites (5'GRGGC'3) in the gelsolin promoter are marked in yellow. Especially the two tandem repeats in the end of the sequence are good candidates for LT-ag binding domains, as the LT-ag domain of polyomaviruses usually preferentially binds tandem repeats of the 5'-GRGGC-3' motif separated by a short interspace.

Gelsolin 419 bp

gctttgcctcctgaagtccgttctctccagggctgaaatctgcctccgctggtgctagttga
gcattgctcgcttgcccgtcccatctgagctctttggccccagcccagctcaggagctgccc
tgggtctcctccccgaccctaggcctcttcagatctcccctccgtgctccgggcctcagttt
cctccaggggaaagcagagggcttggtttggtgccttcctgcgaggtgaagcgaggggtccc
cctggacgaaggcgagcttggagccacccgcccagcagccgacgggagggcctggcgctcct

ccccacccgcctgcccggccgccccgccccgagggcggctcccgcccgcgccctgcccacc
ccggccgcgcgcaccacaacgccccgccccgccgcccggaaccagc

Putative LT-ag binding sites in the thrombospondin promoter

No putative LT-ag binding motifs (5'GRGGC'3) were located in the thrombospondin promoter used in the study.

THBS 235 bp
cctatgctggtggtagactagggttgtttgtcttctctcaagaaatggtgttcttctctgac
ctgaaatacgaatgtagagatccctaatcatcaaattgttgattgaaagactgatcataaac
caatgctggtattgcaccttctggaactatgggcttgagaaaacccccaggatcacttctcc
ttggcttccttcttttctgtgcttgcatcagtgtggactcctagaacgt

Putative LT-ag binding sites in the periostin promoter

No putative LT-ag binding motifs (5'GRGGC'3) were located in the periostin promoter used in the study.

Periostin 339 bp
gatggagtgcctgtggaaataactgaaaaagagacacgagaagaacgaatcattacaggtcc
tgaaataaaatacactaggatttctactggaggtggagaaacagaagaaactctgaagaaat
tgttacaagaagaggtcaccaaggtcaccaaattcattgaaggtggtgatggtcatttattt
gaagatgaagaaattaaaagactgcttcagggagacacacccgtgaggaagtt